IMPACT OF COPPER, ZINC SUPEROXIDE DISMUTASE KNOCKOUT ON LIPID METABOLISM IN MICE

A Dissertation

Presented to the Faculty of the Graduate School

of Cornell University

In Partial Fulfillment of the Requirements for the Degree of

Doctor of Philosophy

by

Shikui Wang

August 2009

IMPACT OF COPPER, ZINC SUPEROXIDE DISMUTASE KNOCKOUT ON LIPID METABOLISM IN MICE

Shikui Wang, Ph. D.

Cornell University 2009

Antioxidant enzymes play important roles in maintaining the cellular redox homeostasis and protecting cell from damage caused by reactive oxygen species (ROS). Copper,zinc superoxide dismutase (SOD1) is an important antioxidant enzyme responsible for the clearance of superoxide anion. It has been suggested that the deficiencies of superoxide dismutases lead to abnormal lipid deposition in different organs. However, the regulatory role of SOD1 in lipid metabolism is largely unknown. The objective of this study was to determine the role of SOD1 in lipid metabolism. The experiments were conducted on the young and adult SOD1 knockout (SOD1-/-) and WT mice fed high fat, copper deficient, copper excess, or normal diets. Under the normal conditions, the SOD1 knockout causes hypercholesterolemia and hypotriglyceridemia with irregular lipids accumulation in liver, heart, kidney, muscle and testis. In contrast to the suppressed accumulation of fatty acids/triglyceride, the cholesterol synthetic pathway was consistently activated in SOD1-/- mice as indicated by increased mRNA and protein levels of related genes. The significant increase of sterol regulatory element binding proteins (SREBP) 2 and decrease of SREBP1 in SOD1-/- mice were observed. SOD1-/- mice fed high fat diet had reduced body weight and very low density lipoproteins (V)LDL triglyceride, although the total plasma cholesterol, total triglyceride and fecal cholesterol was not significantly affected. Copper deficiency did not affect the concentrations of blood lipids in $SOD1^{-/-}$ mice

while high copper was found only to reduce hepatic triglyceride level without effect on plasma cholesterol and triglyceride levels as well as hepatic cholesterol. Surprisingly, significant increase of total plasma cholesterol was observed in mice injected with herbicide diquat (DQ) in addition to the increased mRNA levels of 3 –hydroxy-3-methyl-glutaryl-CoA reductase (HMGCR) and squalene epoxidase. HepG2 cells showed similar responses to diquat treatment with increased HMGCR mRNA level. In conclusion, knockout of SOD1 caused disorder in lipid metabolism associated with the increased transcription of genes involved in cholesterol synthesis. These changes were not reversed by the high fat diet or dietary copper supplementation and might be dependent on increased ROS level following loss of SOD1 function.

BIOGRAPHICAL SKETCH

Shikui Wang was born on October 6, 1978 in Taihu, Anhui, P. R. China, where he spent most of his childhood with his grandmother and sisters. After graduating from Taihu Second High School, Shikui attended Huazhong Agricultural University in 1996 and received the Bachelor of Agricultural Science degree in July 2000. He then attended the Institute of Animal Science at the Chinese Academy of Agricultural Sciences, studying under the guidance of Dr. Jianming Tong and received the Master of Science degree in July 2003. Upon completion of the Master's degree, Shikui was employed by National Center for Clinical Diagnostics & Beijing Hospital, Ministry of Health, P. R. China, where married his classmate, Lifang Han, in July 2004. In August 2005, he left Beijing and started his Doctor of Philosophy degree program under his mentor, Dr. Xin Gen Lei, in the Department of Animal Science at Cornell University. His daughter, Kathy Wang, was born on November 28, 2006. He completed his Doctor of Philosophy in Animal Science with minors in Nutrition and Biomedical Science in August 2009.

ACKNOWLEDGEMENTS

I would first like to thank my advisor, Dr. Xin Gen Lei, for his patient guidance and support throughout my Ph.D. program. I would also like to thank my committee members, Dr. Charles McCormick, Dr. James Thomas Brenna and Dr. Yung-Fu Chang, for their knowledgeable advice and kind assistance.

I would like to thank Dr. Li Li at USDA ARS Robert W. Holley Research Center for Agriculture and Health for generous support during my doctoral research. My thanks also go to her lab members Drs. Xin Zhou and Xiangjun Zhou for assistance with real time PCR analysis.

I would also like to thank Drs. Sheng Zhang, Wei Wang and Xinming Zheng at Institute for Biotechnology and Life Science Technologies and Department of Molecular Biology and Genetics for help in assaying samples and providing technical support. My thanks go to Dr. Martha Stipanuk at Nutrition Science for providing cells, which made it possible to do in vitro studies. I would also like to thank faculty，staff and my peers, in the Department of Animal Science for friendship and support during my past four years. My thanks go to Shuai Li for his technical support and friendship.

I would like to thank Carol Roneker for her excellent animal care and lab management. I would like to thank my labmates, Jianhong Zhu, Jeremy Weaver (also my officemate), Michael Scimeca, Koji Yasuda, Xiaodan Wang, Matt Pepper, Catherine Faber, Xi Yan, Elizabeth Wasmouth and Drs. Marko Vatamaniuk, Ruqian Zhao, Chunxiang Ai, Yuting Hu, Jiang Li and Fang Yang for their help and friendship. I appreciate the kind help from Joanne Parsons, Susan Herbert, and Deloris Bevins for their administrative assistance, and great humor from big Karl Roneker.

I would like to thank my wife Lifang Han and our families, whose love and support have made the completion of my Ph.D. study possible. I would also like to thank my daughter, Kathy Wang, who is an inspiration to me.

TABLE OF CONTENTS

LIST OF FIGURES

LIST OF TABLES

LIST OF ABBREVIATIONS

8-OHdG	=	8-hydroxy-2-deoxyguanosine
ACAA	=	Acetyl coenzyme A acyltransferase
ACAT	=	Acyl coenzyme A:cholesterol acyltransferase
ACC	=	Acetyl coenzyme A carboxylase
ACOX	=	Acyl coenzyme A oxidase
ARE	=	Antioxidant response element
ARH	=	Autosomal recessive hypercholesterolemia
ATF	=	Activating transcription factor
CAT	=	Catalase
CLA	=	Conjugated linoleic acid
CYP7A1	=	Cholesterol 7 alpha-hydroxylase
DHCR7	=	7-dehydrocholesterol reductase
DQ	=	Diquat
ER	=	Endoplasmic reticulum
FALS	=	Familial Amyotrophic lateral sclerosis
FASN	=	Fatty acid synthase
FDB	=	Familial defective apolipoprotein B
GPX1	=	Glutathione peroxidase 1
H_2O_2	=	hydrogen peroxide
HDL	=	High density lipoprotein
HDL-C	=	High density lipoprotein cholesterol
HMG CoA	=	3-hydroxy-3-methylglutaryl coenzyme A
HMGCL	=	3-hydroxymethyl-3-methylglutaryl-coenzyme A lyase
HMGCR	=	3-hydroxy-3-methylglutaryl coenzyme A reductase
HMGCS	=	3-hydroxy-3-methylglutaryl coenzyme A synthase

IDL	=	Intermediate density lipoprotein
IL	=	Interleukin
INSIG	=	Insulin induced gene
LDL	=	Low density lipoprotein
LDL-C	=	Low density lipoprotein cholesterol
MAP	=	Mitogen-activated protein
MCCC	=	Methyl crotonyl coenzyme A carboxylase
MDA	=	Malonaldehyde
MTP	=	Microsomal triglyceride transfer protein
NEFA	=	Non-esterified free fatty acids
NRF	=	Nuclear respiratory factor
$O_2^{\cdot-}$	=	superoxide anion
$^1O_2$	=	singlet oxygen
$^{\cdot}OH$	=	hydroxyl radical
PBS	=	Phosphate-buffered saline
PDH	=	Pyruvate dehydrogenase
PMSF	=	Phenylmethylsufonyl fluoride
PPARG	=	Peroxisome proliferator-activated receptor gamma
PTP1B	=	Protein tyrosine phosphatase-1B
ROS	=	Reactive oxygen species
S1P	=	Site 1 protease
S2P	=	Site 2 protease
SCAP	=	Sterol regulatory element binding proteins cleavage activating protein
SCHAD	=	Short-chain 3-hydroxyacyl- coenzyme A dehydrogenase
SF1	=	Steroidogenic factor

SOD1	=	Copper, zinc superoxide dismutase
SOD1+/-	=	Copper, zinc superoxide dismutase heterozygous knockout
SOD1-/-	=	Copper, zinc superoxide dismutase homozygous knockout
SOD2	=	Mitochondrial manganese superoxide dismutase
SOD3	=	Extracellular copper, zinc superoxide dismutase
SOO	=	Superoxide oxidase
SOR	=	Superoxide reductase
SQLE	=	Squalene epoxidase
SREBP	=	Sterol regulatory element binding proteins
TC	=	Total cholesterol
TG	=	Total triglyceride
TNF	=	Tumor necrosis factor
VLDL	=	Very low density lipoprotein
WT	=	Wild-type

CHAPTER ONE

INTRODUCTION

Oxygen, a final acceptor of electrons in the reactions of respiration coupled with oxidative phosphorylation, is indispensible to aerobic organisms because of energy production. However, it is also a potentially toxic molecule because of the formation of reactive oxygen species (ROS). The survival of all metazoan organisms depends on the balance between the generation of energy and production of potentially toxic oxidants (1). An antioxidant system, including copper (Cu), zinc (Zn) superoxide dismutase (SOD1), makes cells capable of coping with these potentially toxic molecules, and simultaneously maintains the cellular redox homeostasis which affects the cellular signal transduction. The importance of SOD1 has been recognized because it catalyzes the first step of clearance of superoxide. A number of studies have been conducted to investigate the protective roles of SOD1 in different tissues and organs, such as brain, eyes, muscle, and liver (2-9). Linked to the energy metabolism by oxygen, the precursor of superoxide, SOD1 possibly plays an important role in regulation of energy homeostasis and lipid metabolism in cells.

1.1 Reactive Oxygen Species (ROS)

Reactive oxygen species are derived from the metabolism of molecular oxygen, including superoxide anion radical ($O_2^{-}\cdot$), singlet oxygen ($^1O_2$), hydrogen peroxide (H_2O_2), and hydroxyl radical ($^{\cdot}OH$) (10). A one-electron reduction of O_2 results in the formation of superoxide either by enzymatic catalysis or by "electron leaks" from various electron transfer reactions. In contrast to its remarkable stability in many organic solvents, superoxide in aqueous solution is short-lived (11). Unlike superoxide, H_2O_2 is not a free radical and is a much more stable molecule. H_2O_2 is able to diffuse

across biological membranes, whereas superoxide does not (12). H_2O_2 is a weaker oxidizing agent than superoxide. However, in the presence of transition metals such as iron or Cu, H_2O_2 gives rise to the indiscriminately reactive and toxic hydroxyl radical by Fenton chemistry (13).

Due to their higher reactivities relative to molecular O_2, ROS are potentially toxic to cells, and have wide effects on biological molecules, including proteins, nucleotides, carbohydrates and lipids (14). The term oxidative stress refers to damage to these molecules that occurs when ROS generation is higher than the clearance ability of the antioxidant system (15). Several markers which may indicate the oxidative stress level induced by ROS have been identified：1) protein carbonyls are chemically stable biomarkers of oxidative stress. Carbonyl groups are generated by direct oxidation of amino acid residues, particularly lysine, arginine, threonine, and proline, or by secondary reaction with the primary oxidation products of sugars and lipids; 2) the most representative product that may reflect oxidative damage to DNA in the cells is 8-hydroxy-2-deoxyguanosine (8-OHdG), a product of oxidatively modified DNA base guanine; 3) malonaldehyde (MDA) is one of the end products of lipid peroxidation in the cell membranes or in low-density lipoproteins, and F2-Isoprostanes, especially 8-iso-PGF2, also have been proposed as specific, reliable, and non-invasive markers of lipid peroxidation *in vivo* (16-18). These molecules could be used as clinical markers to evaluate the damage caused by ROS because their levels are very low in normal animal biological fluids and tissues (18).

In addition to their deleterious effects on cells, ROS have been proven to act as important signaling molecules in the cell. Early studies have shown that H_2O_2 has an insulin-like effect on glucose transport and oxidation, and enhances lipid synthesis from glucose in adipocytes (19, 20). Mitogen-activated protein (MAP) kinase signaling pathways are well known to be activated by ROS which induce the

phosphorylation of downstream proteins, extracellular signal-regulated kinase (ERK), c-Jun N-terminal kinase (JNK) and p38 MAP kinase, as widely observed earlier (21). It has been suggested that mitochondrial ROS are involved in the process of apoptosis induced by TNF-α and IL-1β, while mediating the hypoxia-induced gene transcription (22, 23). ROS derived from NADPH oxidase in vascular smooth muscle cells regulate the vascular remodeling (24). Recently, protein tyrosine phosphatase-1B (PTP1B) has been identified as a ROS-responsive protein, which could be directly oxidized and inactivated by superoxide and hydrogen peroxide (25, 26). As PTP1B is a key regulator of multiple signaling pathways downstream of receptor tyrosine kinases, it provides a possible target for manipulating cellular responses through ROS. Another example is NF-E2-related factor-2(Nrf2)-Keap1 complex, which functions as a ROS sensor and regulates the expression of antioxidant enzymes, such as catalase (CAT) and glutathione peroxidase 1 (GPX1), through the binding of antioxidant response elements (AREs) in their 5'-flanking promoter regions (27, 28). Other factors including NF-κB, SP1, and YY1 are also involved in the regulation of redox-induced changes (29-31). Therefore, in addition to oxidative damage, ROS are critical to maintain normal physiological reactions.

As potentially toxic molecules, ROS are strictly regulated by the antioxidant system which is made up of antioxidant enzymes and small antioxidant agents. Superoxide generated by the mitochondria and other sources is converted to H_2O_2 and O_2 by superoxide dismutases (SODs), and H_2O_2 is then catalyzed to water by GPX1 and CAT (32, 33). Therefore, SODs provide an important defense against superoxide toxicity. Depending on the species, there are up to three different metal-containing SOD enzymes which, taken together, make up the major superoxide scavenging system in the mitochondrion, nucleus, cytoplasm and extracellular spaces. These SODs are the products of different genes and are historically designated, in higher

eukaryotes, by their primary location as follows: SOD1 (cytoplasmic Cu, Zn SOD), SOD2 (mitochondrial manganese SOD) and SOD3 (extracellular Cu, Zn SOD). The majority of superoxide in mammalian cells is generated by chemiosmotic proton transfer by Complex I and III during mitochondrial ATP production. Superoxide produced by Complex I is exclusively released into the mitochondrial matrix and dismutated by SOD2, whereas Complex III can release superoxide to both extra-mitochondrial and intra-mitochondrial matrix locations, where the superoxide is dismutated by SOD1 and SOD2, respectively (34). The different types of SODs have different roles in maintaining the entire cellular redox environment.

Superoxide is subjected to rapid spontaneous dismutation in aqueous solutions, especially when its concentration reaches a high level in acidic pH conditions. SOD speeds up this reaction almost 10^4-fold and the rate constant reaches 1.6×10^9 M^{-1} s^{-1} (35). Nitric oxide is another biomolecule, which is able to outcompete SOD, and reacts with superoxide at near diffusion-limited rates to form peroxynitrite (36). This reaction provides another significant biological outlet of superoxide because peroxynitrite is a much more active molecule that could nitrate the residues of protein (37). Nitrotryrosine is one of its end products and it may induce alteration of protein conformation leading to changes in enzyme catalytic activity, signal transduction, cytoskeletal organization and inhibition of tyrosine phosphorylation by protein kinase (38). The significance of protein nitration has also been shown in aging, neurodegeneration and cancer (39, 40).

1.2 Superoxide Dismutase (SOD)

Cu, Zn superoxide dismutase is the major cellular isoform of superoxide dismutase, and it is encoded by the SOD1 gene. It is a homodimer of molecular weight 32,500 Daltons and the two subunits that joined primarily by hydrophobic and electrostatic

interactions (41). It is mainly located in cytosol, but also found in the intermembrane space of the mitochondria in which SOD1 might be involved in the protection of mitochondrial proteins from the superoxide-induced damage (42). In addition to its superoxide dismutase activity, SOD1 can function as a superoxide reductase (SOR), and as a superoxide oxidase (SOO) while Mn SOD does not have SOR or SOO activities (43). These differences, in addition to the cellular localization, may be related to their biological functions.

Studies have shown that SOD1 is an indispensible antioxidant enzyme to maintain the normal redox environment and physiological reactions in cells. Mutant SOD1 has been widely linked to neurodegenerative diseases. Up to 25% of familial amyotrophic lateral sclerosis (FALS) are associated with mutations in SOD1 (44). However, the proposed pathogenesis of mutant SOD1 is not because of the loss of functional activity, but of the gain of toxic properties of mutant SOD1 (45, 46). Due to the additional deleterious property of mutant SOD1, knock out or over expression of SOD1 gene provides more specific tools for functional studies. Knockout studies indicate that deficiency of SOD1 results in the widespread oxidative damage and induces various symptoms/phenotypes, related to liver (2-4), eyes (5, 6), infertility (7), neuron (8), muscle (9), kidney (47) and erythrocyte (48) in rodent models. For example, SOD1 deficient mice display a decreased life span and an elevated incidence of liver cancer with an increased frequency of DNA mutation and apoptotic cells (2, 4). Without the protection of SOD1, ethanol accelerates the functional loss of mitochondria by inducing uncoupling, swelling, changing the permeability transition and decreasing adenine nucleotide translocator activity, which leads to the development of necrosis in the alcohol-induced liver injury (3). The deletion of SOD1 also increases the ischemia/reperfusion-induced acute renal failure in mice (47). By contrast, over expression of SOD1 is proved to reduce the superoxide radical level and oxidative

stress. Over expression of SOD1 causes a significant decrease of superoxide production, which affects redox-sensitive inflammatory signaling and neurotoxic inflammation process in microglia (49). The activation of NF-kappa, regulated by ROS, is attenuated by the over expression of SOD1 after transient focal cerebral ischemia, and it blocks the expression of downstream deleterious genes like *c-myc*, thereby reducing ischemic damage in mice (50). So, the deficiency of SOD1 exposes cells to the deleterious superoxide while over expression of SOD1 blocks the signal transduction of superoxide.

Besides the antioxidant activity, SOD1 itself has been found to function as a signal molecule interacting with other proteins. SOD1 can interact with ERα and enhance binding of ERα to estrogen response element-containing DNA (51). SOD1 is required for the effective estrogen responsiveness of the endogenous pS2, progesterone receptor, cyclin D1, and cathepsin D genes in MCF-7 breast cancer cells (51). This suggests the additional function of SOD1, which is different from enzymatic activity. Another possible role of SOD1 is metal chelator for Cu and Zn in cells to maintain the metal homeostasis. Knock out of SOD1 results in a 50% decrease of Cu in the liver of 3-month-old mice while it causes a 50% increase of hepatic iron as well (52).

1.3 Cholesterol and Hypercholesterolemia

Cholesterol, an amphipathic lipid, is an essential structural component of the cell membrane and outer layer of blood plasma lipoproteins. Moreover, cholesterol is a precursor of several other steroids, namely corticosteroids, sex hormones, bile acids, and vitamin D in animals. Cholesterol in animal body originates from two major sources, dietary intake and *de novo* synthesis. Dietary cholesterol comes mainly from animal products, while food of plant origin contains no cholesterol. In animals,

cholesterol can be synthesized in most tissues from acetyl-CoA, and liver is a primary organ for cholesterol synthesis (~40%) in mice (53).

The process of cholesterol synthesis occurs in the endoplasmic reticulum (ER), microsomes and cytosol from the two-carbon acetate group of acetyl-CoA, which is generated in the mitochondria primarily from two sources, the pyruvate dehydrogenase (PDH) reaction, and fatty acid oxidation and is delivered to the cytoplasm. It is noted that acetyl-CoA is the same substrate for both cholesterol and fatty acid synthesis in the cytosol, and it represents different directions of energy flux in cells. For cholesterol synthesis, two molecules of acetyl-CoA are condensed in a reversal of the thiolase reaction, forming acetoacetyl-CoA. Acetoacetyl-CoA and a third molecule of acetyl-CoA are converted to HMG-CoA by the action of HMG-CoA synthase. Unlike the HMG-CoA produced during the synthesis of ketones in the mitochondria, this form is synthesized in the cytoplasm. However, both pathways share the necessary enzymes. Then HMG-CoA is converted to mevalonate by HMG-CoA reductase (HMGR) which is bound in the ER membrane. The reaction is the rate-limiting step of cholesterol biosynthesis, and HMGR is a target for clinical cholesterol-lowering drugs such as statins.

As a precursor for biologically important nonsteroidal isoprenoids, mevalonate is then converted to 3-isopentenyl pyrophosphate in three reactions which require ATP. This molecule is decarboxylated to isopentenyl pyrophosphate, which is a key metabolite for various biological reactions. Three molecules of isopentenyl pyrophosphate condense to form farnesyl pyrophosphate through the action of geranyl transferase. Two molecules of farnesyl pyrophosphate then condense to form squalene by the action of squalene synthase, which is the first enzyme in the committed cholesterol pathway. Squalene is converted to 2, 3- oxidosqualene by squalene epoxidase, which requires NADPH as a reductant and O_2 as an oxidant. This is the first oxidation step in

cholesterol synthesis. Oxidosqualene cyclase then cyclizes 2,3- oxidosqualene to form lanosterol. Finally, lanosterol is then converted to cholesterol involving 19 reactions, catalyzed by enzymes associated with ER membranes. *De novo* synthesized cholesterol as well as dietary source cholesterol is utilized in the formation of membranes and the synthesis of the steroid hormones, bile acids and others, and the greatest proportion of cholesterol is used for bile acid synthesis in hepatocytes.

Although the ER is the primary site of cholesterol synthesis, the concentration of cholesterol in the ER is very low, comprising only about 0.5–1% of cellular cholesterol (54). *De novo* synthesized cholesterol is mostly transported from the ER directly to the plasma membrane, bypassing the Golgi apparatus, but some follows the vesicle-mediated protein secretory pathway from the ER to the trans-Golgi network (55). Excess cholesterol in the ER becomes esterified (CE) by acyl-CoA: cholesterol acyltransferases, after which the cholesterol esters are stored in lipid droplets. Cholesterol can be removed from cells by efflux to extracellular acceptors, especially apoA-I and HDL, which transports cholesterol from extra hepatic tissues to the liver (56, 57). Alternatively, part of the liver cholesterol may be esterified, incorporated into the nascent VLDL particle, and secreted into the plasma to be used by peripheral tissues (58).

As cholesterol is almost insoluble in water, it is stored in lipoproteins in the circulatory systems, which includes chylomicrons, very low density lipoprotein (VLDL), intermediate density lipoprotein (IDL), low density lipoprotein (LDL), and HDL. Many of these lipoproteins are named based on its density while they carry different amount of lipids inside. Chylomicrons mainly carry triacylglycerol, with certain amount of dietary cholesterol, from the intestines to the liver, skeletal muscle, and to adipose tissue. VLDL carries newly synthesized cholesterol and triglyceride from the liver to peripheral tissues. Once depleted of its triacylglycerol, the VLDL is

transformed into cholesterol-rich remnant particles LDL. LDL can be removed from the plasma by receptor-dependent and receptor-independent mechanisms. Receptor-dependent LDL uptake accounts for 60–80% of LDL clearance, most of which occurs in the liver (59). IDL is the intermediate between VLDL and LDL. HDLs are the smallest and densest class of lipoprotein and are produced in nascent form by the liver and the intestine. The role of HDLs are to transport of cholesterol from peripheral tissues, including the artery wall, either directly or via other lipoproteins, to the liver, which is the main reason why HDL-bound cholesterol is sometimes called "good cholesterol". In contrast, high levels of LDL cholesterol can signal medical problems like cardiovascular diseases, so it is sometimes called "bad cholesterol".

Hypercholesterolemia is a condition characterized by a very high level of cholesterol in the blood (60). It is not a disease but a metabolic derangement that can be secondary to many diseases and can contribute to many forms of different diseases, most notably cardiovascular disease. Elevated cholesterol in the blood is due to abnormalities in the levels of lipoproteins, the particles that carry cholesterol in the bloodstream. Many factors, such as diet, receptor dysfunction and hormones, which can affect cholesterol metabolism and transport, may cause this abnormality. It results from a combination of genetic and environmental risk factors. People with hypercholesterolemia have a high risk of developing a form of heart disease called coronary artery disease. This condition occurs when excess cholesterol in the bloodstream is deposited in the walls of blood vessels, particularly in the arteries that supply blood to the heart. The abnormal buildup of cholesterol forms clumps that narrow and harden artery walls. As the clumps get bigger, they can clog the arteries and restrict the flow of blood to the heart. The buildup of plaque in coronary arteries causes a form of chest pain called angina and greatly increases a risk of heart attack.

The most common inherited hypercholesterolemia is known as familial hypercholesterolemia, which results from mutations in the LDLR gene (61). Less commonly, hypercholesterolemia can be caused by mutations in the apolipoprotein B (APOB), low density lipoprotein receptor adaptor protein 1 (LDLRAP1), or proprotein convertase subtilisin/kexin type 9 (PCSK9) genes (62-64). Mutations in the APOB gene result in a form of inherited hypercholesterolemia known as familial defective apolipoprotein B (FDB) (63). LDLRAP1 mutations are responsible for another type of inherited high cholesterol, autosomal recessive hypercholesterolemia (ARH) (64). Proteins produced from the APOB, LDLRAP1, and PCSK9 genes are essential for the normal function of low-density lipoprotein receptors (62). Mutations in any of these genes prevent the cell from making functional receptors or alter the receptors' function and cause severely elevated LDL cholesterol (LDL-C) levels (65). As the excess cholesterol circulates through the bloodstream, it is excessively deposited in tissues such as the skin, tendons, and arteries causing severe health consequences.

Other factors, such as diet, smoking and a life-style, are known to cause or associate with hypercholesterolemia (66, 67). High fat diet can induce hypercholesterolemia in mice and humans with increased LDL cholesterol (66). A strong positive association has been observed between prevalence of hypercholesterolemia and smoking habits, while an inverse association between hypercholesterolemia and adherence to a Mediterranean diet (67).

1.4 Signals Controlling Cholesterol Synthesis

In mammals, regulation of cellular cholesterol content intertwines cellular uptake, biosynthesis, degradation and secretion. Multiple feedback mechanisms that control uptake and synthesis at the transcriptional and posttranscriptional level mainly dictate the cholesterol homeostasis in most cells, while degradation and secretion of

cholesterol also highly contribute to the cellular cholesterol level in hepatocytes.

SREBPs, discovered in 1993, are transcription factors that regulate the expression of genes involved with cholesterol and fatty acid metabolism (68). They are considered as master regulators of cholesterogenesis and lipogenesis. There are three different SREBPs: SREBP-1a, -1c and -2. SREBP-1a and -1c are isoforms produced from a single gene by alternate splicing (69). SREBPs are basic-helix-loop-helix-leucine zipper transcription factors synthesized as inactive precursors bound to the ER membrane (70). In the ER, the C terminus of the SREBP interacts with a protein called Scap (SREBP-cleavage activating protein), which functions as a sterol sensor, specific to the cholesterol level (71-74). Another sterol sensor is Insig (an insulin induced gene) which is an oxysterol binding protein different from Scap (71). When cells have sufficient sterol, Scap and Insig bind its specific sterol, which promote the binding of each other and prevent ER exit of SREBP (75, 76). In sterol-depleted cells, Scap does not bind to Insig, allowing ER exit of SREBP-Scap via COPII vesicles (73). Scap escorts the SREBPs from the ER to the Golgi, where they are processed by two membrane-associated site 1 and site 2 proteases (S1P and S2P), which release the mature forms of the proteins (77, 78). These transcriptionally active fragments of the SREBPs translocate to the nucleus, where they bind to the promoters of SREBP target genes, including genes involved in the synthesis and metabolism of cholesterol, triglyceride, and fatty acid (79-81).

In addition to the direct regulation of SREBPs on the biosynthetic pathway, peroxisome proliferator-activated receptors (PPARs) also regulate diverse aspects of lipid metabolism, including fat mobilization, fatty acids oxidation, and fat cell development (82-84). Moreover, liver X receptors play essential roles in the regulation of cellular cholesterol flux, whole body cholesterol absorption and excretion, and in the biosynthesis and oxidation of fat (85-89). However, fatty acids and cholesterol

metabolites in nucleus can function as natural ligands and regulate the DNA binding activity of PPARs and LXRs (90, 91). Different from the nuclear transcription factors, hormones like insulin and glucagon are also important in regulating lipid metabolism (92, 93).

HMG-CoA reductase is the rate-limiting enzyme of cholesterol synthetic pathway, and its total activity indicates the rate of cholesterol synthesis. This is a transmembrane glycoprotein, located on the ER, which catalyzes the four-electron reduction reaction of HMG-CoA to coenzyme A and mevalonate (94, 95). The activity of HMG-CoA reductase is regulated through synthesis, degradation, and modification in order to maintain the proper concentration of mevalonate derived products (96, 97). When cells are depleted of cholesterol, transcription of HMG-CoA reductase is activated through the binding of SREBP to promoter region of HMG-CoA reductase gene (73). Interestingly, transmembrane segments of HMG-CoA reductase contain a sterol-sensing domain, and products of both the sterol and isoprenoid pathway accelerate the degradation of HMGCR by an ubiquitin-proteasome dependent pathway (98). It is noted that the sterol intermediates lanosterol and 24,25-dihydrolanosterol, rather than the end product cholesterol, stimulate HMGCR degradation (99). HMGCR is also subject to posttranslational modification that regulates enzyme activity. Phosphorylation of hepatic HMGCR by calcium-activated and phospholipid-dependent protein kinase or AMP-activated protein kinase reduces its activity, and it is proposed to protect cells by limiting ATP expenditure in response to metabolic stress (100-102).

1.5 Copper Homeostasis on Hypercholesterolemia

Cu, an essential nutrient has to be obtained from the diet to meet the normal physiological needs. Otherwise Cu deficiency occurs and causes metabolic alterations,

including hypercholesterolemia and lipid disorders (103-106). Cu deficiency-induced hypercholesterolemia has been documented for decades. Cu deficiency induces hypercholesterolemia with 30 to 40% increases of plasma total cholesterol by most studies (103, 104, 107). In rats, HDL and LDL cholesterol, and triglyceride are consistently elevated by Cu deficiency, while VLDL cholesterol varies between studies (103, 108, 109); Cu deficiency also decreases hepatic total cholesterol concentration (108, 110). However, hepatic 3-hydroxy-3- methylglutaryl coenzymeA (HMG CoA) reductase activity is increased by Cu deficiency, which catalyzes the rate-limiting step of cholesterol biosynthesis. The increased synthesis is responsible for the high net efflux of cholesterol from liver to plasma in the Cu deficient rats (111). Hepatic fatty acid synthase (Fasn) is also induced by Cu deficiency in rats (112). The degradation and secretion of cholesterol could reduce cholesterol level in the body, but unlikely account for the Cu deficiency induced hypercholesterolemia, which could be inferred from the results of studies with radiolabeled cholesterol in Cu deficient rats (103, 113). On the other end, the excess Cu could reduce the hepatic and plasma cholesterol. In Wilson disease, elevated hepatic Cu results in the development of liver pathology (114). Most importantly, high Cu suppresses the transcription of HMG CoA reductase inspite of the increased SREBP2 in liver of the mouse model of Wilson disease (115). It shows a 3.6-fold decrease of VLDL cholesterol in serum and a 33% decrease of liver cholesterol (115). In conclusion, these studies suggest that Cu has a significant impact on lipid metabolism.

1.6 Objectives

For the first time we observed the severe lipid disorder in mice caused by the knockout of SOD1, although deficiencies of antioxidant enzymes, including SOD1 and SOD2, showed to cause certain metabolic alterations related to energy and lipids metabolism

as reported. However, the role of SOD1 in lipid metabolism has not been studied well and the mechanism behind the phenotype remained unknown. The present study was conducted to explore the molecular mechanism of the regulation of lipid metabolism in SOD1-/- mice with nutritional and molecular approaches.

Based on the previous characterization of phenotype and molecular studies on the SOD1-/- mice at different developmental stages under normal conditions, we developed and tested a series of hypotheses: 1) the metabolic changes induced by the knockout of SOD1 depended on the dietary energy intake, which could be reversed by high fat diet (Chapter Four); 2), the dietary Cu may counteract the metabolic changes induced by the knockout of SOD1 (Chapter Five), and, 3) ROS are the primary factors in regulation of cholesterol biosynthesis which accounts for the increased plasma cholesterol (Chapter Six). A general conclusion and discussion was stated in Chapter Seven.

CHAPTER TWO

GENERAL MATERIAL AND METHODS

2.1 Animals and Diets

All experiments are approved by the Institutional Animal Care and Use Committee at Cornell University and conducted in accordance with the NIH guidelines for animal care. The SOD1 knockout (SOD1-/-) and wild-type (WT) mice generated from 129SVJ x C57BL/6 strain，were generously provided by Y. S. Ho of Wayne State University, Michigan (116). Mice were kept on a 12-h-light/12-h-dark cycle in a ventilated room with controlled temperature (20–23°C) with the light phase beginning at 7:00 am. All mice were caged with free access to basic or experimental diet and distilled water. Genotypes of mice were verified by DNA analysis using a polymerase chain reaction method. Primers for detection of SOD1 (+) and (-) are: Forward primer: 5'-GGACATCGTGTGATCTCACTCTCAGGAGAG-3'; WT reverse primer 5'-CAAGCGGCTCCCAGCATTTCCAGTCTTTGT-3'; Knockout reverse primer: 5'-AAAAGCGCCTCCCCTACCCGGTAGAATTGA-3'.

Mice were a fed diet as shown in Table 2.1. The diet contained 30% torula yeast, 58.6% sucrose, and 5% tocopherol-stripped corn oil. Vitamin and mineral mix were prepared and added into the diet. Selenium was added into the diet by mixing a stock solution of 0.1 mg Se/ml as Na_2SeO_3. Torula yeast was purchased from Rhinelander Paper Company, Inc., Lake States Division (Rhinelander, WI) and contained less than 0.02 mg Se/kg by analysis. Sucrose, corn oil, DL-methionine and vitamin E (DL-alpha-tocopheryl acetate, 500 IU/g) were purchased from Dyets Inc. (Bethlehem, PA).

2.2 Cell Culture

HepG2/C3A human hepatocellular carcinoma cells (American Type Culture

Table 2.1 Composition of mouse diet[1]

Ingredient	Amount (g/kg)
Torula yeast	300.0
Sucrose	585.9
Corn oil	50.0
DL-methionine	4.0
Choline chlorine	1.0
Vitamin E	0.1
Mineral mix[2]	50.0
Vitamin mix[3]	9.0

[1] Diet is supplemented with Se (Na_2SeO_3) at 0.4 mg/kg.

[2] Mineral mix ingredients (per kg diet): $CaCO_3$, 26.34 g; $MgCO_3$, 1.25 g; $MgSO_4$, 0.79 g; NaCl, 3.45 g; KCl, 5.4 g; KH_2PO_4, 10.6 g; ferric ammonium citrate, 1.03 g; KI, 4 mg; $MnSO_4 \cdot H_2O$, 0.17 g; NaF, 50 mg; $AlNH_4(SO_4)_2 \cdot 12H_2O$, 8 mg; $CuSO_4 \cdot 5H_2O$, 45 mg; $CrCl_3 \cdot 6H_2O$, 26 mg.

[3] Vitamin mix ingredients (per kg diet): sucrose, 8.8 g; thiamin•HCl, 4.0 mg; riboflavin, 2.5 mg; pyridoxine•HCl, 2.0 mg; calcium D-pantothenate, 20.0 mg; niacin, 100.0 mg; menadione sodium bisulfide, 3.0 mg; folic acid, 2.0 mg; D-biotin, 1.0 mg; vitamin B12 (0.1%), 10 mg; vitamin A (650 IU/mg); 38.5 mg; vitamin D (400 IU/mg), 5.0 mg.

Collection CRL-10741) were grown in a humidified incubator at 37°C and 5% CO_2 in Dulbecco's modified Eagle's medium (DMEM) supplemented with 10% fetal bovine serum, 2 mM L-glutamine, 1 mM sodium pyruvate, 0.1 mM L-methionine, 1x MEM nonessential amino acid solution, 100 units/ml penicillin and 100 μg/ml streptomycin. Prior to subculturing, the cells were removed from 100-mm-diameter culture dish using 1 x trypsin solution, washed and re-suspended in fresh complete medium, and replated either in new culture dishes or in 6-well tissue culture plates. Treatment studies were performed within 24 h after reaching 60-70% confluence.

2.3 Sample Collection and Processing

Blood samples were collected from mice through heart puncture with an EDTA-coated syringe immediately after anesthetization with carbon dioxide. Plasma was separated by centrifugation at 3,000×g for 5 min at 4℃. Tissue samples were collected, rinsed in 0.9% saline, frozen in liquid nitrogen, and stored at -80℃ prior to use. Frozen livers were homogenized (Polytron PT3100; Brinkmann Instruments, Littau, Switzerland) in buffer I, II or III. Samples homogenized in buffer I and II were centrifugated at 12,500×g for 20 min at 4℃ (Labnet Spectrafuge, National Labnet Co., Edison, NJ). Supernatants in buffer I were used for Western blot analysis of phophorylated proteins, whereas supernatant in buffer II for Western blot analysis of other proteins. Samples homogenized in buffer III were centrifugated at 105,000 g for 1 h at 4℃ and supernatant was used to determine enzyme activities. Buffer I was 50 mM Hepes, pH 7.4 with 100 mM NaCl, 1% Triton X-100, 5 mM EDTA, 1 mM sodium pyrophosphate, 1 mM sodium orthovanadate, 1 mM NaF, 1 mM phenylmethylsufonyl fluoride (PMSF), 10 μg leupeptin/ml, 10 μg aprotinin/ml, 1 μM microcystin. Buffer II was 50 mM potassium phosphate buffer, pH 7.8, 0.1% Triton X-100, 1.34 mM diethylenetriaminepeantacitic acid, 1 mM PMSF, 10 μg pepstatin

A/ml, 10 μg leupeptin/ml, 10 μg aprotinin/ml. Buffer III was 20 mM Tris-HCl, pH 7.4 with 0.25 M sucrose. Protein concentrations in buffer I were measured with a BCA protein assay kit (Pierce Chemical Co., Rockford, IL). Protein concentrations in buffer II and III were measured by Lowry's method (117).

2.4 Blood and Tissue Chemical Analyses

Plasma total cholesterol (TC), total triglyceride (TG), and non-esterified free fatty acids (NEFA) were determined by using Cholesterol E kit, Triglyceride L-type TG H kit, and NEFA C kit (Wako Pure Chemical Industries, Japan), respectively. Cholesterol and triglycerdide of HDL and (V)LDL fractions were measured using a kit from Biovision Inc. (Mountain View, CA). Total lipids of tissues, organs and feces were extracted by using the Folch extraction procedure and, resuspended in 1% Triton X-100 ethanol (118), and concentrations were determined as indicated above. Tissue cholesterol and triglyceride were calculated based on protein concentration or dry mass.

2.5 Western Blot Analysis

Western blot analysis was used to determine protein expression in tissue homogenates or cell lysates. Briefly, predetermined amounts of proteins were loaded and separated in SDS-PAGE gels, and then transferred to nitrocellulose membranes. Membranes were blocked at room temperature for 1 h, and then incubated with appropriate primary antibodies overnight at 4℃. Thereafter, the membranes were washed and incubated with either anti-mouse or anti-rabbit secondary antibody at room temperature for appropriate time. Anti-rabbit IgG HRP was from Bio-Rad Laboratories (Hercules, CA), and anti-mouse IgG HRP was from Pierce (Rockford, IL). Signals were detected with SuperSignal West Pico Kit (Pierce Chemical Co.,

Rockford, IL) and exposed to imaging films (Kodak, Rochester, NY) according to the manufacturer's instructions. The source, dilution and preparation of primary antibodies are listed in Table 2.2.

2.6 Total RNA Extraction

Total RNA was extracted from livers or cultured cells using Trizol reagent (Life Technologies, Bethesda, Maryland, USA), according to the manufacturer's recommendation. Briefly, 50 mg of frozen liver or about 10^6 cultured cells were transferred to 1ml of Trizol solution and homogenized with a Polytron (Brinkmann Instruments, Littau, Switzerland), following phenol-chloroform extraction, and precipitation with isopropanol. Precipitated RNA was washed with 75% ethanol. RNA pellet was dissolved in DEPC-treated water. RNA concentration was assessed by absorbance spectrophotometry, and RNA integrity was confirmed either by nondenaturing agarose gel electrophoresis or Agilent Bioanalyzer 2100 (Foster City, CA). RNA was stored at -80°C.

2.7 Reverse Transcription and Real Time Quantitative PCR

One microgram of total RNA was used to synthesize the first strand of cDNA using SuperScript III reverse transcriptase (Invitrogen Life Technologies). The ABI Prism 7700 Sequence Detection System and the SYBR Green Master Mix kit (both from Applied Biosystems) was used to detect real-time PCR products from cDNA samples. The total volume of reaction mixture was 10 µl (5µl 2× SYBR Green master mix, 0.5 µl primers (10 µM), 1µl cDNA and 3.5 µl nuclease-free sterile water). PCR was performed for 40 cycles at 95°C for 15 seconds and 60°C for 1 minute after initial incubations at 95°C for 10 minutes. The specific primers of each gene are listed in Table 2.3. The specificity and purity were evaluated by agarose gels. Sample Ct values

Table 2.2 Source, dilution and preparation of primary antibodies

Antibody	Species	Dilution	Buffer[1]	Source
CAT	Goat	1:500	5% milk TTBS	Santa Cruz Biotechnology (Santa Cruz, CA)
GPX1	Rabbit	1:5000	5% milk TTBS	Lab Frontier (Seoul, Korea)
SOD1	Rabbit	1:5000	5% milk TTBS	Chemicon (Temecula, CA)
SREBP1	Rabbit	1:1000	5% milk TTBS	Santa Cruz Biotechnology (Santa Cruz, CA)
SREBP1[2]	Mouse	1:500	5% milk TTBS	Gift from Dr. Chang (Dartmouth University)
SREBP2	Rabbit	1:1000	3% milk TTBS	Santa Cruz Biotechnology (Santa Cruz, CA)
SREBP2[2]	Mouse	1:500	5% milk TTBS	Gift from Dr. Chang (Dartmouth University)
HMGCR	Mouse	1:500	3% milk TTBS	Gift from Dr. Chang (Dartmouth University)
P38[2]	Rabbit	1:1000	3% milk TTBS	Cell Signaling (Beverly,MA)
Phophorylated-P38[2]	Rabbit	1:1000	3% BSA TTBS	Cell Signaling (Beverly,MA)

[1] TBS represents Tris buffered saline, pH 7.4, while TTBS represents TBS buffer with 1% Tween 20.

[2] Used in related studies which are not shown in this thesis

Table 2.3 Gene specific primers for the polymerase chain reactions

Name	Gene ID.	Sense	Antisense	Amplicon(bp)	Tm(℃)
Transcriptional factors					
Srebp1a	BC056922	5' GGAACAGACACTGGCCGAGA 3'	5' GCATAGGGGGCGTCA 3'	116	60
Srebp1c	BC056922	5'	5'	106	60
Srebp2	NM_03321	5' GCGTTCTGGAGACCATGGA 3'	5'	131	60
ATF4	NM_00971	5' CAATGACAGTGGCATCTGTATGAG 3'	5' GCTGTCTTGTTTTGCTCCATCTT 3'	222	60
PPARG	EF062476	5' CCGTGATGGAAGACCACTCG 3'	5' CAGGTCATATTTGTAATCAGCAACC	140	60
SF1	NM_13905	5' GGCTTCTAACCATTCCTTCCTC 3'	5' TGCCCTCATTGATGCCTGTA 3'	175	60
Cholesterol synthesis					
HMGCS	BC023851	5' GCCGTGAACTGGGTCGAA 3'	5' GCATATATAGCAATGTCTCCTGCAA	77	60
HMGCS	NM_00825	5' CCGTATGGGCTTCTGTTCAG 3'	5' AGCTTTGTGCGTTCCATCAG 3'	84	60
HMGCR	NM_00825	5' CTTGTGGAATGCCTTGTGATTG 3'	5' AGCCGAAGCAGCACATGAT	76	60
SQLE	MUSERG1	5' GGAAGAGCCTCATCTCCAGTAAA 3'	5' CCCGAATATCAACAAGTACCCTAG	174	60
DHCR7	NM_00785	5' CTGGAATCTTCTGAGGGCAG 3'	5' CGTGTGAATTCAGCTCTCCA 3'	184	60
Bile acid synthesis					
Cyp7A1	BC130261	5' AGCAACTAAACAACCTGCCAGTACTA	5' GTCCGGATATTCAAGGATGCA 3'	90	60
Fatty acid synthsis and oxidation					
ACC1	AY451393	5' TGAGGAGGACCGCATTTATC 3'	5' GCATGGGATGGCAGTAAGGT 3'	97	60
Fasn	AF127033	5' AGGATGTCAACAAGCCCAAG 3'	5' ACAGAGGAGAAGGCCACAAA 3'	100	
ACOX1	BC056448	5' GAGTGAGCTGCCTGAGCTTCA 3'	5' TCTTCGATACCAGCATTGGCT 3'	81	60
HMGCL	AK077842	5' CTGCTCTATAGAGGAGAGTTTC 3'	5' TGGCAGTGGACAGCCAATGC 3'	280	60
Acat1	BC029345	5' GTTCCAGAAAGAAAATGGCACA 3'	5' TCTACGGCAGCATCAGCAAA 3'	153	60
ACAA1	BC026669	5' GCTCTACCACGGCTGGAAAC 3'	5' CGACCACTGCATAGGACCTCA 3'	129	60
ACAA2	BC028901	5' GGGACAGTCACAGCAGGGAA 3'	5' GCCAGGGGCGTGAAGTTAT	104	60
Leucine (BCAA)					
MCCC1	BC021382	5' GGAAAATCGGGTATCCTGTTATG 3'	5' AGACTTCTTCGCCTCCCTCC 3'	128	60
Lipids transport					
MTP	BC012686	5' TGAGCGGCTATACAAGCTCAC 3'	5' CTGGAAGATGCTCTTCTCGC 3'	220	60

were normalized to Ct values of mouse 18s rRNA, all of which were calculated from two PCR reactions performed in triplicates from each genotype. Relative gene induction values were calculated following the manufacturer's recommendations as $2^{\Delta\Delta Ct}$, ($\Delta\Delta Ct = (Ct_{\text{gene interested of WT}} - Ct_{\text{18s of WT}}) - (Ct_{\text{gene interested of KO}} - Ct_{\text{18s of KO}})$).

2.8 Enzyme Activities Analysis

Acetoacetyl CoA thiolase activity was assayed with 15 μM of Acetoacetyl-CoA (AACoA) and 50 μM of CoA in 0.1 M Tris-HCl (pH 8.0), 25 mM MgCl2, 0.5 mM DTT, 50 mM potassium chloride. Enzyme activity was monitored by a decrease of AACoA at 303nM. The activity was normalized by protein concentration.

Short-chain 3-hydroxyacyl-CoA dehydrogenase (SCHAD) activity was determined spectrophotometrically at 340 nm with the C_4 substrates and NADH as the electron donor. The final assay mixture contained, in a final volume of 250 ul, 100 mmol/L potassium phosphate, pH 6.5, 0.1 mmol/L EDTA, and 0.1 mmol/L NADH. Buffer was warmed to 30℃ and all assays were carried out in Biotek plate reader at 30 °C. Samples (1–20 μL, containing 2–10 μg of soluble protein) were added to this mixture and the basal rate (for 1–3 min) was determined. The baseline was generally stable and showed minimal bias over 10 min. The reaction was initiated by the addition of C_4 substrate with final concentration 50 μmol/L.

2.9 Statistical Analysis

Values were expressed as mean ± SE. Statistical comparisons between each group were performed by using one way ANOVA for repeated measures followed by Dennett's test using SAS software (release 6.11, SAS Institute, Cary, NC). Significance was defined as $P < 0.05$.

CHAPTER THREE

ACTIVATION OF CHOLESTEROL BIOSYNTHETIC PATHWAY IN CU,ZN-SUPEROXIDE DISMUTASE KNOCKOUT MICE

3.1 Abstract

Knockout of superoxide dismutase has been shown to cause abnormal lipid distribution in liver and heart (119-121). This study was conducted to investigate the role of Cu, Zn superoxide dismutase (SOD1) in lipids metabolism. Wild-type (WT) and SOD1 knockout (SOD1-/-) mice at 3 and 9 weeks of age were used to examine the phenotype and molecular signal transduction in the regulation of lipids metabolism. Interestingly, knockout of SOD1 caused hypercholesterolemia and hypotriglyceridemia with abnormal lipid accumulation in liver, heart, kidney, muscle and testis. The cholesterol synthetic pathway was consistently activated in SOD1-/- mice as indicated by increased mRNA and protein level of related genes at 3 and 9 weeks of age. Moreover, SOD1-/- had reduced mRNA level of hepatic fatty acid synthase and increased hepatic LPL mRNA; at the same time, they had increased activities of mitochondria short-chain-3-hydroxyacyl-coenzyme A dehydrogenase and thiolase as well as increased plasma ketones level. We observed increased SREBP2 but decreased SREBP1 protein, which might be responsible for the changes of its target genes in SOD1-/- mice. Our data suggest that SOD1 is indispensible in maintaining the normal lipid metabolism through, at least in part, the SREBPs pathway.

3.2 Introduction

Cholesterol is an essential structural component of cells as well as a precursor of important hormones in animals. The cellular cholesterol level has to be maintained at a

steady level to meet the requirement of normal cellular metabolism. This is achieved by a feedback regulatory system that senses the level of cholesterol in the ER membranes and modulates the transcription of genes encoding enzymes of cholesterol biosynthesis and uptake from plasma lipoproteins (122). Therefore, two sources provide mammalian cells with cholesterol: receptor-mediated endocytosis of LDL by LDL receptor (LDLR) and *de novo* synthesis from acetyl-CoA by synthetic pathway (75). The biosynthesis of cholesterol occurs in the ER, cytosol and microsomes, and is catalyzed by specific enzymes. The first related enzyme is HMG-CoA reductase, which catalyzes the rate-limted step of cholesterol synthesis. This is an ER membrane-spanning enzyme, catalyzing the four-electron reduction of HMG-CoA to CoA and mevalonate (MVA), which is then converted to isopentenyl pyrophosphate, the building block for cholesterol and nonsterol isoprenoids (123). Many studies have been conducted to explore the regulatory mechanisms of this enzyme *in vivo* as a potential target for lowering-cholesterol drugs. HMG-CoA reductase can be phosphorylated or dephosphorylated by AMPK and PP2A and it is physiologically present in cells in unphosphorylated active form (~30%) and phosphorylated inactive form (~70%) (124). The enzymatic inactivation is due to the phosphorylation of the serine 871 present in the catalytic domain (102). The existence of HMG-CoA reductase in interchangable active and inactive forms provides a mechanism for the rapid short-term regulation of the pathway for cholesterol biosynthesis (125). The enzyme can also be inactivated by dithiol oxidation, and its activity depends on thiol/disulfide oxidation state of the cellular glutathione (126).

At the transcriptional level, cholesterol biosynthesis is well known to be regulated by SREBPs. There are three different SREBPs: SREBP-1a, -1c and -2. SREBP1a and 1c are isoforms produced from a single gene by alternate splicing (69). SREBP 2 isoform preferentially regulates genes involved in cholesterol homeostasis including all the

cholesterol biosynthetic enzymes (127). SREBPs are basic-helix-loop-helix-leucine zipper transcription factors synthesized as inactive precursors bound to the membranes of the ER (70). In the ER, the C terminus of the SREBP interacts with a protein called Scap (SREBP-cleavage activating protein), which functions as a sterol sensor, specific to the cholesterol level. (71-74). Another sterol sensor is Insig (Insulin induce gene) which is an oxysterol binding protein different from Scap (71). When cells have sufficient sterol, Scap and Insig bind their specific sterol, which promote the binding of each other and prevent ER exit of SREBP (75, 76). In sterol-depleted cells, Scap does not bind to Insig, allowing ER exit of SREBP-Scap via COPII vesicles (73). Scap escorts the SREBPs from the ER to the golgi, where they are processed by two membrane-associated proteases, the site 1 (S1P) and site 2 (S2P) proteases, which release the mature forms of the proteins (77, 78). These transcriptionally active fragments of the SREBPs translocate to the nucleus, where they bind to the promoters of SREBP target genes and interact with other signaling proteins (79-81). This pathway provides a long-term regulation of cellular cholesterol level and makes cells efficiently integrate the signals from different responses at the transcriptional level. For example, the binding of ATF6 to SREBP attenuates its transcriptional activity and reduces the lipogenic effect of SREBP2 (128). SCF(Fbw7), a ubiquitin ligase, can regulate lipid metabolism through the control of the phosphorylation-dependent degradation of the SREBPs family (129). Upstream stimulatory factor (USF) directly interacts with SREBPs and synergistically activates the target genes (130).

SOD1 is the major cellular isoform of superoxide dismutase and catalyzes superoxide conversion into hydrogen peroxide, which is then converted into water by catalase or glutathione peroxidase 1 (131). SOD1 is located mainly in cytosol, but also found in the intermembrane space of the mitochondria (42). As an important antioxidant enzyme, SOD1 protects cells from the damage of superoxide. The SOD1 deficiency

results in an increased incidence of pathological changes, such as hepatocarcinogenesis, hearing loss, muscle atrophy and others (2-9). As a consequence, the lifespan of SOD1 knockout mice is reduced by approximately 30% (52). Basically, this phenotype is deemed as the outcome of increased oxidative stress. However, SOD1 is also found to play an important role in nucleus as a co-activator of particular transcriptional factors. SOD1 enhances the binding of ERα to estrogen response element-containing DNA and is required for effective estrogen responsiveness of the endogenous pS2, progesterone receptor, cyclin D1, and cathepsin D genes (51). SOD1or SOD2 knockout have been reported to cause hepatic lipid accumulation and dyslipidemia in mice (132, 133). However, the exact role of SOD1 in lipid metabolism has still remained unknown. In the present study we examined the impact of SOD1 knockout on lipid metabolism in mice, focusing on alterations of hepatic cholesterol metabolism. Our data indicate that the hypercholesterolemia, hypotriglyceridemia and fatty liver result from the increased biosynthesis of cholesterol which is activated at transcriptional level of cholesterol synthetic pathway genes. The results of the present study establish a new link between oxidative stress and the regulation of lipid metabolism at the transcriptional level.

3.3 Experimental Design

Chemicals and antibodies. All chemicals were purchased from Sigma Chemical Co. (St. Louis, MO) unless otherwise indicated. Reagents for cholesterol, triglyceride and non-esterified fatty acids determination were from Wako Chemicals USA, Inc. (Richmond,VA). Antibodies used in this chapter are listed in Table 2.2. Gene expression profile was assessed by real time PCR using ABI Prism 7700 Sequence Detection System as indicated before.

Animals. The SOD1 knockout (SOD1-/-) and wild-type (WT) mice generated from 129SVJ x C57BL/6 strain，were generously provided by Y. S. Ho of Wayne State University, Michigan (116). Mice were weaned at 3 weeks of age and fed normal diet for 6 weeks based on the design of experiments. All mice used were male and their genotypes were verified by PCR.

Plasma and tissue lipids measurements. Total plasma cholesterol, triglyceride and non-esterified fatty acids levels were measured by using commercially available kits (Wako Pure Chemical Industries). Total cholesterol and triglyceride in HDL and (V)LDL lipoproteins were measured by using a kit from Biovision Inc. (Mountain View, CA). Tissues or organs were collected from 9 week old mice and were rinsed in cold PBS buffer to remove blood, and then homogenized in PBS buffer before lipids extraction. The final cholesterol and triglyceride levels were measured as indicated previously and normalized based on the protein levels.

Total RNA extraction, cDNA synthesis and real time PCR. Total RNA was extracted from 50mg frozen liver samples with Trizol reagent. Reverse transcription was performed on 1 μg total RNA per sample. Real time PCR was conducted with gene specific primers as listed in table 2.3. The generation of specific PCR products was confirmed by melting-curve analysis and gel electrophoresis.

Mitochondria isolation. Mitochondria were isolated by differential centrifugation (10). Livers were finely minced and then homogenized in a 10-ml Wheaton Scientific Teflon-to-glass homogenizers in sucrose buffer III. The homogenate was centrifuged at 600 g for 10 minutes to remove cell and tissue fragments and cell nuclei, and then supernant was transferred into a new tube and spinned at 8,000×g for 15minutes. Mitochondrial pellets were washed with the same buffer for 3 times, and then resuspended in 600 μl buffer I. Sonication was performed to release the mitochondrial protein.

Nuclei isolation. Nuclei were isolated by Dounce homogenization and sucrose gradient centrifugation. Whole livers were minced in 5 ml of ice cold buffer A (10 mM Hepes, pH 7.9; 25 mM KCl; 1 mM EGTA; 1 mM EDTA; 0.32 M sucrose; 0.15 mM spermine; 0.5 mM spermidine; 1 mM DTT; 0.5 mM PMSF; 0.5 μg/ml leupeptin; 1 μg/ml aprotinin; 1 μg/ml pepstatin) and homogenized in a 10-ml Potter-Elvehjem (Wheaton Science Products, Millville, NJ) Dounce homogenizer. Crude nuclei were collected by centrifugation (800×g, 10 min, 4 ℃). The nuclei pellet was diluted with 2 vol. of buffer B (buffer A with 2 M sucrose) and layered onto buffer B sucrose cushions in polyallomer centrifuge tubes. The gradient was centrifuged for 60 min at 1,00,000×g (Beckman Coulter). The pure nuclear pellet was then resuspended in 2.5 ml of buffer A, diluted with 5 ml of buffer B, and layered onto a second 3.5-ml cushion of buffer B for centrifugation. Nuclei were resuspended and sonicated in NP40 buffer with protein inhibitors, and stored in -80℃.

Western blot analysis. Liver homogenate (30 μg of protein) or nucleus extract (10 μg of protein) was used for Western blot analysis as described in the General Material and Methods section. Antibodies used in this chapter are listed in Table 2.2.

3.4 Results

Knockout of SOD1 caused hypercholesterolemia and hypotriglyceridemia in mice. At 3 weeks of age, body weight of SOD1-/- was slightly less than that of WT ($P = 0.07$). Concentrations of plasma total cholesterol (TC) and non-esterified fatty acids (NEFA) in SOD1-/- mice was 59% and 76% higher as compared to WT mice, respectively ($P < 0.001$), while total triglyceride (TG) level was 42% lower ($P < 0.001$) (Table 3.1). Both genotypes had similar concentrations of plasma total protein. Therefore, the genotype difference in plasma lipids did not vary by the calculation based on either the total plasma volume or total plasma protein levels (Table 3.2). The

Table 3.1 Body weight, plasma lipids and protein concentrations of WT, SOD1+/- and SOD1-/- mice at 3 weeks of age[1]

	BW(g)	TC(mg/dl)	TG(mg/dl)	NEFA(mg/dl)	Protein (g/dl)	Ratio(TC/TG)
WT	10.75±1.13	90.09±4.00	31.69±2.39	9.52±0.56*	3.78±0.16	2.90±0.27
SOD1+/-	10.53±0.50	96.27±3.74	32.58±3.52	17.36±1.12	3.89±0.17	2.75±0.39
SOD1-/-	9.10±0.55	142.79±7.65*	18.36±2.04*	16.80±0.28	3.70±0.01	8.16±0.94*

[1]All mice (n = 5~10) were males and were fasted for 8 hours before being the experiment. Blood samples were collected by cardiac puncture into EDTA-coated tubes, and plasma was immediately separated. Total cholesterol, triglyceride and NEFA were measured by using kits from Wako Chemicals USA Inc. Values represent mean ± SE. *indicates the significant difference between genotypes ($P < 0.05$). BW, body weight; TC, total cholesterol; TG, total triglyceride; NEFA, non-esterified fatty acids.

Table 3.2. Body weight and plasma lipids concentrations of WT and SOD1-/- mice at 9 weeks of age[#]

	BW(g)	TC(mg/dl)	TG(mg/dl)	NEFA(mg/dl)
WT	24.92±0.95[a§]	176.68±9.63	121.93±18.43	23.01±2.43
SOD1+/-	23.16±0.70[ab]	175.13±7.73	118.37±14.95	22.96±1.53
SOD1-/-	21.64±1.46[b]	225.33±10.43*	48.61±8.38*	23.74±1.92

[#] All mice (n = 8~12) were males and were fasted for 8 hours before the experiment. Blood samples were collected by cardiac puncture into EDTA-coated tubes. Total cholesterol, triglyceride and NEFA were measured by using kits from Wako Chemicals USA Inc.

[§] Different letters indicate the significant difference between genotypes ($P < 0.05$). Values are mean ± SE. BW, body weight; TC, total cholesterol; TG, total triglyceride; NEFA, non-esterified fatty acids.

TC:TG ratio of SOD1-/- mice was 8.2 *vs.* 2.9 of WT ($P < 0.001$). There was no difference in body weight, TC and TG between WT and SOD1+/- mice, while plasma NEFA of SOD1-/- was higher than that of WT mice ($P < 0.01$). The increase in total plasma cholesterol was mainly due to increased high density lipoproteins (HDL), while the decreased total plasma triglyceride was due to (V)LDL in SOD1-/- mice, although some changes were found in other fractions (Figure 3.1 & 3.2). At 9 weeks of age, SOD1-/- was lighter as compared to WT ($P < 0.05$); SOD1-/- mice had 27% higher TC and 61% lower TG in plasma ($P < 0.05$) as compared to WT, (Table 3.2). There was no difference in plasma NEFA between genotypes. The TC:TG ratio of SOD1-/- was more than 3 times of WT, 4.51 vs. 1.38, respectively.

Abnormal lipid profile in tissues and organs in SOD1-/- mice. The organs or tissues weight values were expressed as a ratio according to body weight in 9 week old mice (Figure 3.3). Compared to WT, SOD1-/- mice had enlarged livers and spleens, and reduced kidney, testis and abdominal fat pad weights ($P < 0.05$). The concentrations of cholesterol in liver, heart and muscle were 52%, 23%, 15%, and 14% higher in SOD1-/- than in WT ($P < 0.05$). SOD1-/- mice also had 225%, 173%, 43%, 16% more triglyceride in testis, liver, heart and kidney, respectively ($P < 0.05$) (Figure 3.4, Figure 3.5), while 30% ($P < 0.05$) less triglyceride in spleen as compared to WT.

Elevated hepatic gene expression of cholesterol, but not fatty acids, synthetic pathways in SOD1-/-. Microarrays and real time PCR were used to further explore changes in gene expression in the livers of SOD1-/- mice. Microarray results showed that, at 9 wk, over 30 genes, which expressions were changed more than two folds, were related to lipid metabolism (Figure 3.6). Among these genes, 23 up-regulated genes were specifically related to cholesterol synthesis and fatty acids mobilization and oxidation, and 8 down-regulated genes, including Fasn, were related to fatty acid synthesis. The second largest group changed genes is related to oxidoreductase family.

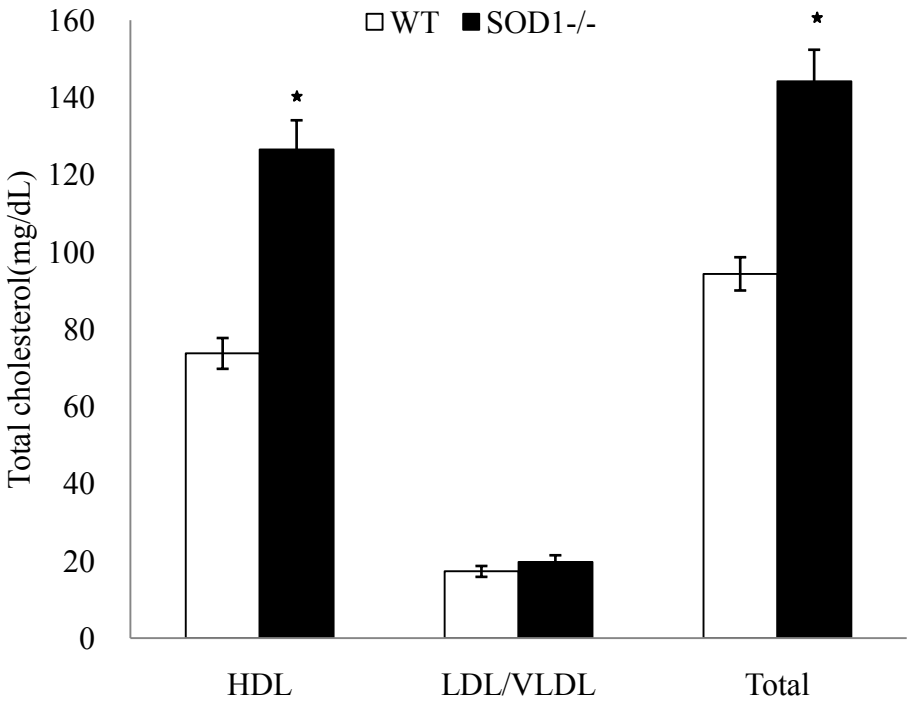

Figure 3.1. The distribution of cholesterol in HDL and (V)LDL lipoproteins in WT and SOD1-/- mice at 3 weeks of age. All mice (n = 6) were male and fasted for 8 hours before being sacrificed. Blood samples were collected by cardiac puncture into EDTA-coated tubes, and plasma was separated immediately. HDL and (V)LDL lipoproteins were analyzed by using a kit from Biovision Inc. Cholesterol of each fraction was measured by using kits from Wako Chemicals USA Inc. An asterisk indicates the significant difference between genotypes ($P < 0.05$). HDL, high density lipoprotein; (V)LDL, (Very) low density lipoprotein.

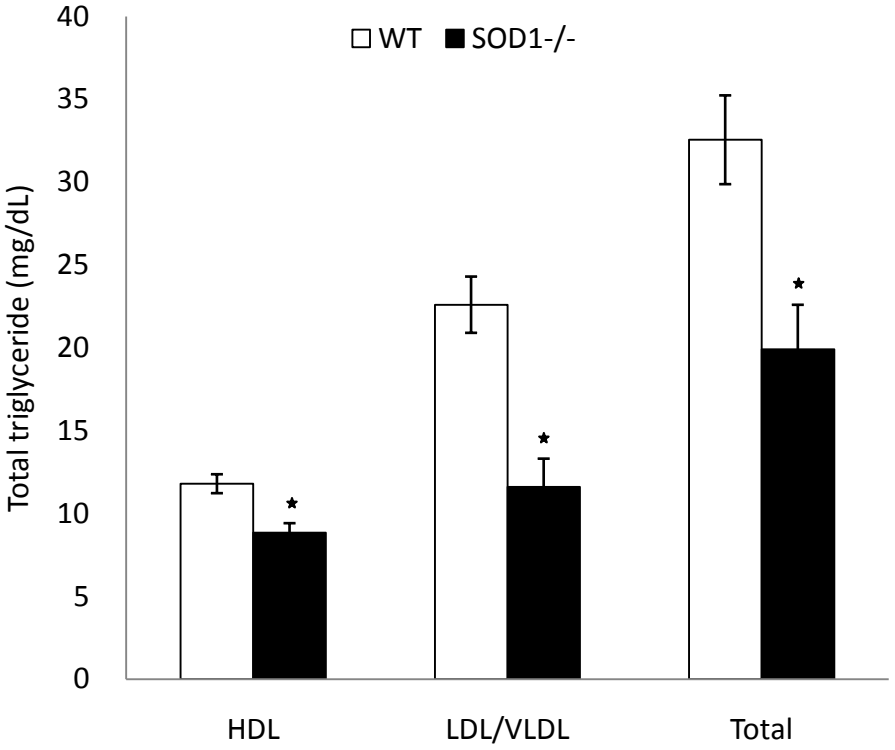

Figure 3.2. The distribution of triglyceride in HDL and (V)LDL lipoproteins in WT and SOD1-/- mice at 3 weeks of age. All mice (n = 6) were male and fasted for 8 hours before being sacrificed. Blood samples were collected by cardiac puncture into EDTA-coated tubes, and plasma was separated immediately. HDL and (V)LDL lipoproteins were analyzed by using a kit from Biovision Inc. Triglyceride of each fraction was measured by using a kit from Wako Chemicals USA Inc. An asterisk indicates the significant difference between genotypes ($P < 0.05$).

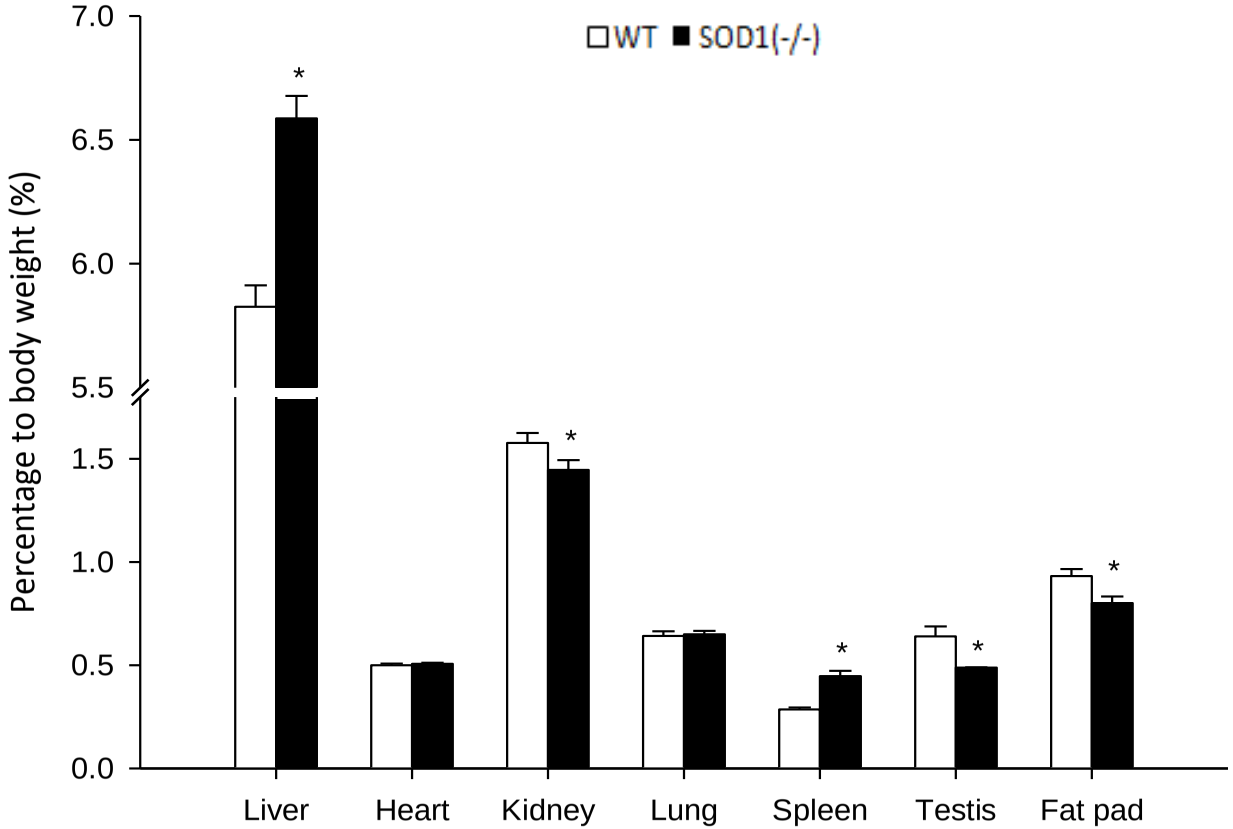

Figure 3.3. The percentage of tissue and organ weight to body weight of WT and SOD1-/- mice at 9 weeks of age. Fresh tissues and organs were collected from 9 week old mice fed normal diet and weighed immediately after dissection. All mice (n = 6) were male and were fasted for 8 hours before the experiment. *indicates the significant difference between genotypes at $P<0.05$ level.

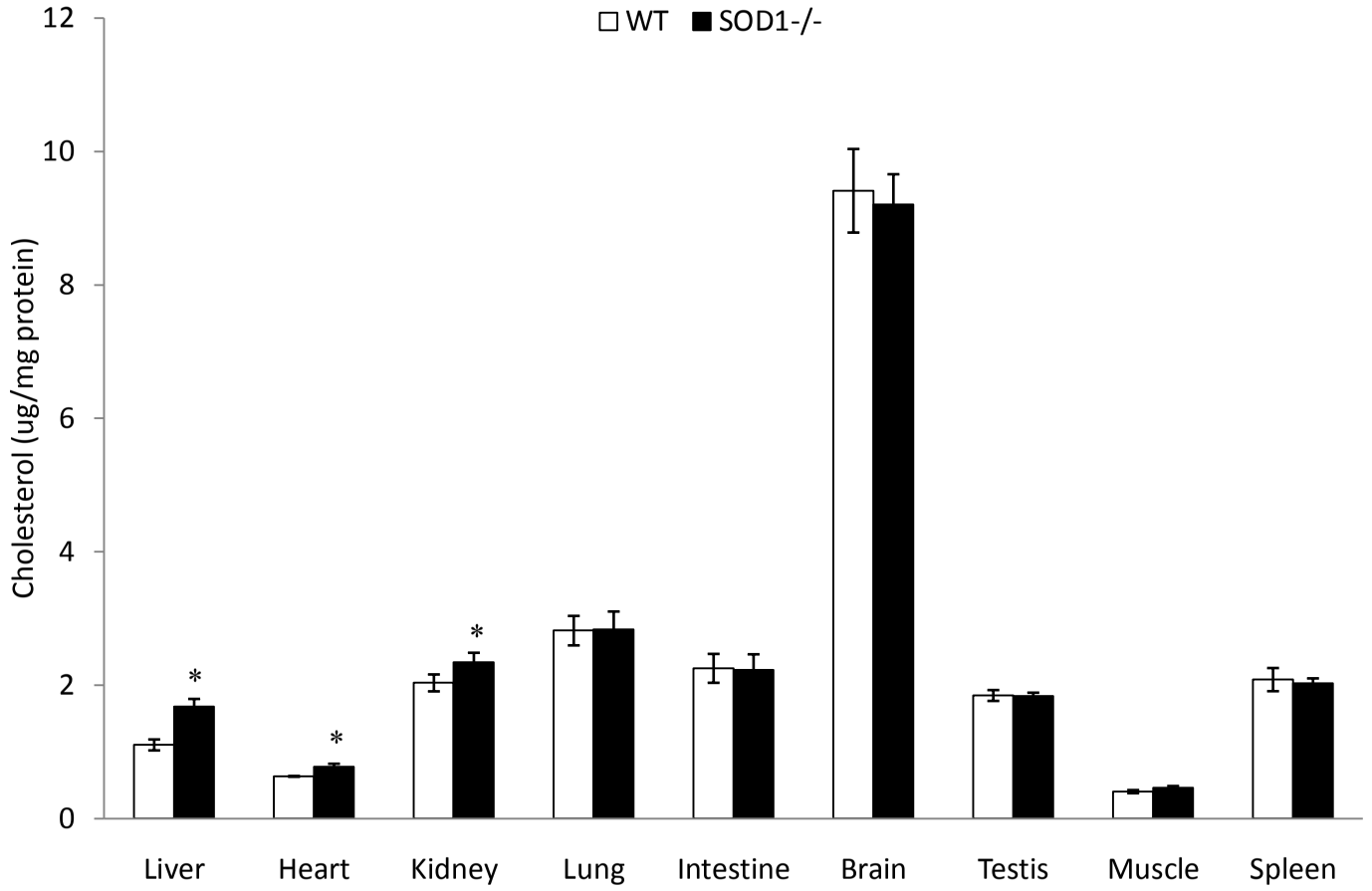

Figure 3.4. The concentrations of total cholesterol in tissues and organs. Tissues and organs were collected from 9 week old mice fed normal diet and total lipids were extracted by using Folch method. Cholesterol was measured by using a kit from Wako Chemicals USA Inc. All mice (n = 6) were males and were fasted for 8 hours before the experiment. The concentrations are expressed based on the protein concentrations. *indicates the significant difference between genotypes at $P<0.05$ level.

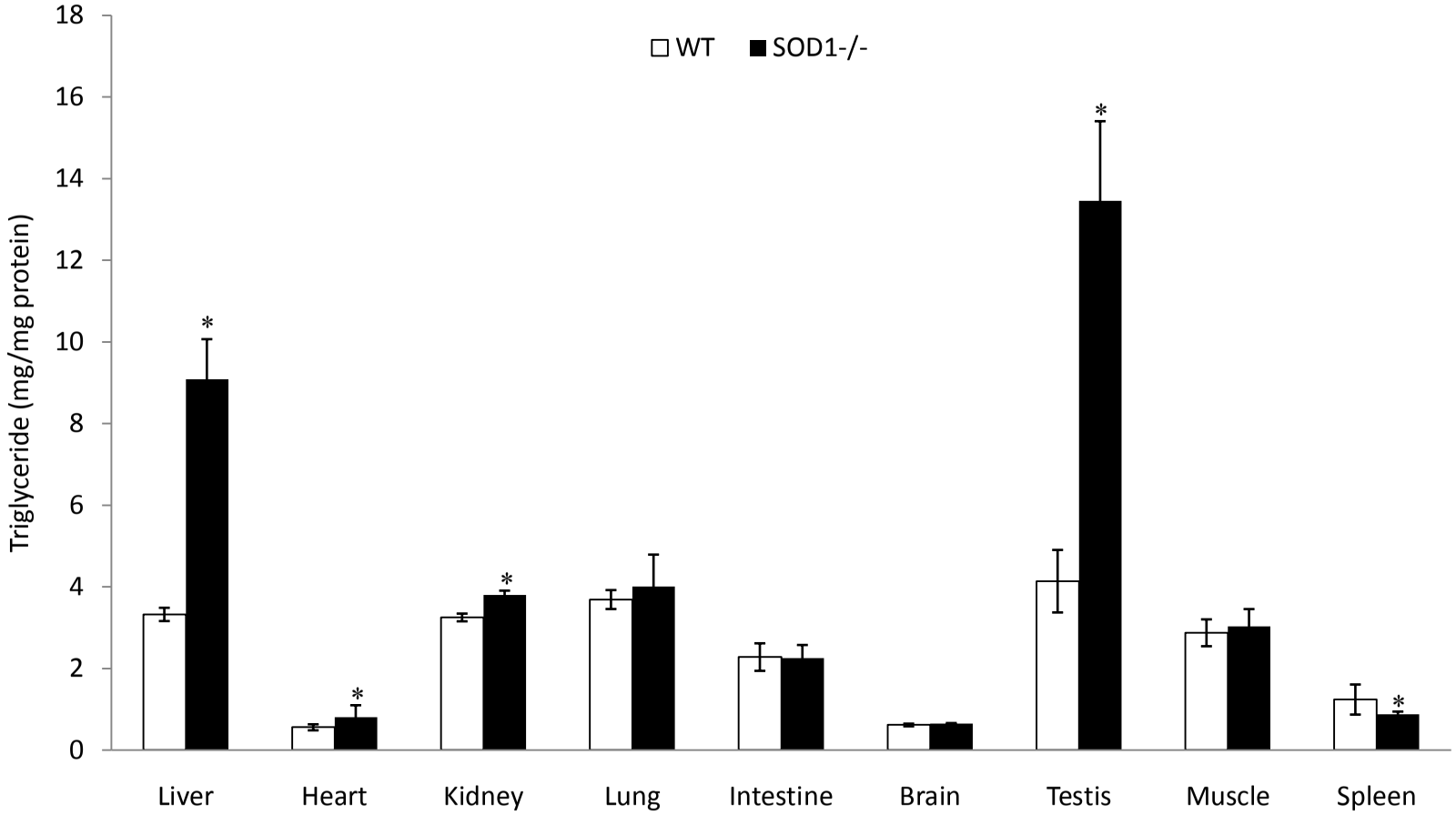

Figure 3.5. The concentrations of total triglyceride in tissues and organs. Tissues and organs were collected from 9 week old mice fed normal diet and total lipids were extracted by using Folch method. Triglyceride was measured by using a kit from Wako Chemicals USA Inc. All mice (n = 6) were male and fasted for 8 hours before being sacrificed. The concentrations are expressed based on the protein concentrations. *indicates the significant difference between genotypes at $P<0.05$ level.

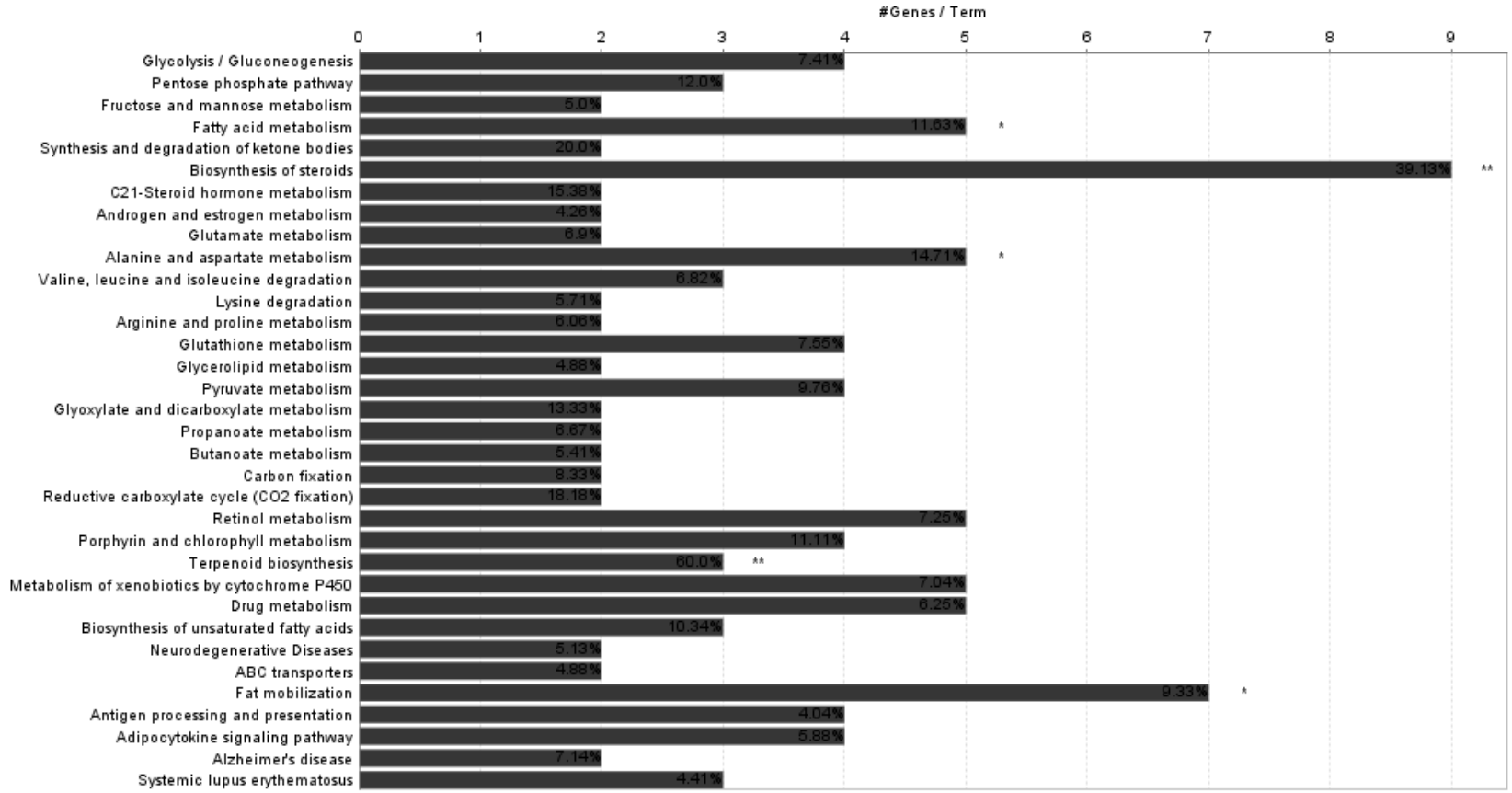

Figure 3.6. Functional clustering analysis of hepatic genes affected by the knockout of SOD1 in mice. The bars represent the number of the genes from the analyzed cluster found to be associated with the term, and the label displayed on the bars is the percentage of found genes compared to all the genes associated with the term. Term significance information (P Value) included in the chart was calculated with a two-sided minimal-likely-hood test on the hypergeometric distribution, equivalent to a classical Fisher's exact test (134, 135) **: if the term/group is over significant, P value < 0.001; *:if 0.001 <=P value < 0.05.

Real time PCR was used to confirm these same changes. As indicated in Figure 3.7, there was a significant increase of mRNA levels of gene controlling cholesterol synthesis, including HMG-CoA synthase (2.9-fold), HMG-CoA reductase (3.1-fold), Farnesyl diphosphate synthase (4.6-fold), qualene synthase (4.1-fold), squalene epodase (4.7-fold), and lanosterol synthase (4.2-fold) in the liver of 9 week old SOD1-/- mice. Similar changes were also observed in 3 week old mice (Figure 3.8). Squalene epoxidase was the most changed gene of cholesterol synthetic pathway and was increased by 2.9 times in SOD1-/- mice. Consistent with the change at mRNA level, the amount of HMG-CoA reductase protein was higher in SOD1-/- mice than WT mice as shown in Figure 3.11. In addition, there were a 20% decrease of Fasn mRNA and a 60% increase of lipoprotein lipase mRNA in the liver of SOD1-/- mice ($P < 0.05$) as compared to WT mice.

Increased fatty acid mobilization and oxidation in SOD1-/- mice. Our previous data indicated the increased fatty acid mobilization and oxidation in SOD1-/- mice, therefore activities of a few important enzymes were assessed. The activity of short-chain 3-hydroxyacyl-CoA dehydrogenase (SCHAD) was significantly higher in the mitochondria of SOD1-/- than that of WT mice ($P < 0.001$) (Figure 3.9), thus pointing on possible increased fatty acid oxidation in mitochondria. Moreover, in SOD1-/- mice, the activity of acetoacetyl CoA thiolase was 40% higher in mitochondria, though 40% lower in cytosol, thus totally not different from WT (Figure 3.10), and consistent with the increased fatty acid oxidation. The concentration of plasma beta-hydroxybutyrate after 8 hours fasting in SOD1-/- was 64% higher than in WT ($P < 0.001$) (Figure 3.11), proving higher fatty acid oxidation rate in SOD1-/- mice.

Increased mature SREBP2 in nuclei may be responsible for the new metabolic pattern of SOD1-/- mice. As shown in Figure 3.12, SOD1-/- mice expressed less

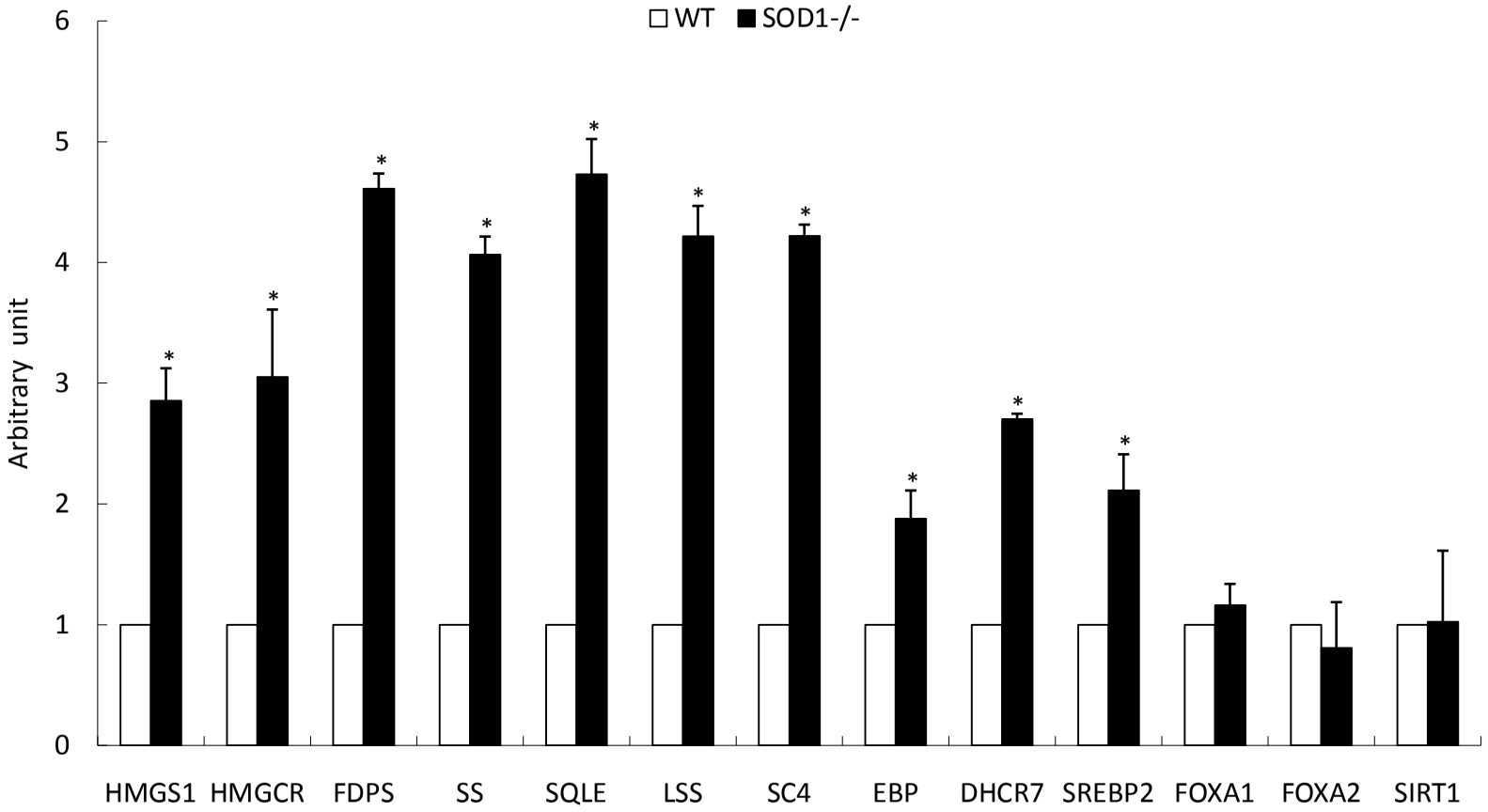

Figure 3.7. Messenger RNA levels of genes related to lipids metabolism in liver of SOD1-/- mice at 9 weeks of age. Total mRNA was extracted from the livers of 9-week-old male mice (n = 4 per genotype) fed normal diet. Real time PCR was performed with specific primers as listed in Table 2.3. The threshold cycle (Ct) was determined for each sample. mRNA expression levels were normalized to 18S rRNA concentration. The values in above figure are presented as $2^{\Delta\Delta Ct}$.($\Delta\Delta Ct = (Ct_{\text{gene of interested of WT}} - Ct_{\text{18s of WT}}) - (Ct_{\text{gene of interested of ko}} - Ct_{\text{18s of ko}})$). * indicates the significant difference between genotypes at $P<0.05$ level.

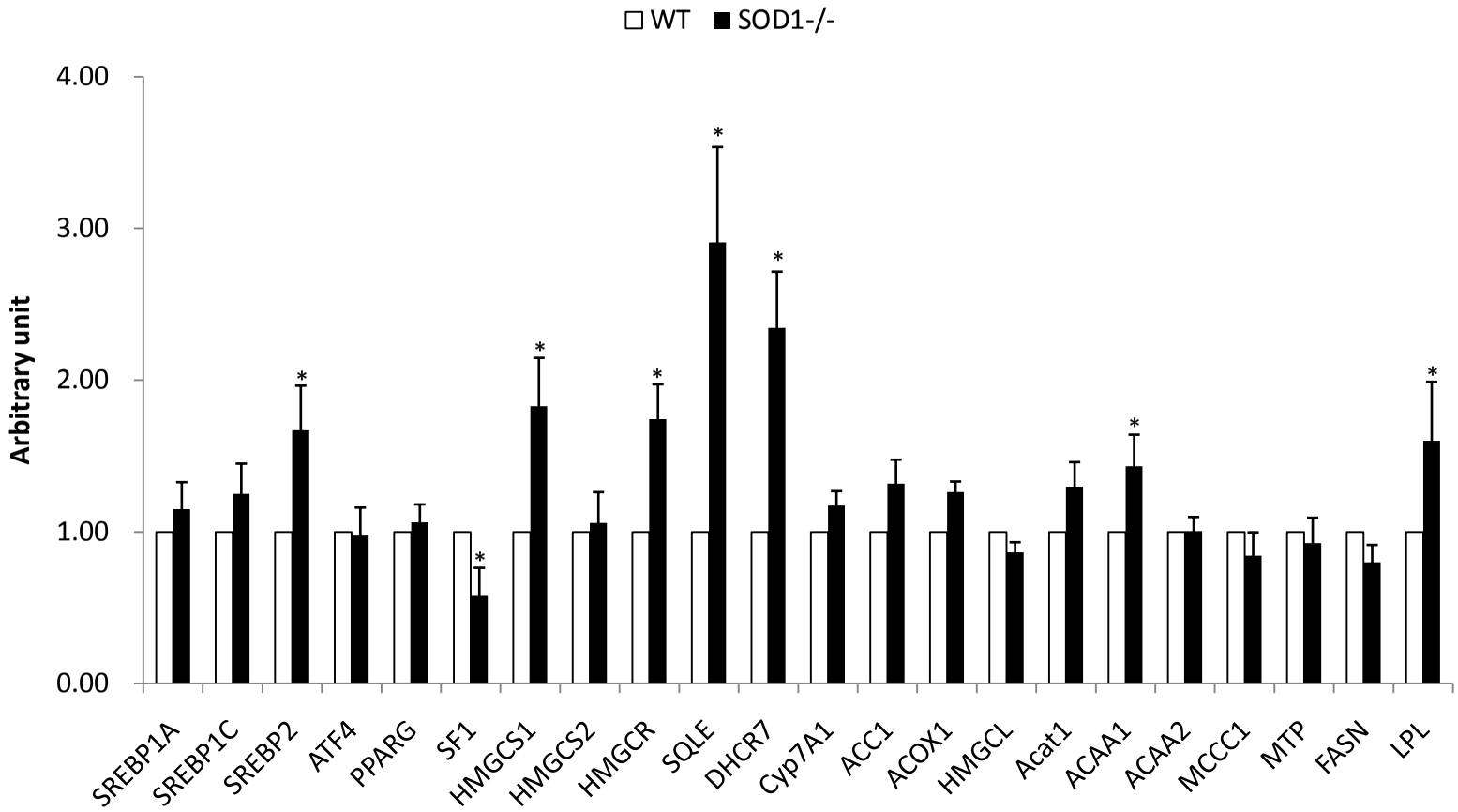

Figure 3.8. Messenger RNA levels of genes related to lipids metabolism in liver of SOD1-/- mice at 3 weeks of age. Total mRNA was extracted from the livers of 3-week-old male mice (n = 4 per genotype) fed normal diet. Real time PCR was performed with specific primers as listed in Table 2.3. The threshold cycle (Ct) was determined for each sample. mRNA expression levels were normalized to 18S rRNA concentration. The values in above figure are presented as $2^{\Delta\Delta Ct}$.($\Delta\Delta$ Ct= ($Ct_{\text{gene of interested of WT}}$-$Ct_{\text{18s of WT}}$)- ($Ct_{\text{gene of interested of ko}}$-$Ct_{\text{18s of ko}}$)). * indicates the significant difference between genotypes at $P<0.05$ level.

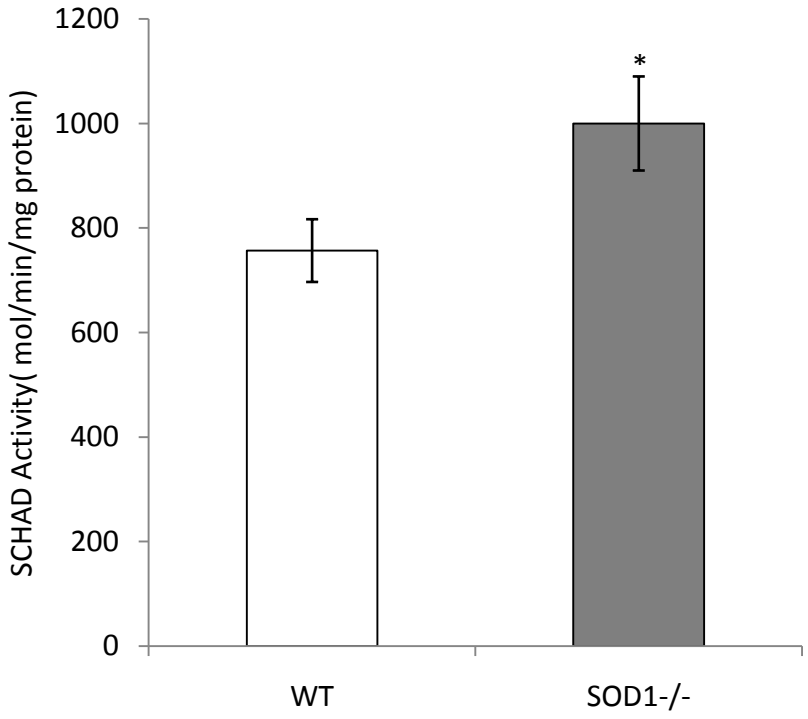

Figure 3.9. Effect of SOD1 knockout on hepatic SCHAD activity. Mice (n = 5, male) were sacrificed at 9 weeks of age after being fasted for 8 hours. Mitochondria were isolated from the fresh liver homogenates by centrifugation in sucrose buffer as described previously. The SCHAD activity was measured as stated in *Experiment design.* *indicates the significant difference between genotypes ($P < 0.05$).

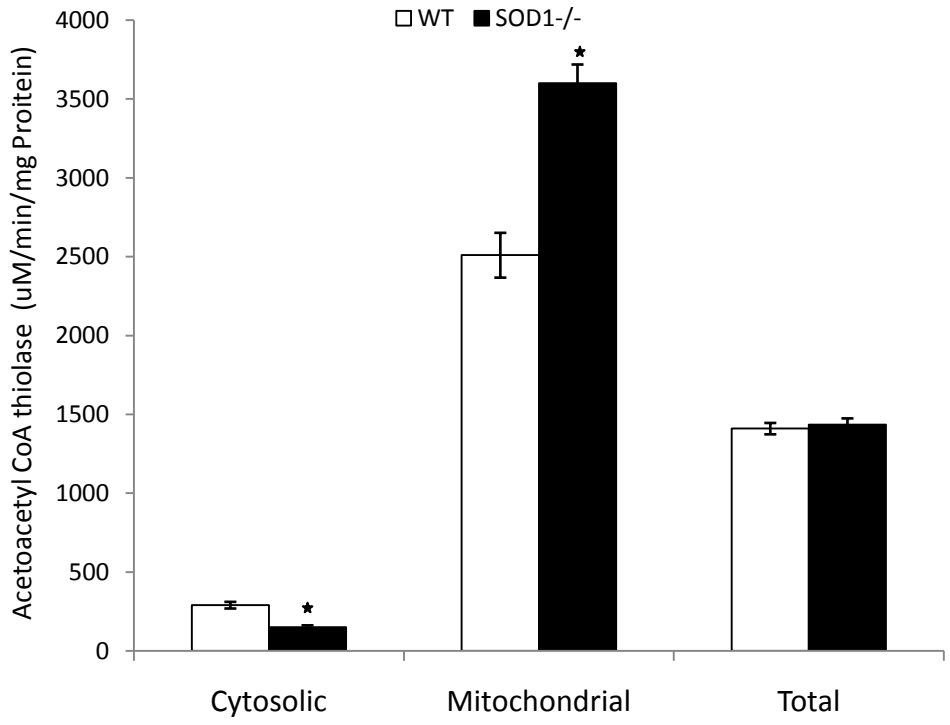

Figure 3.10. Effect of SOD1 knockout on hepatic acetoacetyl CoA thiolase activity. Mice (n = 5, male) were sacrificed at 9 weeks of age after being fasted for 8 hours. Mitochondrial and cytosolic fractions were prepared from the fresh liver homogenates by centrifugation in sucrose buffer as described previously. Acetoacetyl CoA thiolase activity was measured as stated in *Experiment design.* *indicates the significant difference between genotypes ($P < 0.001$).

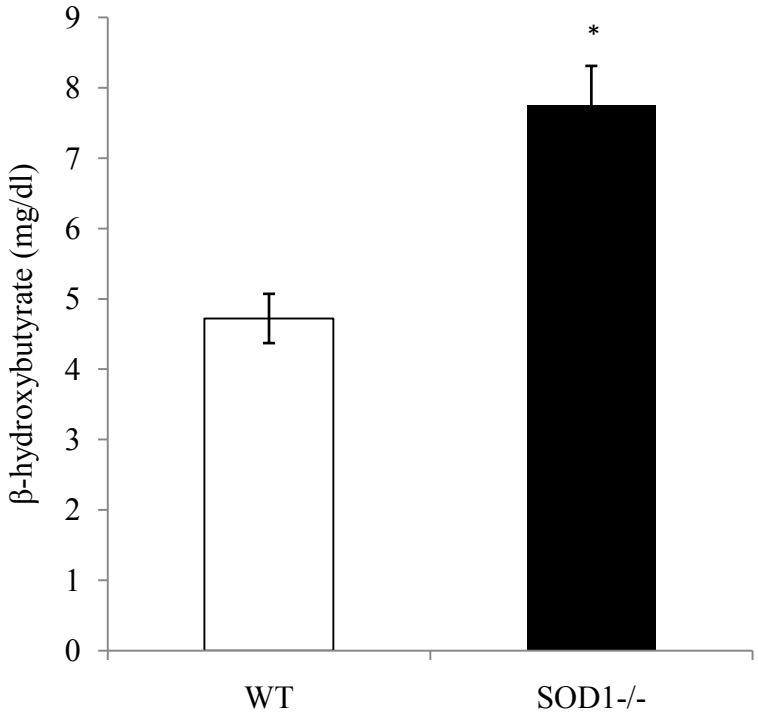

Figure 3.11. Concentrations of plasma β-hydroxybutyrate in WT and SOD1-/- mice. Mice (n = 5, male) were sacrificed at 9 weeks of age after being fasted for 8 hours. Blood samples were collected by cardiac puncture into EDTA-coated tubes, and plasma was immediately separated after collection. The concentrations of β-hydroxybutyrate were measured as described previously. *indicates the significant difference between genotypes ($P < 0.001$).

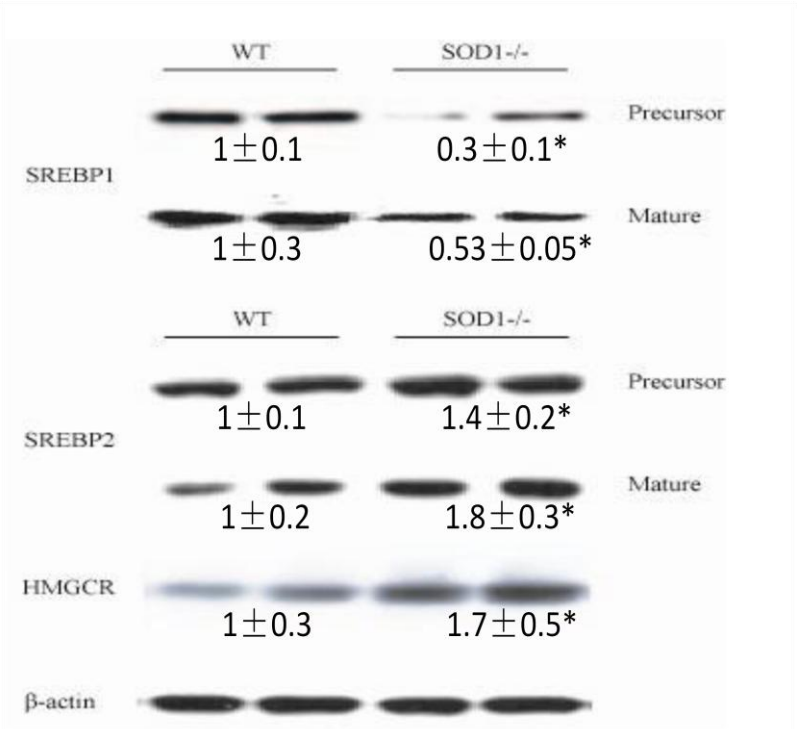

Figure 3.12. Western blot analysis of SREBP1, SREBP2 and HMG-CoA reductase in livers of WT and SOD1-/- mice. Liver samples were collected from male mice (n = 5 per genotype) at the age of 3 weeks. Mice were fasted for 6 hours before killing. Total protein was extracted from livers as described in the text.

SREBP1 protein, but much more SREBP2, in both the precursor and the mature proteins, when whole-cell lysates were subject to analysis. To further explore SREBPs localization, nuclei fractions were used to test the presence of SREBPs. Indeed, mature SREBP2 in nuclei of SOD1-/- was about two times of WT, as indicated by Figure 3.13.

3.5 Discussion

The most interesting finding from this study is that the knockout of SOD1 causes hypercholesterolemia and hypotriglyceridemia in mice. Compared with the WT mice, SOD1-/- mice showed increased level of *de novo* synthesized cholesterol in plasma, tissues and organs. The elevated cholesterol level correlated with increased expression of cholesterol synthetic pathway genes, increased mobilization, oxidation and reduced synthesis of fatty acids. Deletion of SOD1 leads to the energy usage for excessive cholesterol synthesis rather than fat accumulation. We hypothesize the priority of cholesterol synthesis, as hormones precursor which essential for survival under oxidative stress because of SOD1 deficiency, and as new building blocks for the cell membranes repair, increasingly damaged because of SOD1 absence. It is worthwhile to mention another metabolic symptom caused by over expression of cellular antioxidant enzyme, glutathione peroxidase 1, which results in obesity and affected glucose metabolism, discovered in our lab (131).

Superoxide dismutase is responsible for the clearance of toxic superoxide, which is also a signaling agent (42). It has been reported that knockout of either cellular SOD1 or mitochondrial SOD2 increases triglyceride accumulation in liver and heart (119-121), which is consistent with our results. However, Uchiyama et al. (121) did not observed the lipid change in the liver of SOD2-/- mice and in the plasma of SOD1-/- mice, which had been found by others (119, 120). The difference may

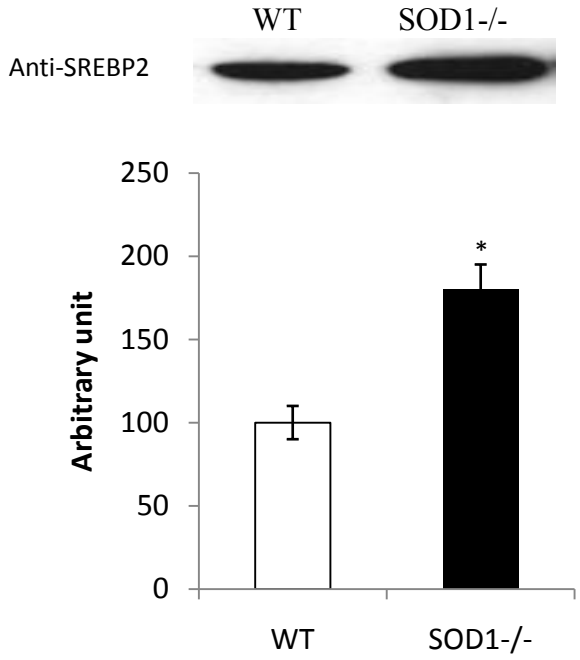

Figure 3.13. Western blot analysis of nuclear SREBP2 in livers of WT and SOD1-/- mice. Liver samples were collected from male mice (n = 4 per genotype) at the age of 9 weeks. Mice were fasted for 8 hours before killing. Nuclei were isolated by centrifugation in sucrose buffer. The density was measured by software. *indicates the significant difference between genotypes ($P < 0.05$).

depend on a different genetic background, in which other antioxidant agents might compensate for the loss of target gene. Together, it is clear that SODs could affect lipid and energy metabolism as indicated by majority of relevant studies.

In this study, the symptom of severe dyslipidemia is very striking and indicates a role of SOD1 in lipid and energy metabolism, directly or indirectly. Most interestingly, the concentrations of cholesterol and triglyceride change in opposite directions in SOD1-/- mice at the different age. This phenomenon is a rare case in mammals. The TC:TG ratio is maintained in a certain range to meet the needs of extra hepatic tissues and organs for lipids. The irregular profile of plasma lipids indicates the abnormal distribution of lipids among tissues and organs (136). Elevated plasma cholesterol and triglyceride can contribute to many forms of disease, most notably cardiovascular disease. The well-known cause of hypercholesterolemia is the compromised ability of clearance of LDL lipoprotein in blood. For example, mutations of LDL receptor, APOB and PCSK9, which interrupt the uptake of plasma LDL, results in familial hypercholesterolemia (61-64). Hypotriglyceridemia has been found in patients with acute exercise, autoimmune disease, and subjects consuming conjugated linoleic acid (CLA) contained in high fat diet (137-139).

Endogenous source was responsible for the increased cholesterol in plasma, liver and other tissues in SOD1-/- mice, because no dietary cholesterol was consumed by these mice, while the cholesterol synthetic pathway was consistently activated as indicated by increased mRNA and protein levels of related genes. Under the normal conditions, the cellular cholesterol synthesis is strictly regulated based on the cellular cholesterol level which is sensed by proteins located on the ER membrane (77, 78, 122). The well-known SREBP2 is the master regulator of cholesterol synthesis genes, and is activated and translocated into nucleus as a part of transcription machinery when the cell is depleted of cholesterol. When the cell is replete with cholesterol, the process of

translocation is blocked by the interaction of Scap/Insig (70, 71, 73, 75, 76, 127). The mature SREBP2 in nucleus is degraded rapidly by the ubiquitin-proteasome pathway (129). Based on the consistent activation of cholesterol synthetic pathway and the increased premature and mature SREBP2 protein level, the feed-back regulation mechanism appears to be dysfunctional in SOD1-/- model. It is possible that this pathway is disrupted at the step of translocation of SREBP2, which normally takes place only when cells are depleted of cholesterol. ER membrane is the headquarters for sensing cholesterol and housing SREBP2 in cells, and it is also a factory for assembling and folding proteins (70, 71, 140). It has been shown that the accumulation of aberrantly folded protein or ROS in ER leads to ER stress (141-143). Interestingly, SOD1 is required for tolerance of ER stress induced by superoxide accumulation in *Saccharomyces cerevisiae* (144). Further, Ye et al. (2000) reported SREBPs are cleaved by proteases induced by ER stress (145). Therefore, the knockout of SOD1 may lead to the ER stress induced by accumulated superoxide, and, then, ER stress promotes the cleavage of SREBP2 which is translocated to nucleus and initiates the transcription of its target genes.

In addition to the increased level of cholesterol, knockout of SOD1 caused the reduction of plasma triglyceride, increased plasma NEFA and ketone bodies. And the genes coding enzymes for catalyzing these metabolites were demonstrated to have corresponding changes at mRNA levels and functional activities as well. Fasn is the key enzyme for fatty acid synthesis, which catalyzes the conversion of acetyl-CoA and malonyl-CoA, in the presence of NADPH, into long-chain saturated fatty acids (146). Thus, the reduced level of Fasn mRNA may indicate the reduced synthesis of fatty acid in SOD1-/- mice. Lipoprotein lipase is an enzyme that hydrolyzes lipids in lipoproteins, such as those found in chylomicrons and VLDL, into three free fatty acids and one glycerol molecule (147). Compared to the WT mice, knockout of

SOD1 significantly increased the LPL mRNA level. This provides a strong evidence for the reduced plasma triglyceride and increased plasma NEFA, as it was reported by Merkel, et al., (1998) (148). Consequently, largely increased NEFA raise the ß-oxidation of fatty acid and the production of ketone bodies. Short-chain 3-hydroxyacyl-CoA dehydrogenases (SCHAD) resides in the mitochondrial matrix and is involved in the mitochondrial ß-oxidation (149). Mitochondrial acetoacetyl-CoA thiolase (commonly called ß-Ketothiolase) is an enzyme with a dual function in metabolism, which acts in the breakdown of acetoacetyl-CoA generated from fatty acid oxidation and regulates production of ketone bodies(150), while cytosolic acetoacetyl-CoA thiolase is likely to be involved in the pathway of steroid biosynthesis, catalyzing the synthesis of cytoplasmic acetoacetyl-CoA for substrate conversion into 3-hydroxy-3-methyglutaryl-CoA (151). All of above reactions are reversible, and the exact functions of both enzymes are still uncertain as the outcome of deficiency of both is similarly ketosis (152, 153). The changes of these activities in SOD1-/- mice indicate increased fatty acid oxidation and ketone bodies production, while the mitochondria is one of the targets that are mostly affected by knockout of SOD1. It is clear that the knockout of SOD1 increases ROS production and has a remarkable impact on the mitochondrial function (9, 154, 155). Mutated human SOD1 causes a dysfunction of oxidative phosphorylation in mitochondria of transgenic mice (154). To compensate the functional loss and meet the normal demand of ATP, it is possible that cell accelerates fatty acid oxidation to increase the energy production in SOD1-/- mice. PGC1 and PPARγ are important regulators of mitochondria biogenesis, which are induced by ROS and also control the antioxidant system in cell (156, 157). It is of an interest that neither was affected by the knockout of SOD1 at mRNA level.

The opposite change of cholesterol and fatty acids in SOD1-/- mice intrigues the management strategy of energy balance under the unfavorable conditions. SREBP

pathway responds to the oxygen level and regulates sterol synthesis under hypoxia in fission yeast (158). The activation of SREBP offers the advantage for survival as sterols are the more important precursors of signal agents than energy molecules. It is possible that cholesterol synthesis is activated to ensure the adequate substrate for hormones synthesis when cells lose the full ability to cope with superoxide and endure the oxidative stress. The biosynthetic pathways of cholesterol and fatty acids share the same substrate acetyl-CoA in cytosol, but are governed, at least, by the two close though different transcriptional factors, SREBP1c and SREBP2 (159). The functional change of one of them drastically alters the ratio of cholesterol and fatty acids in liver and plasma (160). Therefore, these proteins dictate the direction of energy flow for the synthesis of either cholesterol or fatty acids, and the proper SREBPs ratio determines the balance of two lipids. Compared with WT, SOD1-/- mice had significantly higher SREBP2 and lower SREBP1 level, as indicated by Western blot analysis. This strongly suggests that these two proteins are altered by the deficiency of SOD1, directly or indirectly, and these changes are responsible to some extent for the increased cholesterol and decreased fatty acid biosynthesis. In addition to the fulfilling of energy requirement, increased beta oxidation of fatty acids may be considered as a secondary response to the activated biosynthesis of cholesterol, providing adequate acetyl-CoA and ATP, while ketone bodies, as by-products, are formed in the altered metabolic reaction.

In summary, this study demonstrates that the important role of SOD1 in lipids and energy metabolism has multiple physiological and potentially pharmacological implications. First, antioxidant enzyme SOD1 affects de novo cholesterol synthesis, while its deficiency causes hypercholesterolemia. Our data suggest the SOD1 related pathway is a possible *in vivo* target for regulation of plasma cholesterol, as in vitro studies suggest SOD1 inhibits the cholesterol synthesis (161, 162). Second, SOD1 is

important in maintaining the normal function of mitochondria, which is the powerhouse of the cell. It is most likely that increased fatty acid oxidation and ketones formation result from the functional loss of SOD1, which reminds us of the importance of SOD1 in the treatment of mitochondrial related diseases and management of mitochondrial biogenesis. Third, it may suggest the new strategy to manage the energy balance by SOD1 or other antioxidant enzymes, such as GPX1 (131). SREBPs mediate the metabolic changes induced by SOD1 deficiency to some extent. Cholesterol, synthesized from acetyl-CoA which is also substrate for fatty acid synthesis, could be used as a carrier to excrete energy in feces, and it may shed light on the treatment of obesity. Finally, the phenotype of the SOD1-/- mice, including hypercholesterolemia, hypotriglyceridemia, liver steatosis, and ketosis, offers a desirable model for the study of links among antioxidant balance, lipids metabolism and obesity.

CHAPTER FOUR

EFFECT OF HIGH FAT DIET ON THE LIPID METABOLSIM IN COPPER, ZINC-SUPEROXIDE DISMUTASE KNOCKOUT MICE

4.1 Abstract

Our previous study showed that the knockout of Cu, Zn superoxide dismutase (SOD1) caused disorders in lipid and energy metabolism. Diet is an important factor which could influence the metabolism of lipid and energy *in vivo*. We hypothesized that the metabolic changes induced by the knockout of SOD1 depend on the dietary energy, and can be reversed by high fat diet. Three-week-old WT and SOD1-/- male mice were fed the normal (11% energy by fat) or high fat diet (58% energy by fat) for 6 weeks. After the feeding period, we examined metabolic changes and signaling proteins. Interestingly, we found that high fat diet reduced body weight of SOD1-/- mice by 17% and plasma (V)LDL triglyceride by 15% although the plasma total cholesterol and total triglyceride, and fecal cholesterol in SOD1-/- mice were not significantly affected. High fat diet significantly increased nuclear SREBP1 and SREBP2 proteins in both genotypes but did not reverse the changes induced by the knockout of SOD1 in mice fed normal diet. Therefore, the metabolic changes in SOD1-/- mice did not depend on the dietary energy source. A high fat diet was not able to recover the metabolic symptom induced by the knockout of SOD1.

4.2 Introduction

Obesity is becoming a serious heath problem worldwide. In 2005, the World Health Organization reported that more than 400 million adults worldwide were obese (163). In industrialized countries overeating of high energy-containing food leads to the excess accumulation of body fat, causing metabolic syndrome-related diseases. In

obese individuals the elevated level of lipids promotes excessive production of ROS, and systemic oxidative stress, which is considered an important pathogenic mechanism of obesity-associated metabolic syndrome (164-167). Antioxidant enzymes, as a major part of the antioxidant system, protect cells against the damage of ROS. However, the roles of antioxidant enzymes in lipid metabolism and in the development of obesity largely remain unknown.

Energy homeostasis is achieved when anabolic and catabolic processes are in balance over long intervals (168). Obesity, a result of the continuous positive balance of energy metabolism, is characterized by exceedingly increased mass of adipose tissue. Adipose tissue has been appreciated as the energy warehouse to accumulate triglyceride in hypertrophied adipocytes during periods of caloric excess, but to release these lipids for use by the organism during periods of caloric restriction (169). Beyond a warehouse of energy storage, adipose tissue is also an important endocrine organ, which secrets a variety of bioactive peptides, called adipocytokines (170). The dysfunction of adipocytes and adipose tissue belongs to the primary defects in obesity, which is caused by the interaction of genetic and environmental factors (171). Adipocytes and hepatocytes serve as the primary sites for fatty acids synthesis, which are further transported and incorporated into triglyceride in adipocytes (172). This process is under the regulation of various transcriptional factors, including SREBPs, AMPK, PPAR gamma and XBP (173-176).

Many diseases, particularly atherosclerotic cardiovascular disease, type 2 diabetes and osteoarthritis, are associated with obesity, and dyslipidemia is one of the major changes of obesity induced metabolic syndrome (177, 178). Obese persons release increased amounts of fatty acid into the circulation, which can be easily taken up by the tissues and oxidized in mitochondria (179). The mitochondrion is the major place where ROS are formed during the process of respiration (180). The production of ROS

is increased when the concentration of circulating fatty acids rises (181, 182). It has been shown that the levels of ROS is increased in fatty liver, plasma and adipose tissue, along with increased antioxidant enzymes activities in obese subjects (164, 183). Adipocytokines, such as tumor necrosis factor-α and angiotensinogen, secreted from adipose tissue are also able to increase the ROS production and related to the oxidative stress (184). More than an outcome of obesity, the increased ROS also could affect the physiological reactions. ROS have been proved to act as intracellular second messengers, which lead to induction of unique signal transduction pathways (185). Production of ROS is increased selectively in adipose tissue of obese mice, accompanied by augmented expression of NADPH oxidase and decreased expression of antioxidative enzymes. Moreover, NADPH oxidase inhibitor reduces ROS production in adipose tissue, attenuates the dysregulation of adipocytokines, and improves diabetic condition, hyperlipidemia, and hepatic steatosis (164). Oxidative stress impairs glucose uptake in muscle and fat, and decreases insulin secretion from pancreatic β cells (186, 187). ROS derived from NADPH oxidase in vascular smooth muscle cells are important to vascular remodeling (24). During hypoxia, ROS act as signaling elements in human umbilical vein endothelial cells, regulating secretion of the proinflammatory cytokines that lead to alterations of endothelial permeability (188).

The antioxidant system, involving antioxidant enzymes and small chemicals, prevents the accumulation of ROS. Cu, Zn superoxide dismutase (SOD1) is an important cellular enzyme, catalyzing the dismutation of superoxide to hydrogen peroxide, which is further cleared by glutathione peroxidase 1 (GPX1) or catalase. Lack of SOD1 significantly impairs the cellular antioxidant ability and promotes oxidative stress (5, 155, 189). The expressions of these antioxidant genes are regulated by ROS mediated by NF-kB, AP-1, AP-2 and Sp1, as well as C/EBP (see review by Miao,

2009) (190). Recently, numbers of studies show that PGC1 and Sirt1, which control mitochondrial biosynthesis and lipid metabolism, also regulate the expression of antioxidant enzymes, including SOD1, SOD2 and GPX1 (191-194). Furthermore, over expression of GPX1 causes obesity and related metabolic syndrome in mice, while knockout of GPX1 extremely reduces plasma triglyceride in mice fed a high fat diet for a prolonged period (131, 195). It has been reported that knockout of either cellular SOD1 or mitochondrial SOD2 increases triglyceride accumulation in liver and heart in mice (119-121). Taken together, these results strongly suggest that antioxidant enzymes play regulatory roles in lipid and energy metabolism.

Our previous results showed that knockout of SOD1 significantly activated the cholesterol synthetic pathway with outcome of hypercholesterolemia. At the same time fat synthesis was suppressed while its mobilization and oxidation were increased in mice. There processes were mediated at least in part by SREBPs. Considering that dietary energy could affect the energy and lipid metabolism, we hypothesized that high fat diet might reverse the observed phenotype. This study was conducted to test the effect of high fat (coconut butter) diet on the body weight, blood lipids, and signal proteins in WT and SOD1-/- mice. Interestingly, high fat diet did not ameliorate the loss of body weight and dyslipidemia caused by the knockout of SOD1 although signaling proteins, SREBP1 and SREBP2, were remarkably improved.

4.3 Experimental Design

Chemicals and antibodies. All chemicals were purchased from Sigma Chemical Co. (St. Louis, MO) unless otherwise indicated. Reagents for cholesterol, triglyceride and non-esterified fatty acids were from Wako Chemicals USA, Inc. (Richmond ,VA).

Animals and diets. The SOD1 knockout (SOD1-/-) and wild-type (WT) mice, generated from 129SVJ x C57BL/6 strain, were generously provided by Y. S. Ho of

Wayne State University, Michigan (116). After weaning at three weeks of age, male mice were divided into two groups and were fed either a high-fat or a normal diet for 6 weeks. The content of normal diet is listed in Table 2.1. Coconut butter was used as the energy source of the high fat diet. On caloric basis, the high-fat diet consisted of 58% energy from fat, 27% from carbohydrate, and 15% from protein, whereas the normal diet contained 11% from fat, 74% from carbohydrate, and 15% from protein.

Plasma and fecal lipid measurements. All mice were sacrificed at 9 weeks of age after an 8-hour-fast. Tissues and organs were collected and frozen immediately. Total plasma cholesterol (TC), triglyceride (TG) and non-esterified fatty acids (NEFA) levels were measured using commercially available kits (Wako Pure Chemical Industries). Total cholesterol and triglyceride in HDL and (V)LDL lipoproteins were measured by using a kit from Biovision Inc. (Mountain View, CA). Fecal cholesterol was extracted by using Folch method from dried feces and measured by the method stated above.

Nuclei isolation. Nuclei were isolated by Dounce homogenization and sucrose gradient centrifugation as described previously.

Western blot. Nuclei extract (10 μg of protein) was used for Western blot analysis as described in the General Material and Methods. Antibodies used in this chapter were listed in Table 2.2.

4.4 Results

High fat diet did not improve body weight of SOD1-/- mice. Compared with normal diet, high fat diet did not improve the body weight of SOD1-/- mice. SOD1-/- mice had 21% less body weight than WT, 17.99±1.11 vs. 22.92±0.45 grams ($P < 0.05$), respectively, after feeding high fat diet for 3 weeks (Table 4.1). The difference between genotypes was increased by 38% after an additional 3 weeks' feeding with

Table 4.1. Comparison of body weight (g) of WT, SOD1+/- and SOD1-/- mice fed normal diet and high fat diet *

	Normal diet		High fat diet	
	6 Wk	9 Wk	6 Wk	9 Wk
WT	21.88±0.44[a §]	25.31±0.95[a]	22.92±0.45[a]	28.58±0.94[a]
SOD1+/-	20.84±0.73[a]	23.02±0.70[ab]	23.76±0.65[a]	27.32±0.83[a]
SOD1-/-	18.66±0.96[b]	22.02±1.46[b]	17.99±1.11[b]	18.20±1.27[b]

* All mice (n = 5~8, male) were weighed after an 8-hours-fast at the age of 6 and 9 weeks. Mice were fed normal or high fat diet after weaning at 3 weeks of age.

§ Values not sharing a common letter within column were different ($P < 0.05$). All values represent mean ± SE.

high fat diet. Furthermore, compared with normal diet, high fat diet did not result in extra gain of body weight in SOD1-/- mice, but adversely reduced the body weight by 17% ($P < 0.05$) after 6 weeks' feeding. The body weight of SOD1-/- mice was consistently less than those of WT and SOD1+/- mice, and the trend was not changed by the age and diet. There was no difference in body weight between WT and SOD1+/- mice on either diet.

Plasma lipid profile was not affected by high fat diet in SOD1-/- mice. Similar to the results of the previous study, severe hypercholesterolemia and hypotriglyceridemia were present in SOD1-/- mice fed normal diet at 6wks and 9wks of age as shown in Table 4.2. High fat diet did not affect the plasma TC and TG concentrations in SOD1-/- mice, compared with the normal diet. However, plasma TC of WT mice was increased to a similar level of SOD1-/- mice when high fat diet was consumed. Therefore, high fat diet resulted in a 27% increase of plasma TC in WT mice. There was no significant difference in NEFA between the genotypes. To further detail the changes of lipids in plasma, cholesterol and triglyceride of HDL and (V)LDL were measured. As expected, most plasma cholesterol is located in HDL lipoprotein in WT and SOD1-/- mice. As shown in figure 4.1, knockout of SOD1 did not change the distribution of major cholesterol, as the percentage of HDL-cholesterol in the plasma cholesterol pool of SOD1-/- mice was similar to that of WT. Further, there was no effect of high fat diet on the cholesterol distribution among lipoproteins in WT or SOD1-/- mice, compared to the normal diet. Figure 4.2 shows that the percentage of (V)LDL-triglyceride was higher ($P < 0.05$) in SOD1-/- mice than in WT mice fed normal diet at 9 weeks of age, although the total amount was less ($P < 0.05$). However, high fat diet reversed the trend, and reduced the total amount and percentage of (V)LDL-triglyceride in the plasma of SOD1-/- mice by about 25% and 15%, respectively ($P < 0.05$), compared to normal diet.

Table 4.2. Plasma TC, TG and NEFA in WT, SOD1+/- and SOD1-/- mice fed normal and high fat diets (Unit: mg/dl) [§]

	Normal diet				High fat diet			
	6 Wk	9 Wk			6 Wk	9 Wk		
	TC	TC	TG	NEFA	TC	TC	TG	NEFA
WT	175.51±9.56	178.69±11.64	129.46±22.74	25.48±2.52	160.47±3.45	205.38±12.82	83.90±10.45	29.68±4.48
SOD1+/-	171.50±7.63	177.54±6.86	122.83±15.32	24.64±1.40	169.32±9.48	197.28±11.24	112.02±11.03	26.32±1.12
SOD1-/-	209.62±10.77*	227.89±9.12*	50.41±9.67*	22.40±1.68	198.92±6.92*	203.73±10.94	44.52±3.63*	24.92±2.52
P value [#]	0.043	0.030	0.015	0.602	0.002	0.187	0.031	0.094

[§] Each value represents the mean ± SE of 8~12 mice. Mice were fed normal or high fat diet after weaning at 3weeks of age. Blood samples were collected from tails at 6wk and from hearts at 9wk with anti-coagulant EDTA. Plasma was immediately separated. All mice were male and fasted for 8 hours before being sacrificed. Total cholesterol, triglyceride and NEFA were measured by using kits from Wako Chemicals USA Inc. Values are mean ± SE. TC, total cholesterol; TG, total triglyceride; NEFA, non-esterified fatty acids.

[#] P values indicate the significant level of the effect of genotype on the plasma TC, TG and NEFA by one way ANOVA.

* indicates the values which are different from others within the group ($P < 0.05$).

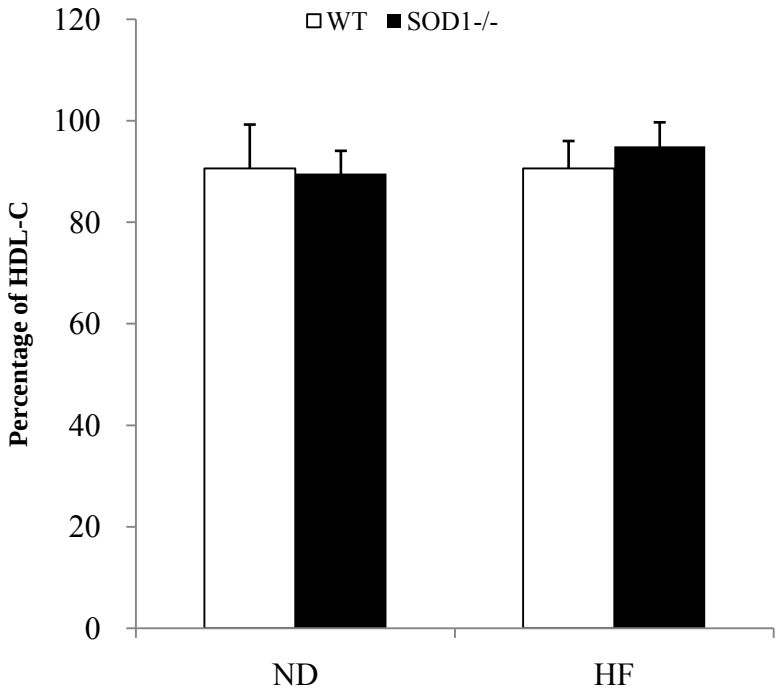

Figure 4.1. The percentage of plasma HDL-cholesterol in WT and SOD1-/- mice fed normal diet (ND) and high fat diet (HF). All mice (n = 6~10) were male and fasted for 8 hours before the experiment. Blood samples were collected by cardiac puncture into EDTA-coated tubes, and plasma was immediately separated after collection. HDL and (V)LDL were separated before the measurement of total cholesterol as described in Materials and Methods.

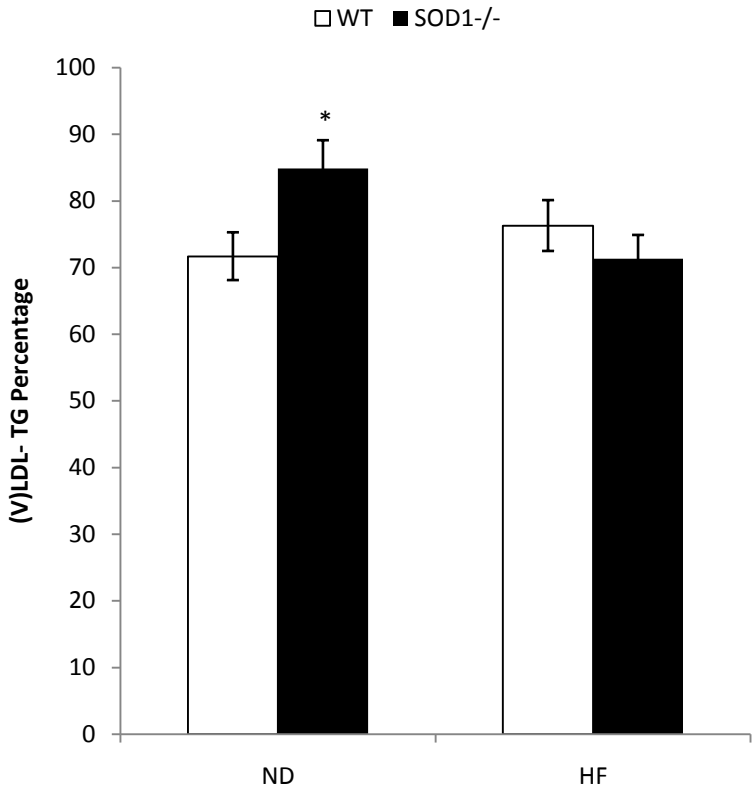

Figure 4.2. The percentage of plasma (V)LDL-triglyceride in WT and SOD1-/- mice fed normal diet (ND) and high fat diet (HF). All mice (n = 6~10) were male and fasted for 8 hours before being sacrificed. Blood samples were collected by cardiac puncture into EDTA-coated tubes, and plasma was immediately separated after collection. HDL and (V)LDL were separated before the measurement of total cholesterol as described in Materials and Methods. *indicates significant differences between genotypes ($P < 0.05$).

High fat diet reduced the fecal cholesterol in WT but not in SOD1-/- mice. As indicated in Figure 4.3, fecal cholesterol of SOD1-/- mice was significantly higher ($P < 0.05$) than that of WT mice fed either normal or high fat diet. Interestingly, high fat diet reduced fecal cholesterol of WT, but not SOD1-/- mice, by 30% ($P< 0.001$), compared to normal diet. Therefore, the difference between WT and SOD1-/- was amplified by high fat diet.

Increased nuclear SREBPs proteins were found in WT and SOD1-/- mice fed high fat diet. Figure 4.4 shows that high fat diet significantly increased nuclear SREBP1 and SREBP2 proteins in both genotypes. Interestingly, nuclear SREBP1 in SOD1-/- mice was significantly less than in WT on normal diet, while high fat diet minimized the genotype differences although SOD1-/- was still lower. Opposite to SREBP1, the level of nuclear SREBP2 was higher in SOD1-/- mice fed either normal or high fat diet, but high fat diet significantly enhanced the presence of SREBP2 in nuclei of both genotypes with a similar range, compared to normal diet.

4.5 Discussion

The most significant finding from this study is that high fat diet did not ameliorate the loss of body weight and dyslipidemia caused by the knockout of SOD1. Normally high fat diet produces the higher body weight and obesity, and affects the concentrations of blood lipids in human and animals (196-198). This was observed in the WT, but not in SOD1-/- mice. It is obvious that SOD1-/- mice were resistant to the high fat diet induced gain of body weight and obesity. Abundant evidence from preclinical and clinical studies indicate that fat promotes excess energy intake and positive energy balance (199-201). Dietary fat does not promote its own oxidation in the body and is stored efficiently, promoting a positive energy balance (202). However, the status of energy balance in SOD1-/- mice was not increased by feeding high fat

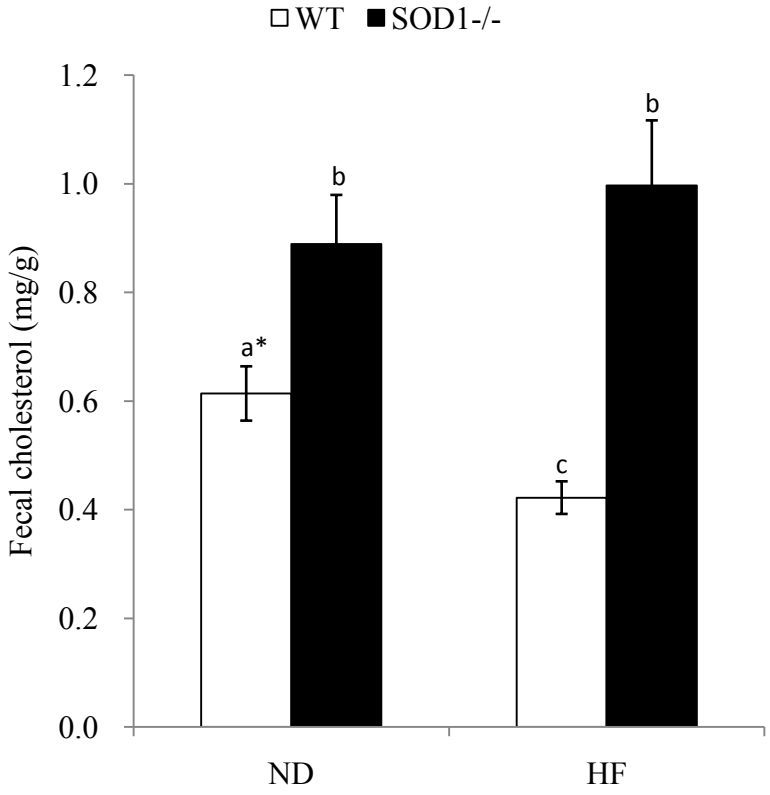

Figure 4.3. Comparison of fecal cholesterol of WT and SOD1-/- mice. Feces was collected from 9 week old mice (n = 5) on normal and high fat diet for one week. Total lipids were extracted by using Folch method from dried feces. The final concentration was calculated based on the total dry weight and the values are expressed as mg/g. * the different letters indicate significant differences between groups ($p < 0.05$).

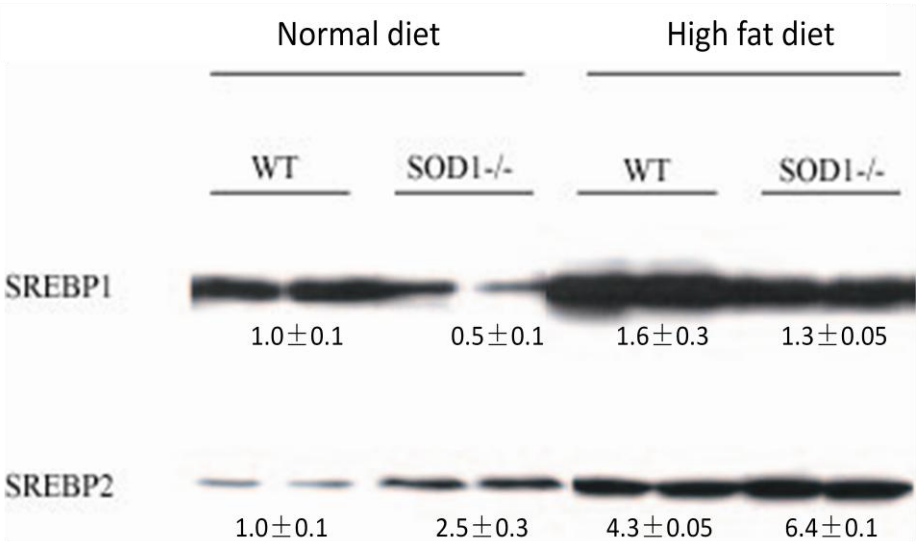

Figure 4.4. Western blot analysis of SREBP1 and SREBP2 in livers of WT and SOD1-/- mice on normal diet (ND) and high fat diet (HD). Nuclear proteins were prepared from fresh livers as described previously. All mice were male (n = 5 per genotype) and were sacrificed at the age of 9 weeks after being fasted for 8 hours. Western blot was performed as stated in General Material and Methods.

diet, and the deficiency of SOD1 interrupts the normal physiological response in mice, as inferred from the lower body weight of SOD1-/- mice under the normal nourishment in this study and others (52). The knockout or overexpression of the antioxidant enzymes has been found to affect the cellular energy homeostasis. The deficiency of mitochondria manganese superoxide dismutase causes slow growth and fatty liver (119), while over expression of the antioxidant enzyme, glutathione peroxidase 1 causes obesity and related metabolic syndrome (131, 203).

The regulatory mechanism of antioxidant enzymes in controlling energy balance might be mediated by ROS. A large amount of ROS are produced by mitochondria during cellular respiration. In addition to their deleterious effects, ROS have been proven to function as signaling molecules in many processes (185). A hypothalamic ROS is required for insulin-induced food intake inhibition, and the pharmacological suppression of this insulin-stimulated ROS elevation, either by antioxidant or by a NADPH oxidase inhibitor abolishes the anorexigenic effect of insulin (204). ROS also affect the mitochondrial biogenesis in cells. It has been shown that ROS is an important mediator of mitochondrial biogenesis induced by homocysteine, and that antioxidants may block the process (205).

Based on the concentration of plasma total cholesterol, high fat exerted a stronger impact on the cholesterol metabolism in WT than in SOD1-/- mice, possibly because there was no capacity for a further increase in the blood of SOD1-/- mice. The previous study showed the cholesterol synthetic pathway was highly activated in the livers of SOD1-/- mice with increased level of SREBP2, which is the master regulator of cholesterol biosynthesis (206). Actually, high fat diet promoted the increased level of the nuclear SREBP2 in both genotypes compared with normal diet as indicated by Western blot. Therefore, SOD1-/- mice might reach the maximal level of plasma cholesterol, thereby excess of endogenous cholesterol was secreted as fecal cholesterol,

as indicated by Figure 4.3. High fat diet significantly increased plasma cholesterol as well as SREBP2, but reduced the fecal cholesterol in WT mice, in comparison with normal diet. Fecal cholesterol is mainly secreted by the gall bladder and the intestine in mice (207). All of the fecal cholesterol was endogenous because there was no dietary cholesterol in this study. Cholesterol can be re-absorbed with chylomicrons in small intestine (208). Therefore, there might be two reasons for the increased plasma cholesterol: reduced loss and increased biosynthesis. However, Bosch and co-authours showed that the high-fat diet almost doubled fecal neutral sterol excretion with diminished cholesterol absorption while did not affect biliary cholesterol secretion (209). Satchithanandam et al., (1993) showed reduced cholesterol absorption in rats only when fed 24% sesame oil diet, but no effect was observed with 24% coconut oil diet (210). Brussaard et al., (1983) showed that fecal excretion of neutral steroids on diets differed in type and amount of dietary fat in young healthy persons (211). Therefore, the effect of high fat on the fecal loss of cholesterol varies with the types of fat and models. It is reasonable to infer that the fecal cholesterol reflects the body status of cholesterol, as higher fecal cholesterol in SOD1-/- was always observed. As for the potentially increased biosynthesis of cholesterol induced by high fat diet, the SREBP2 mediated pathway could be considered as the major mechanism. Generally, SREBP2 controls the cholesterol synthesis by a feedback mechanism based on the cellular cholesterol level to meet the requirement of normal physiological reactions (77, 78, 122). Consistent with our results, diet with high saturated fat significantly increased hepatic total cholesterol contents via enhancing the activity and mRNA expression of 3-hydroxy-3-methylglutaryl coenzyme A reductase with increased SREBP2 in mice, which could be alleviated by antioxidant compounds, as reported by Lin et al., (2008) (212). Dietary fat elevates the ROS production and increases oxidative stress (181, 182, 213). Further, oxidative stress induced by different factors,

such as virus and oxidant substrates, has been shown to activate the SREBPs pathway (214, 215). Therefore, compared to the normal diet, high fat diet increased the mature SREBP2, while the knockout of SOD1 showed an additional effect in this study.

In terms of plasma triglyceride, high fat diet did not increase the concentration in SOD1-/- mice. On the normal diet, SOD1-/- mice had only about 40% plasma triglyceride of the WT mice. However, there was a decrease of plasma triglyceride in WT fed high fat diet, similar to the phenomenon observed by Fearnside et al., (2008) in C57BL/6 strain mice (198), from which our lines were developed. There might be a relevant metabolic adjustment to the high fat intake with regard to plasma triglyceride, which is specific to the genetic background. Nevertheless, we observed a significant increase of mature SREBP1 in both genotypes under the high fat feeding, compared with normal diet. SREBP1 is an important transcriptional factor for the regulation of fatty acid synthesis. High fat diet has been shown to increase hepatic triglyceride via enhancing the activity and mRNA expression of malic enzyme and Fasn, mediated by SREBP1 (202, 212). The lower level of SREBP1 in SOD1-/- mice accounts for, at least partially, the lower level of triglyceride as discussed elsewhere (159). It seems that the knockout of SOD1 has an effect on the SREBP1 which could not be reversed by the high fat diet. However, energy deficiency or fasting suppresses the expression of SREBP1, while feeding reverses the change (216, 217). The increased accumulations of subsarcolemmal mitochondria in SOD1-/- mice indicate the metabolic adaptation to the mitochondrial dysfunction and reduced biogenesis (9). Therefore, there might be an energy deficient condition in SOD1-/- mice which was slightly improved by the high fat diet.

In conclusion, the knockout of SOD1 interrupted the normal metabolic response to high fat diet in mice. There was no positive effect on body weight and plasma lipids of high fat diet in SOD1-/- mice although nuclear SREBP1 and SREBP2 were increased

remarkably, compared to normal diet. The results indicate that SOD1 is essential for the SREBPs-mediated process, which could lead to future phenotype changes. Multiple adaptive mechanisms could be involved in these processes, which together provide the basis for the regulation of energy homeostasis and lipid metabolism with altered energy intake in SOD1-/- mice.

CHAPTER FIVE

EFFECT OF DIETARY COPPPER ON THE METABOLIC ABNORMALITIES IN COPPER, ZINC SUPEROXIDE DISMUTASE KNOCKOUT MICE

5.1 Abstract

Our previous studies showed that the knockout of SOD1 caused severe dyslipidemia in mice. Cu deficiency occurs in SOD1-/- mice，while Cu deficiency-induced hypercholesterolemia in mammals has been documented for decades (ref. 52, 103 and 107). This study was conducted to test our hypothesis that dietary Cu might counteract the metabolic changes induced by the knockout of SOD1. Three-week-old WT and SOD1 male mice were fed Cu deficient (less than 1 ppm), normal (11ppm) and excess (110 ppm) diet for 6 weeks. We investigated and compared the metabolic changes of WT and SOD1-/- mice induced by Cu deficient and Cu excess diet with normal diet as control. We found that dietary Cu deficiency elevated plasma cholesterol of WT mice, which is comparable to that of SOD1-/- mice, but did not affect the concentrations of blood lipids in SOD1-/- mice. Dietary Cu deficiency elevated (V)LDL cholesterol while SOD1 deficiency reduced plasma triglyceride and increased hepatic cholesterol and triglyceride. Cu excess diet was only found to reduce hepatic triglyceride in terms of metabolic changes in this study with no effect on plasma cholesterol and triglyceride as well as hepatic cholesterol. We also found that the expression of SOD1 and catalase proteins negatively correlated to the dietary Cu in WT mice. SREBPs proteins were remarkably changed, partially explaining the alterations of phenotype. Therefore, excess of dietary Cu supplementation was unable to recover the defects of SOD1 deficiency despite of the similarities of symptoms in regard to Cu and SOD1 deficiency.

5.2 Introduction

The knockout of Cu, Zn superoxide dismutase (SOD1) causes severe dyslipidemia and metabolic syndrome in mice as demonstrated in our previous studies and others (9, 121). It also has been suggested that Cu deficiency gives rise to hypercholesterolemia in mammals (103-106). Cu deficiency decreases the SOD1 activity while the genetic loss of SOD1 reduces Cu concentration in organs and tissues (52, 106). However, it is still unknown whether the nutritional Cu supplementation could reverse the metabolic changes caused by the genetic loss of SOD1.

SOD1 catalyses the dismutation of superoxide radicals to molecular oxygen and hydrogen peroxide, and the latter is converted into water by catalase or glutathione peroxidase 1 (131, 218). SOD1 is a dimer, which is located in intracellular compartments, including the cytosol, nucleus, lysosome and mitochondrial intermembrane space in all eukaryotes (42, 219). Each subunit of SOD1 contains one Cu and one Zn atom. Cu is essential for catalysis, and reversibly oxidized and reduced by successive encounters with superoxide radicals to yield dioxygen and hydrogen peroxide, while Zn mainly serves as a structural purpose in addition to a less catalytic role (220). Adequate cellular Cu is essential for the formation of active SOD1 from its apoprotein which is newly synthesized. Cu deficiency significantly reduces the activity of SOD1 in tissues and organs when the dietary supplementation is not met (106, 221).

Coper deficiency as a cause of hypercholesterolemia has been documented decades ago. Copper, an essential nutrient, has to be obtained from the diet to support normal physiological needs. Otherwise Cu deficiency occurs and causes the metabolic alterations, including hypercholesterolemia and lipid disorders (103-106). Hypercholesterolemia is a condition characterized by very high levels of cholesterol in the blood, which may cause many forms of disease, most notably cardiovascular

disease (60). Copper deficiency induces hypercholesterolemia with 30 to 40% increases of plasma total cholesterol by most studies (103, 104, 107). HDL and LDL cholesterol, triglyceride in rats are consistently elevated by Cu deficiency, while VLDL cholesterol varies between studies (103, 108, 109). But Cu deficiency reduces cholesterol deposition in livers of rats (108, 110). However, hepatic 3-hydroxy-3-methylglutaryl coenzyme A (HMG CoA) reductase activity is increased by Cu deficiency, which catalyzes the rate-limiting step of cholesterol biosynthesis; the increased synthesis is responsible for the high net efflux of cholesterol from liver to plasma in Cu deficient rats (111). Hepatic fatty acid synthase is also induced by Cu deficiency in rats (112). The degradation and secretion of cholesterol could also affect the cholesterol status in bodies, but unlikely account for the Cu deficiency-induced hypercholesterolemia based on the studies with radio labeled cholesterol in Cu deficient rats (103, 113). On the other end, the excess Cu could reduce the hepatic and plasma cholesterol. In Wilson disease, elevated hepatic Cu results in the development of liver pathology (114). Most importantly, high Cu suppresses the transcription of HMG CoA reductase in spite of the increased SREBP2 in liver of the mouse model of Wilson disease (115). And this model also shows a 3.6-fold decrease of VLDL cholesterol in serum and a 33% decrease of liver cholesterol (115). Together, Cu has a significant impact on cholesterol metabolism.

The knockout of SOD1 significantly increases plasma cholesterol, but decreases triglyceride with abnormal lipid deposition in liver, kidney and heart, as shown in previous studies (9, 121), which is similar to the Cu deficiency induced lipids disorder. Further, both the knockout of SOD1 and Cu deficiency affect mitochondrial function and metal homeostasis (9, 48, 222, 223). Considering that SOD1 is the major Cu contained protein (52), it is possible that the phenotype of SOD1-/- mice may results from the Cu deficiency. On the contrary, SOD1 may mediate the Cu deficiency

induced metabolic changes as Cu deficiency-reduced the SOD1 activity (106, 221). To test our hypothesis that dietary Cu might alter the metabolic abnormalities caused by the knockout of SOD1, WT and SOD1-/- mice were fed diets with different levels of Cu. And the metabolic changes and signaling proteins were monitored. Interestingly, Cu deficiency caused hypercholesterolemia in WT mice, while excess Cu diet had only a partial alleviation of the metabolic changes in SOD1-/- mice. The regulatory proteins, SREBP1 and SREBP2, were significantly affected by the level of dietary Cu. These results suggest that dietary Cu supplementation could not effectively reverse the physiological changes in the subjects with the genetic loss of SOD1.

5.3 Experimental Design

Chemicals and antibodies. All chemicals were purchased from Sigma Chemical Co. (St. Louis, MO) unless otherwise indicated. Reagents for cholesterol, triglyceride and non-esterified fatty acids were from Wako Chemicals USA, Inc. (Richmond ,VA).

Animals and diets. SOD1-/- and WT mice, generated from 129SVJ x C57BL/6 strain, were generously provided by Y. S. Ho of Wayne State University, Michigan (116). After weaning at 3 weeks of age, male mice were subjected to Cu deficient (CD, no Cu added) diet, normal (ND, supplemented with 11ppm) diet or Cu excess (HC, supplemented with 110ppm) diet for 6 weeks. The complete ingredients of normal diet is listed in Table 2.1. The Cu level was fulfilled with the supplementation of $CuSO_4 \cdot 5H_2O$ into the diet.

Plasma and hepatic lipids measurements. Plasma was collected from the tail at 6 weeks old mice for monitoring plasma cholesterol and triglyceride levels. Mice were sacrificed at 9 or 12 weeks of age after an 8-hour-fast, and tissues and organs were collected and frozen immediately. Total plasma cholesterol, triglyceride and non-esterified fatty acids levels were measured using commercially available kits

(Wako Pure Chemical Industries). Total cholesterol in HDL and (V)LDL lipoproteins was estimated by using a kit from Biovision Inc.(Mountain View, CA). Liver cholesterol and triglyceride were extracted by Folch method and measured by the method stated above.

Total superoxide dismutase activity assay. Liver samples were homogenated in 50mM PBS buffer (pH 7.4) containing 0.1% Triton X-100 and 1.34 mM diethylenetriaminepeantacitic aicd. The total activity was determined using a water-soluble Formazan dye kit (Dojindo Molecular Technologies, Gaithersburg, MD). Enzyme unit was defined as the activity needed to inhibit 50% 2-(4-iodophenyl)-3-(4-nitrophenyl)-5-(2,4-disulfophenyl)-2H-tetrazolium mono-sodium salt reduction.

Nuclei isolation. Nuclei were isolated by Dounce homogenization and sucrose gradient centrifugation as described previously.

Western blot. Liver homogenate or nuclei extract (10 μg of protein) was used for Western blot analysis as demonstrated in the General Material and Methods section. Antibodies used in this chapter were listed in Table 2.2.

5.4 Results

The levels of dietary Cu did not affect the body weight of SOD1-/- mice. Table 5.1 shows that the body weight of SOD1-/- mice was not affected by the levels of dietary Cu after 3 or 6 weeks of feeding. Compared with ND, either CD or HC did not increase the difference in body weight between WT and SOD1-/- mice. Although all mice had a similar body weight at the beginning of the experiment, at 9wk of age, SOD1-/- mice weighed 80%, 77% and 82% of WT mice on CD, ND and HC, respectively. The difference between genotypes reached the significant level ($P < 0.05$) at 6wk of age. CD insignificantly reduced body weight of WT mice, while HC

Table 5.1. Body weights of WT and SOD1-/- mice fed diets with different Cu levels

Diet	Genotype	Body weight (g)		
		Initial	3 Wk	6 Wk
Cu deficient diet	WT	11.22±0.62	18.48±1.35[a*]	23.02±1.65[a]
	SOD1+/-	11.70±0.50	18.72±0.93[a]	22.90±1.14[a]
	SOD1-/-	10.71±0.75	15.29±1.02[b]	18.44±1.40[b]
Normal diet	WT	11.54±0.92	19.08±1.13[a]	24.26±1.79[a]
	SOD1+/-	11.68±0.78	19.19±0.67[a]	24.11±1.87[a]
	SOD1-/-	10.34±1.18	15.94±1.23[b]	18.57±1.54[b]
Cu excess diet	WT	11.86±0.79	19.85±1.01[a]	23.88±1.12[a]
	SOD1+/-	10.92±0.57	18.68±0.93[a]	22.79±1.03[a]
	SOD1-/-	10.34±0.90	16.15±1.04[b]	19.58±1.55[b]

All mice (n = 7~10, male) were weighed after being fasted for 8 hours at the age of 6 weeks 9 weeks. Mice were fed experimental diets after weaning at 3 weeks of age. *The same letter in the same vertical row means no difference ($P > 0.05$). All values represent mean ± SE.

insignificantly increased body weight of SOD1-/- mice ($P > 0.05$). Different Cu levels did not significantly influenced body weight of WT and SOD1+/- mice.

Cu deficient diet caused hypercholesterolemia in WT mice, similar to the phenotype of SOD1-/- mice. As shown in Table 5.2, CD had a stronger effect on the concentrations of plasma lipids than Cu excess diet. Specifically, CD increased plasma TC in WT and SOD1+/- mice by 11% and 18%, respectively ($P < 0.05$), but not in SOD1-/-, compared to normal diet at 6wk. However, these changes were not observed at 3wk in both WT and SOD1+/- mice. CD also did not affect the concentrations of plasma TC in SOD1-/- mice. HC diet did not influenced plasma TC level in WT mice, while insignificantly reduced its level in SOD1-/- mice. Neither CD nor HC significantly affected the levels of plasma TG in WT and SOD1-/- mice, compared to ND. Even after 12 weeks on HC, there was only a subtle decrease of plasma TC in SOD1-/- mice (Figure 5.1). However, there was a dose dependent relation between dietary Cu level and plasma TG level ($P < 0.05$) in SOD1-/- mice. In regard to NEFA, CD showed negative effects in all genotypes, compared to ND. The most decrease in NEFA was observed in WT mice (60%, $P < 0.05$), and the least in SOD1+/- (21%, $P < 0.05$). No effect of HC on NEFA was found among the genotypes, compared with ND control. The distribution of cholesterol among the lipoproteins was measured to specify the profile of plasma lipids. Figure 5.2 shows that the levels of HDL-cholesterol of WT and SOD1-/- mice on CD were similar. CD did not affect the lipoprotein cholesterol in SOD1-/-, compared with ND. However, compared to SOD1-/- mice, CD led to a higher level of (V)LDL cholesterol in WT mice ($P < 0.05$), although the total cholesterol in plasma between them was not different.

Cu excess diet alleviated the fatty liver of SOD1-/- mice. As shown in Figure 5.3, SOD1-/- mice had a large amount of cholesterol in liver, and the phenomena did not depend on the diets. However, CD increased the hepatic cholesterol in SOD1-/- mice

Table 5.2. Plasma TC, TG and NEFA concentrations of WT and SOD1-/- mice fed diets with different Cu levels (Unit: mg/dl) [§]

Diet	Genotype	6 Wk		9 Wk		
		TC	TG	TC	TG	NEFA
Cu deficient diet	WT	178.82±10.81[a*]	39.13±7.51[a]	202.52±9.60[b]	76.67±10.71[a]	9.52±2.52[a]
	SOD1+/-	182.48±9.33[a]	36.61±6.14[a]	217.66±11.59[ab]	73.84±8.20[a]	13.72±1.96[b]
	SOD1-/-	238.85±18.31[b]	16.50±1.98[b]	235.34±14.45[a]	19.12±7.00[b]	11.48±0.56[ab]
Normal diet	WT	168.95±5.67[a]	36.74±6.16[a]	182.15±10.17[c]	68.07±9.12[a]	24.36±2.24[c]
	SOD1+/-	185.62±9.32[a]	36.99±7.23[a]	184.71±11.56[c]	65.80±3.58[a]	17.36±3.08[c]
	SOD1-/-	241.17±16.36[b]	11.04±3.78[b]	231.43±15.49[a]	25.37±11.82[b]	21.56±4.2[c]
Cu excess diet	WT	168.21±10.58[a]	29.22±6.10[a]	187.54±11.43[c]	69.64±9.81[a]	20.44±5.04[c]
	SOD1+/-	191.67±9.42[a]	31.86±4.15[a]	185.19±9.73[c]	68.32±8.25[a]	18.76±2.52[c]
	SOD1-/-	231.37±11.45 [b]	10.26±2.94[b]	218.72±10.63[ab]	31.78±6.59[b]	22.12±3.08[c]

[§]Each value represents the mean ± SE of 7~10 mice. Mice were fed experimental diets after weaning at 3wk. Blood samples were collected from tails at 6wk and from hearts at 9wk with anti-coagulant EDTA, and plasma was immediately separated. All mice were male and fasted for 8 hours before the experiment. Total cholesterol, triglyceride and NEFA were measured by using kits from Wako Chemicals USA Inc. Values are mean ± SE. TC, total cholesterol; TG, total triglyceride; NEFA, non-esterified fatty acids.

*different letters mean the significant difference between groups within the column ($P < 0.05$).

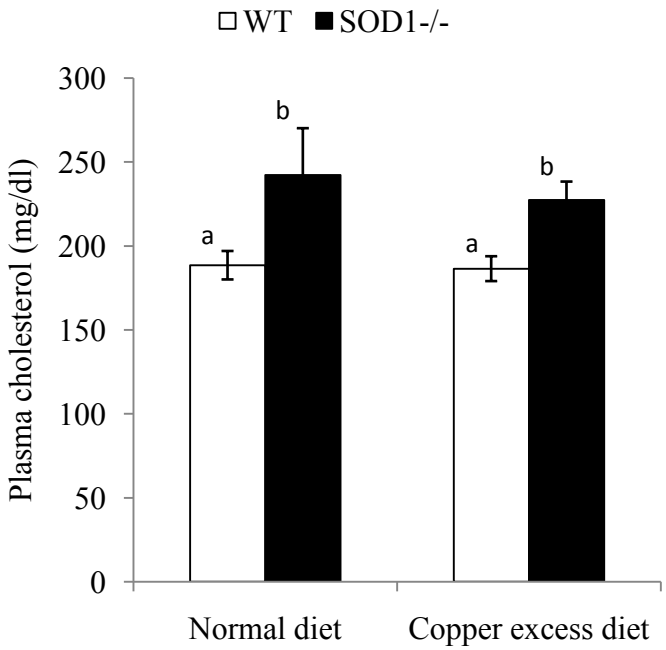

Figure 5.1. Plasma total cholesterol of WT and SOD1-/- mice after 12 weeks of feeding Cu excess and normal diet. Mice (n = 5) were fed experimental diets for 12 weeks after weaning at 3wk. Blood samples were collected from hearts with anti-coagulant EDTA, and plasma was immediately separated. All mice were male and fasted for 8 hours before the experiment. Total cholesterol was measured by using a kit from Wako Chemicals USA Inc. *different letters mean the significant difference between groups within the column ($P < 0.05$).

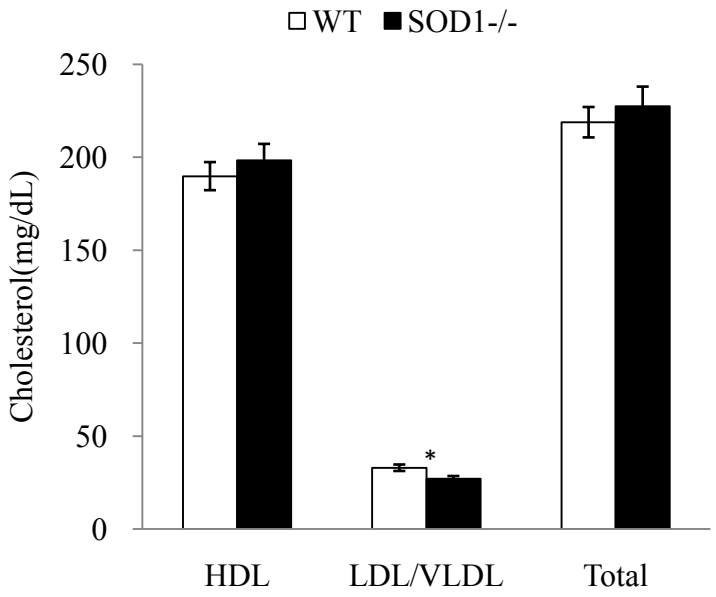

Figure 5.2. Distribution of plasma cholesterol in WT and SOD1-/- mice after 6 weeks of feeding Cu deficient diet. Mice (male, n = 7~10) were fed experimental diets for 6 weeks after weaning at 3wk. Blood samples were collected by cardiac puncture into EDTA-coated tubes, and plasma was immediately separated after collection. HDL and (V)LDL was separated before the measurements of total cholesterol as described in General Material and Methods. *indicates the significant difference between genotypes ($P < 0.05$).

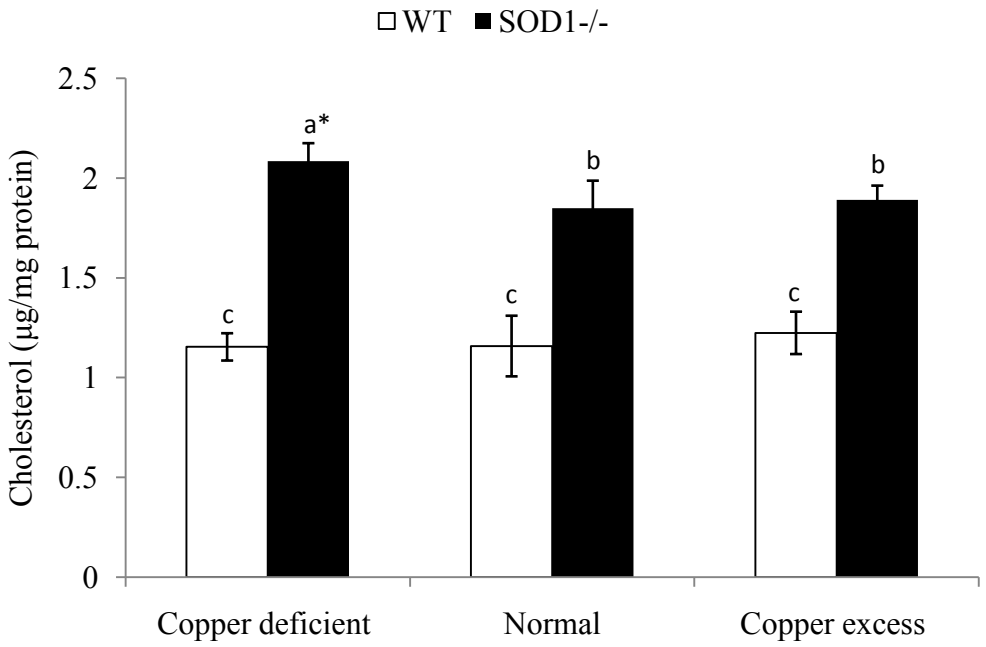

Figure 5.3. Effect of dietary Cu on hepatic cholesterol in WT and SOD1-/- mice. Livers were collected from 9 week old mice (n = 7~10 per genotype) after 6 weeks of feeding different diets. Total liver lipids were extracted by using Folch method. Cholesterol was measured by using a kit from Wako Chemicals USA Inc. All mice were male and fasted for 8 hours before being killed. The cholesterol concentrations were expressed based on the total protein concentrations. * The different letters indicate the significant differences between groups ($p < 0.05$).

($P < 0.05$), but not in WT mice. Moreover, HC did not show any impact on hepatic cholesterol in both genotypes. Figure 5.4 indicats that the hepatic triglyceride of WT and SOD1-/- mice was strongly affected by experimental diets. SOD1-/- mice displayed severe fatty liver and the symptoms were alleviated by the increased dietary Cu. However, both CD and HC reduced hepatic triglyceride ($P < 0.05$) in the WT mice, compared to ND, while CD had the strongest effect.

Cu deficiency reduced the total SOD activity in WT mice. As expected, the knockout of SOD1 caused the major loss of total SOD activity. Compared with ND, CD reduced the total SOD activity for about 43% in WT mice, while HC did not show a significant effect (Figure 5.5). However, the SOD1 protein in WT was negatively correlated with the Cu level, while Cu deficiency elevated and high dietary Cu reduced the total SOD1 protein (Figure 5.6). Also, dietary Cu caused a dose-dependent decrease of catalase protein, but no effect on GPX1 protein was observed in both genotypes.

Effects of dietary Cu on SREBP1/2, and HMGCR in the livers of the WT and SOD1-/- mice. Results of Western blot (Figure 5.6) show that SREBP1 was decreased in WT and increased in SOD1-/- mice by CD, compared to ND control, while HC had similar but stronger effects on SREBP1. With comparison to ND, SREBP2 was increased in WT but decreased in SOD1-/- mice by CD. HC diet reduced SREBP2 in both genotypes, but its level in SOD1-/- mice was still higher. Interestingly, HMGCR was higher in SOD1-/- than in WT mice, regardless of which diet was consumed. However, HC led to a higher level of HMGCR protein in both genotypes, compared to CD and ND.

5.5 Discussion

In the present study, we demonstrated that the excess of dietary Cu did not completely

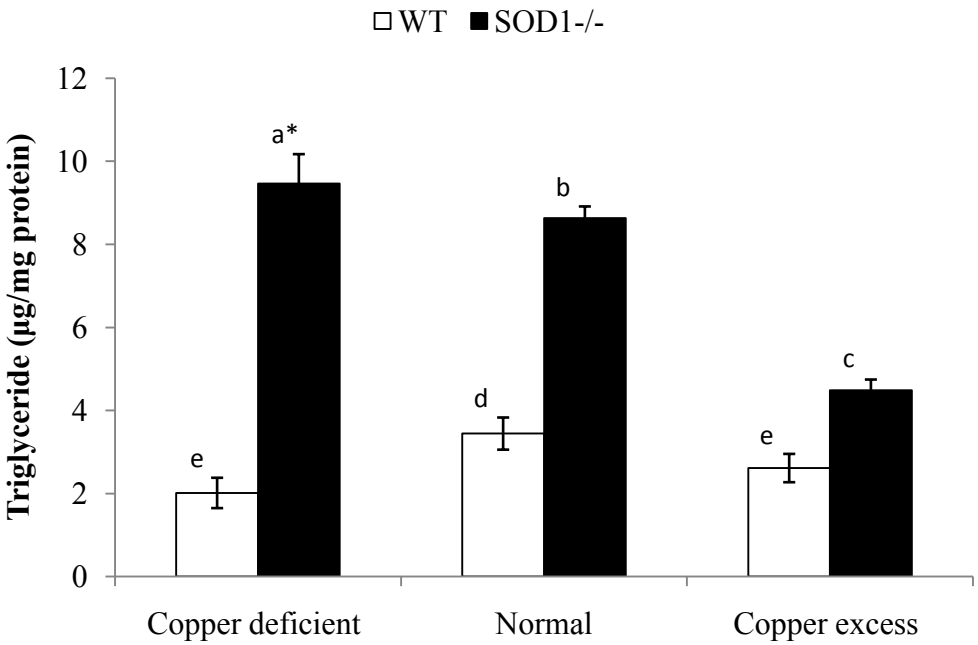

Figure 5.4. Effect of dietary Cu on hepatic triglyceride in WT and SOD1-/-mice. Mice (n = 7~10 per genotype) were weaned at 3 weeks of age and fed Cu deficient diet, normal diet, and Cu excess diet for 6 weeks. All mice were male and fasted for 8 hours before the experiment. Total lipids were extracted from livers by using Folch method. Triglyceride was measured by using a kit from Wako Chemicals USA Inc. The concentrations are expressed based on the protein concentrations. * The different letters indicate the significant differences between groups ($p < 0.05$).

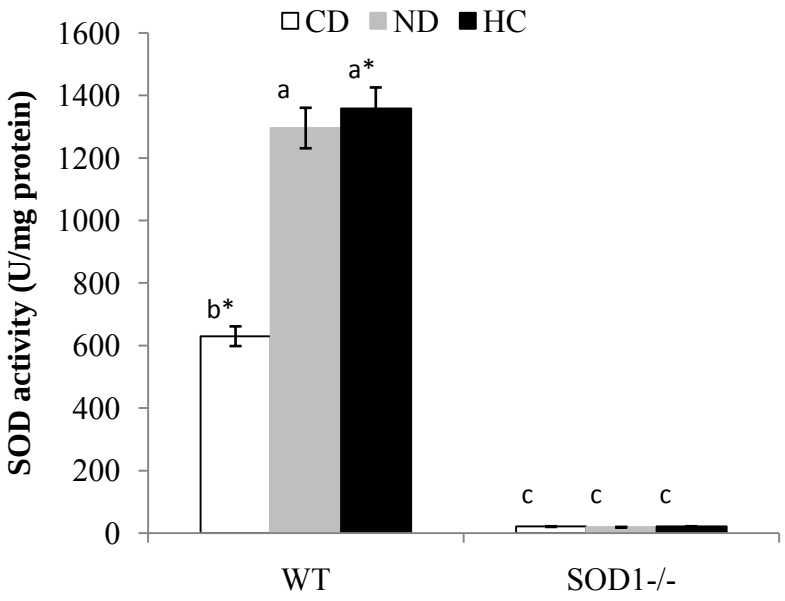

Figure 5.5. Effect of dietary Cu on total SOD activity in livers of WT and SOD1-/- mice. Mice (n = 7~10) were weaned at 3 weeks of age and fed Cu deficient diet (CD), normal diet (ND), and Cu excess diet (HC) for 6 weeks. All mice were male and fasted for 8 hours before the experiment. Total proteins were prepared from livers before the analysis of SOD activity as described previously. * The different letters indicate the significant differences between groups ($p < 0.05$).

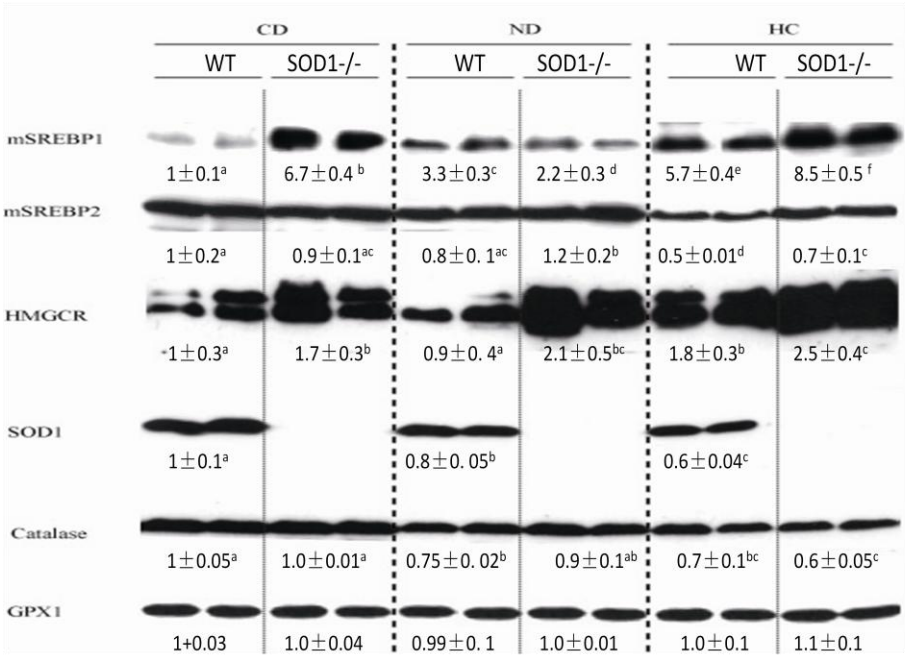

Figure 5.6. Western blot analysis of SREBP1, SREBP2, HMGCR, SOD1, CAT and GPX1 proteins in livers of WT and SOD1-/- mice. Mice were weaned at 3 weeks of age and fed Cu deficient (CD), normal (ND), and Cu excess (HC) diet for 6 weeks. All mice were male and fasted for 8 hours before the experiment. Liver homogenates (for HMGCR, SOD1, catalase and GPX1) or nuclear proteins (for SREBP1 and SREBP2) were prepared from livers before running gel as described previously. The antibodies used are listed in Table 2.2.

restore the metabolic changes caused by the knockout of SOD1, although some benefits were observed. The phenotypes of Cu deficient mice and SOD1-/- mice were similar but not exactly the same. We found that, in SOD1-/- mice, dietary Cu did not affect body weight, plasma TC and TG concentrations, while Cu deficiency increased hepatic cholesterol and triglyceride, and Cu excess diet reduced the hepatic triglyceride but not cholesterol levels. Cu deficiency elevated (V)LDL cholesterol in WT mice as reported (108), which was different from SOD1-/- mice. SREBP2 might mediate the cholesterol biosynthesis in Cu deficient WT mice as well as in SOD1-/- mice. The level of hepatic SOD1 protein in WT was adversely correlated with dietary Cu level, while total activity was reduced if Cu deficiency existed, in agreement with results reported previously (106, 221) .

Compared with Cu deficiency in WT, the knockout of SOD1 caused more severe metabolic changes in mice. It has been established previously that Cu deficiency-caused hypercholesterolemia in rats (103, 104, 107) and in mice (106). The increased HMG CoA reductase activity, induced by dietary Cu deficiency, accounts for the elevated level of cholesterol in blood (111). Further study indicates that Cu deficiency increased hepatic GSH, which activates HMG-CoA reductase activity, and hypercholesterolemia is abolished by the suppression of GSH (107). However, the knockout of SOD1-/- does not affect the basic level of hepatic GSH in mice (224, 225). In this study, the level of proteins of HMG-CoA reductase, and its transcriptional factor, SREBP2, were also increased in WT mice on CD although the reductase activity was not examined. In SOD1-/- mice, hepatic HMG CoA reductase was increased at both mRNA and protein levels, as well as SREBP2, which level was also remarkably increased. These data suggest that the Cu deficiency and the knockout of SOD1 could alter cholesterol biosynthesis at least on the transcriptional level. We also found that the knockout of SOD1 eventually led to the increased level of hepatic

cholesterol as a result of its increased biosynthesis, while WT mice on Cu deficient diet did not show any similar increase of hepatic cholesterol. Our data are in agreement with previously reported findings of others (108, 110, 111).

Compared with the WT mice on ND, dietary Cu deficiency did not affect plasma triglyceride, but reduced hepatic triglyceride, while the knockout of SOD1 significantly reduced plasma triglyceride but increased hepatic triglyceride. As shown by Uchiyama et al., (2006), the knockout of SOD1 does impair the secretion of lipoprotein from the liver as the degradation of ApoB is promoted, which is responsible for carrying cholesterol to tissues (121). SREBP1 is a transcriptional factor which could activate the transcription of lipogenic genes, including fatty acid synthase (226). Interestingly, either Cu deficiency or SOD1 knockout reduced SREBP1 protein, while Cu deficiency reversed the decrease of SREBP1 caused by SOD1 deficiency in the mouse model. It is possible that the reduced triglyceride in plasma or liver caused by Cu deficiency or the knockout of SOD1 resulted from the loss of regulation of SREBP1. However, the increased SREBP1 level in SOD1-/- mice on CD and HC remains a mystery as there was no corresponding metabolic change observed. Moreover, hepatic fatty acid synthase was found to be induced by Cu deficiency in rats (112, 227).

Excess dietary Cu could not counteract the effects caused by the knockout of SOD1 in mice. We hypothesized that the phenotype of SOD1-/- mice might result from the Cu deficiency, because hepatic Cu is reduced by 47% in SOD1-/- mice (52). Excess of dietary Cu did not improve body weight, plasma lipid concentrations and hepatic cholesterol, but reduced hepatic triglyceride in SOD1-/- mice. We found that the excessive supplementation of Cu increased SREBP1 but reduced SREBP2 in SOD1-/- mice, though both proteins were more abundant in SOD1-/- than in WT on the same diet. The decreased SREBP2 protein by the diet was not sufficient to affect the plasma

and hepatic cholesterol. It is obvious that excess dietary Cu reversed the changes of SREPB1 induced by the knockout of SOD1. However, plasma triglyceride was only slightly increased, while hepatic triglyceride was significantly decreased in SOD1-/- mice consuming an excess of Cu. It is not surprising because the transcription activity of SREBP1 is modified by many factors, such as phosphorylation and sumoylation (228, 229).

SOD1 apoprotein is not a decisive factor in cholesterol biosynthesis. An interesting observation from this study was that Cu deficiency reduced total SOD activity but induced SOD1 protein, while Cu overdose reduced its protein expression. The loss of total SOD activity in SOD1-/- mice suggests that SOD1 accounts for the major activity in WT mice, as reported by Lei, et al. (2006) (225). Cu deficiency induced the oxidative stress because of decreased SOD1 activity (230, 231). The expression of SOD1 is under the regulation of NF-kB, AP-1, AP-2, Sp1, and C/EBP transcription factors, which are responsive to ROS-induced stress (see reviewed by Miao, 2009) (190). Therefore, SOD1 expression is induced as a result of oxidative stress caused by Cu deficiency. Similarly, the Cu excess diet maximizes the antioxidant ability of SOD1 and therefore reduces protein expression. Another explanation for the increased SOD1 in mice on Cu deficient diet is that the enzyme degradation is decreased. SOD1 stability is governed by post-translational modification factors that target the SOD1 disulfide, but oxidation of the disulfide *in vivo* depends on Cu proteins which could be blocked by Cu deficiency (232). Therefore, dietary Cu deficiency stabilizes SOD1 for accumulation and excess Cu promotes its degradation in cells. The increased level of SOD1 protein in WT mice with hypercholesterolemia is very interesting, because it suggests that SOD1 protein itself, at least apoprotein, is not a decisive factor in cholesterol metabolism elevated by SOD1 deficiency. This finding may help to exclude the possibility that the SOD1 apoprotein is directly involved the regulation of

cholesterol metabolism.

Taking together, our results suggest that dietary Cu could not fully counteract the metabolic changes induced by the knockout of SOD1 in spite of the similarities between symptoms induced by the Cu deficiency and genetic SOD1 deficiency in mice. Hypercholesterolemia is the shared phenotype, while the regulatory mechanism might be different. The significance of this study for clinical treatment and therapy of lipids disorder is that the nutritional interference of Cu supplementation may not be adequate for the genetic loss of SOD1 and the SOD1 apoprotein may not be a useful candidate for the treatment of hypercholesterolemia.

CHAPTER SIX

EFFECT OF REACTIVE OXYGEN SPECIES ON THE ELEVATED CHOLESTEROL BIOSYNTHESIS IN COPPER, ZINC SUPEROXIDE DISMUTASE KNOCKOUT MICE *IN VIVO* AND *IN VITRO*

6.1 Abstract

Our previous studies show development of severe hypercholesterolemia and increased biosynthesis of cholesterol in SOD1-/- mice. Here we hypothesized that reactive oxygen species (ROS) were primary factors in regulation of cholesterol biosynthesis which affect plasma cholesterol. By using diquat（DQ） as a superoxide generator, we examined the impact of ROS on cholesterol biosynthesis in mice and cultured cells. Interestingly, significant increases, of 23% and 29%, of total plasma cholesterol were observed within two hours in mice injected with DQ dose of 10mg/kg BW and 30mg/kg BW, respectively. We also found that HMG CoA reductase and squalene epoxidase mRNA levels were elevated by 18% and 13%, respectively, compared with control. However, at 6 hours after treatment, the mRNA levels were reduced, and plasma cholesterol concentrations of mice injected with 30mg/kg BW were decreased. In treated mice, the mRNA and protein levels of transcriptional regulator, SREBP2, were elevated at early stage. HepG2 cells showed a similar response to DQ treatment with increased mRNA levels of HMGCR. In conclusion, ROS may play an important role in regulation of cholesterol biosynthesis, and there is a possibility that this regulation is mediated by SREBP2. These findings suggest the potential clinical usage of ROS generator or scavenger to interfere with problems related to cholesterol biosynthesis.

6.2 Introduction

ROS, including superoxide anion ($O_2^{-\bullet}$) and hydrogen peroxide (H_2O_2), are molecular oxygen metabolites, which are produced during the process of respiration in mitochondria as well as other cellular reactions. ROS have been traditionally regarded as toxic by-products of metabolism with the potential to cause damage to lipids, proteins, and DNA (233). However, recent studies have demonstrated that ROS actively participate in a diverse array of biological processes and many functions as cellular signaling molecules. However, the role of ROS in the cholesterol metabolism remains uncertain.

Cellular ROS are formed in both enzymatic and nonenzymatic reactions. More than just by-products of mitochondria biogenesis which could be affected by the energy substrate, the production of mitochondrial ROS can be induced by many stimuli, such as tumor necrosis factor (TNF)-α , interleukin (IL)-1β and radiation (22, 179, 234, 235). The ER and peroxisomes are also important sources of cellular ROS, which are abundant in membrane-associated oxidoreductases responsible for metabolizing drugs or fatty acids (236, 237). Other enzymes, including xanthine oxidase and NADPH oxidase, also affect the local as well as the total levels of ROS in cells upon different stimuli (238, 239). Therefore, many processes may affect the cellular redox microenvironment.

To protect organisms from the potential damage of ROS, cells develops specific cellular antioxidant system able to scavenge ROS and converts potentially toxic molecules into water and others. However, ROS are also essential for the maintenance of normal biological processes and enable cells to adjust to the changed environment or respond to the extracellular stimulus. Early studies show that hydrogen peroxide plays an insulin-like effect on glucose transport and oxidation, and enhances lipid synthesis from glucose in adipocytes (19, 20). Mitogen-activated protein kinase

(MAPK) signaling pathways are well known to be activated by ROS-induced phosphorylation of downstream proteins, ERK, JNK and p38, as widely observed earlier (21). It has been suggested that mitochondrial ROS are involved in the process of apoptosis induced by TNF-α , IL-1β , while mediate the hypoxia-induced gene transcription (22, 23). ROS derived from NADPH oxidase in vascular smooth muscle cells mediate the vascular remodeling (24). Recently, protein tyrosine phosphatase-1B (PTP1B) has been identified as a ROS-responsive protein, which could be directly oxidized and inactivated by superoxide and hydrogen peroxide (25, 26). As PTP1B is a key regulator of multiple signaling pathways downstream of receptor tyrosine kinases, it provides a possible target for manipulating cellular responses through ROS. Another example is NF-E2-related factor-2(Nrf2)-Keap1 complex, which functions as a ROS sensor and regulates the expression of antioxidant enzymes, such as catalase and glutathione peroxidase, through the binding of antioxidant response elements (AREs) in their 5'-flanking promoter regions (27, 28). Other factors, including NF-κB, SP1, and YY1, are also involved in the regulation of redox-induced changes (29-31).

Molecular oxygen could be considered as one substrate of energy production in mitochondria, but it is interesting to note that the derivative of oxygen, ROS, have been specifically linked to the regulation of the mitochondrial biogenesis. The peroxisome proliferator-activated receptor-gamma (PPARγ) coactivator‑1α (PGC1α) stimulates mitochondrial biogenesis in response to increased energy demand, while ROS promote its expression via Cre-binding protein (CREB); it also suggests that PGC1α regulates an antioxidant transcriptional program that includes SODs, catalase and GPX1 (192). PGC1α thus establishes an important link between ROS and mitochondrial respiration. Moreover, Forkhead box O (FOXO) transcription factors are key regulators in response to ROS, but also control the expression of critical enzymes which are involved in cellular energy homeostasis (240-242). Also,

mitochondrial ROS dictate the hypoxic activation of AMPK, which is a sensor of cellular energy status, found in metazoans and is known to be activated by the increased cellular AMP/ATP ratio (243, 244). It suggests that cells possess a delicate mechanism which controls ROS production and energy homeostasis as both are critical to maintain the normal metabolism.

Cholesterol is an essential structural component of cells as well as a precursor of important hormones in animals. The biosynthesis of cholesterol is strictly under control to meet the cellular metabolic needs. As stated above, ROS widely influence cellular biological processes. It has been reported that 3-Hydroxy-3-methylglutaryl CoA (HMG CoA) reductase, the rate controlling enzyme of cholesterol biosynthesis, is activated by the cellular glutathione, an antioxidant peptide (107). ROS has been shown to activate the HMG CoA reductase by dephosphorylation mediated through activation of PP2A/p38/MAPK pathway, which is responsible for the age-related hypercholesterolemia as a result of increased ROS (245, 246). The suppression of ROS production by HMG CoA reductase inhibitors indicates the interesting link between ROS and the synthetic pathway (247, 248). Squalene epoxidase (SQLE), another rate limiting enzyme, catalyses the epoxidation of squalene to yield 2,3-oxidosqualene in the process of cholesterol biosynthesis (249-251). Interestingly, the promoter region of SQLE gene contains the binding sites of SP1 and YY1, while the transcriptional activities of SP1 and YY1 are determined by the redox changes (30, 31, 252). It may suggest the possible role of ROS in cholesterol biosynthesis.

As ROS scavengers, antioxidant enzymes, including superoxide dismutase and glutathione peroxidase, significantly affect the levels of cellular ROS. The deficiencies or over expressions of these genes result in changes of ROS level with altered cellular signaling transductions as revealed by a variety of studies (4, 131, 253, 254). Our previous studies showed that the knockout of SOD1 caused hypercholesterolemia with

activated biosynthetic pathway in mice. Here, we hypothesized that ROS are primary factors responsible for the activation of cholesterol biosynthetic pathway, and may be a reason to cause hypercholesterolemia in mice. By using DQ as a superoxide generator, we found that DQ increased the gene expression of HMGCR and SQLE in the livers of mice as well as in HepG2 cells in *in vitro* studies.

6.3 Experimental Design

Treatment of animals and HepG2 cells. WT mice, 8-10 weeks old, were injected intraperitoneally with phosphate-buffered saline (PBS) or DQ (10mg/kg and 30mg/kg BW) (n = 3-4 per treatment) and euthanized at 2h and 6h post-injection. HepG2 cells were cultured and maintained in DMEM medium as described previously. Cells were plated at a density of 1 x 10^6 cells per 100-mm-diameter culture dish. When the cells reached 60–70% confluence, the medium was replaced with experimental medium, containing 0, 0.25, 0.5 and 0.75 micromole DQ, respectively. After two hours' incubation, cells were collected and RNA was extracted.

Plasma cholesterol measurement. Blood samples were collected from tails of live animals or from hearts after the mice were sacrificed. Plasma total cholesterol was measured as described previously.

RNA extraction and RT-PCR. Total RNA and cDNA were prepared by following the procedures stated in General Material and Methods section. PCR amplifications were carried out using a PTC-100TM Programmable Thermal Cycler with gene specific primers, as listed in Table 2.2. The total volume of reaction mixture was 25µl (2.5µl 10×buffer, 0.5µl each primer (10mM), 1µl 10mM dNTP and 1µl cDNA synthesis reaction product, 1.25U ExTaq polymerase and 19.25µl nuclease-free sterile water). PCR was performed at 95°C for 30 seconds, 60°C for 30 seconds, 72°C for 30 seconds after initial incubations at 95°C for 5 minutes. The reactions were stopped in

the early linear phase which was previously evaluated. PCR products were analyzed on 2% agarose (Gibco BRL, Gaithersburg, MD, USA) gels with ethidium bromide staining at 1 mg/ml TAE buffer for 25 min followed by destaining for 5min with TAE buffer. The density of each band was measured and the values were normalized by 18S of each sample.

Nuclei isolation. Nuclei were isolated from livers by Dounce homogenization and sucrose gradient centrifugation as described in the General Material and Methods section.

Western blot. Nuclei extract (10 μg of protein) was used for Western blot analysis as described in the General Material and Methods section. Antibodies used in these experiments were listed in Table 2.2.

6.4 Results

DQ treatment increased the plasma cholesterol in mice. Compared with PBS control, concentrations of plasma total cholesterol were increased ($P < 0.05$) by 23% and 29% in mice at two hours after treatments with 10mg/kg and 30mg/kg BW DQ, respectively (Figure 6.1). The average plasma total cholesterol was relatively higher in 30mg/kg BW group than in 10mg/kg BW group. At 6 hours after treatment, mice injected with 10mg/kg BW DQ had 28% ($P < 0.05$) increase of plasma cholesterol, while mice injected with 30mg/kg BW DQ showed no increase, compared with the PBS control.

Messenger RNA levels of HMGCR, SQLE and SREBP2 were increased in livers of mice treated with DQ as well as nuclear SREBP2 protein. As shown in Figure 6.2, at 2 hours after treatment, mRNAs level of HMGCR, SQLE and SREBP2 were increased ($P < 0.05$) by 18, 13 and 22% in mice injected with 10mg/kg BW DQ, respectively. Of mice treated with 30mg/kg BW DQ, HMGCR, SQLE and SREBP2

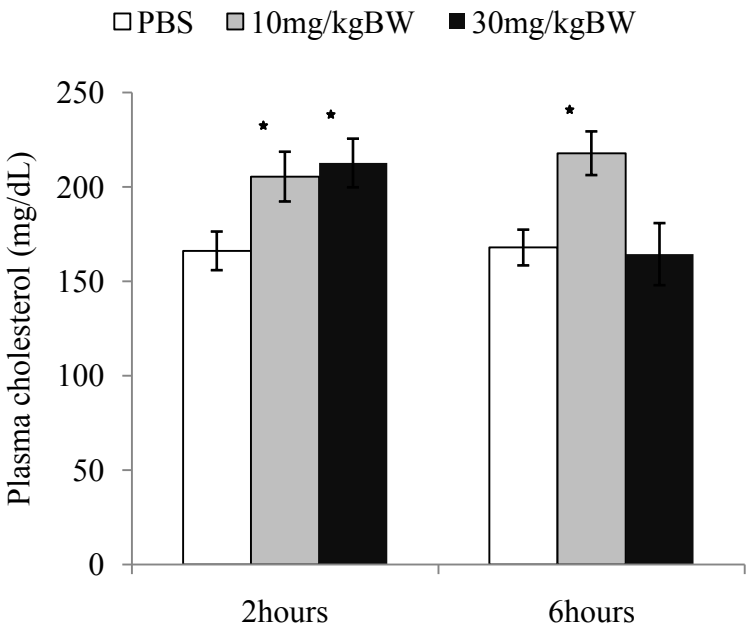

Figure 6.1. Effect of DQ treatment on plasma cholesterol in mice. WT male mice were 8~10 weeks old and injected intraperitoneally with PBS or DQ (10mg/kg BW and 30mg/kg BW). Mice were sacrificed at 2 hours or 6 hours after injections and blood samples were collected from hearts with anti-coagulant EDTA, and plasma was immediately separated. Total cholesterol was measured by using a kit from Wako Chemicals USA Inc. Values are mean ± SE (n = 3). * $P < 0.05$ vs. PBS within the same time.

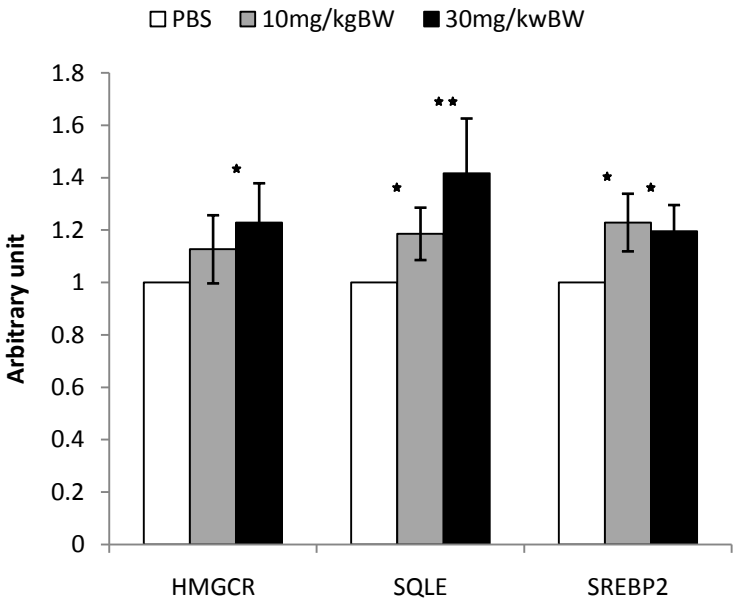

Figure 6.2. Effect of DQ on mRNA levels of hepatic HMGCR, SQLE and SREBP2 after 2 hours of treatment. WT male mice were 8~10 weeks old and intraperitoneally injected with PBS or DQ (10mg/kg BW and 30mg/kg BW). Mice were sacrificed at 2 hours after injections and livers were collected and stored at -80℃. Total RNA were extracted from the frozen livers as described previously. RT-PCR was conducted with gene specific primers as listed in Table 2.3. The amplicons were analyzed by agarose gel electrophoresis with EB staining. Density of each band was measured by using computerized software. Values of DQ treated samples (n = 3) were calculated as ratio to PBS control. * $P < 0.05$ vs. PBS; ** $P < 0.01$ vs. PBS within the same time.

were 42%, 23 and 19% higher ($P < 0.05$) than PBS control. As indicated by figure 6.3, at 6 hours after treatments, SQLE mRNA was consistently higher in the livers of mice treated with 10mg/kg BW or 30mg/kg BW DQ, compared with control; however, the mRNA levels of HMGCR and SREBP2 were decreased after the treatment, and were 17% and 24% lower ($P < 0.05$) in the mice injected with 30mg/kg BW DQ as compared with PBS control. Figure 6.4 indicatesthat DQ treatment increased nuclear SREBP2, while decreased SREBP1 protein, in livers of mice after two hours of injection with 10mg/kg BW DQ.

HepG2 responded to DQ treatment with increased mRNA of HMG CoA reductase. As indicated in Figure 6.5, there was a dose-dependent increase of HMG CoA reductase mRNA in HepG2 cells. The mRNA level of HMG CoA reductase was elevated by 17% ($P < 0.05$) when cells were subjected to 0.75 μM DQ for two hours and cell viability remained at 90% at the end of treatment as shown in Figure 6.5.

6.5 Discussion

The results indicate that superoxide-generator DQ elevated plasma total cholesterol and increased mRNA levels of cholesterol biosynthetic genes, HMG CoA reductase and squalene epoxidase, in the livers of mice at two hours after treatments with 10mg/kg BW and 30mg/kg BW DQ. At the same time, DQ also increased the mRNA level of SREBP2 as well as level of nuclear SREBP2 protein. Similar responses were also observed in HepG2 cells where DQ treatment increased mRNA level of HMGCR. Consistent with our findings, xanthine/xanthine oxidase generated superoxide has been shown to activate the transcription of cholesterol biosynthesis pathway genes in human neuronal cells (255).

To our surprise, DQ treatment was able to increase plasma total cholesterol within two hours, and the high dose treatment resulted in a stronger response. The increase of

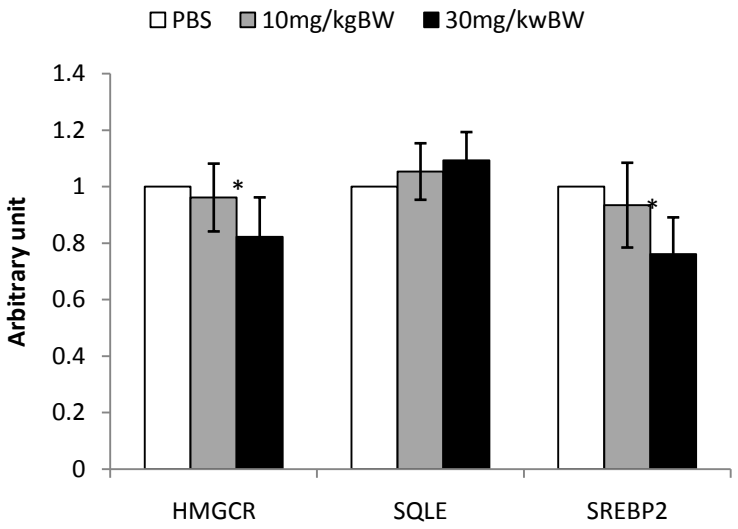

Figure 6.3. Effect of DQ on mRNA levels of hepatic HMGCR, SQLE and SREBP2 after 6 hours of treatment. WT male mice were 8~10 weeks old and intraperitoneally injected with PBS or DQ (10mg/kg BW and 30mg/kg BW). Mice were sacrificed at 6 hours after injections and livers were collected and stored at -80℃. Total RNA was extracted from the frozen livers as described previously. RT-PCR was conducted with gene specific primers as listed in Table 2.3. The amplicons were analyzed by agarose gel electrophoresis with EB staining. Density of each band was measured. Values of DQ treated samples (n = 3) were calculated as ratio to that PBS control. * $P < 0.05$ vs. PBS within the same time.

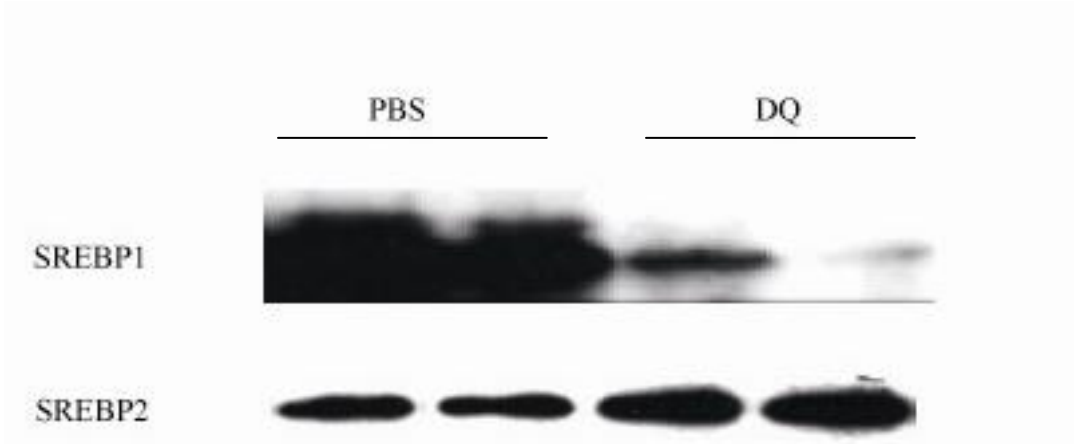

Figure 6.4. Western blot analysis of SREBP1 and SREBP2 in the liver of WT mice treated with DQ. WT male mice were 8~10 weeks old and intraperitoneally injected with PBS or 10mg/kg BW DQ. Mice (n = 3) were sacrificed at 2 hours after injections and livers were collected for nuclei isolation as described previously. Western blot were conducted with 10 microgram nuclear proteins and membranes were probed with anti-SREBP1 and SREBP2 antibodies listed in Table 2.2.

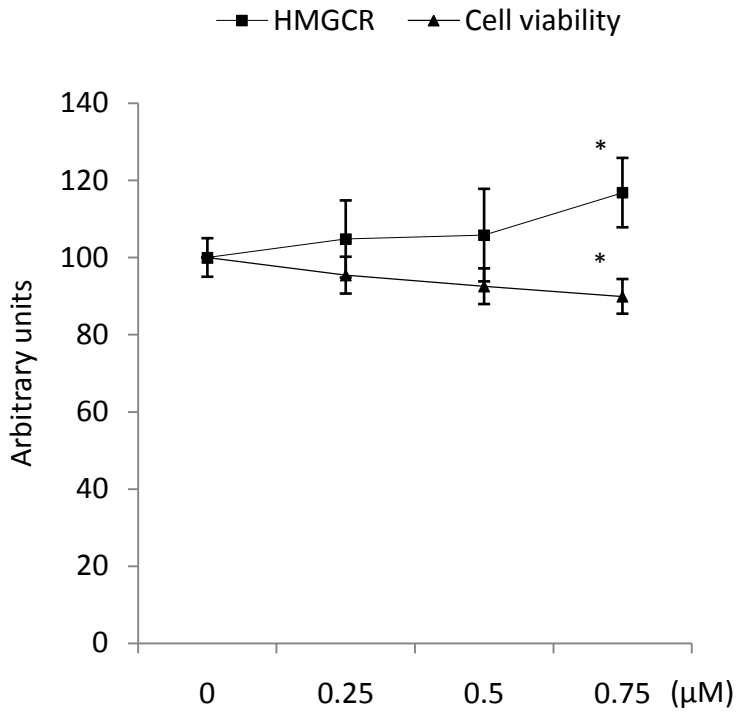

Figure 6.5. Expression of HMG CoA reductase gene in HepG2 cells treated with DQ. HepG2 cells were maintained in DMEM medium. When the cells reached 60–70% confluence, the medium was replaced with experimental medium, which containing 0, 0.25, 0.5 and 0.75 micromole of DQ. After two hours' incubation, cells were washed with warm PBS, and used for total RNA extraction or measuring cell viability. RT-PCR and agarose gel electrophoresis were performed as stated before. Values of DQ treated samples were calculated as ratio to that of non-treated. * $P < 0.05$ vs. non-treated. The figures represent one of three independent experiments with essentially the same results.

plasma total cholesterol in mice injected with low dose (10mg/kg BW) was observed at 6 hours after injection, while high dose (30mg/kg BW) did not produce similar effect. Similar responses were also observed at the level of mRNA. This intrigued us because the high dose DQ treatment showed stronger but shorter effect on plasma cholesterol than the low dose. It may indicate that cells have different mechanisms to cope with the different levels of DQ-induced stress, as observed by Haudek et al. (2008) (256). It is possible that week oxidative stress just tunes the metabolic pathways which are maximally changed under the extreme conditions. Another explanation for dose effect might be that plasma cholesterol is under the feedback control which promotes the clearance when the cholesterol concentration reaches a certain level. The feedback regulation of cholesterol biosynthesis has been well characterized in cells (257).

Oxidative stress induced by DQ has been studied widely in animals (32, 258). DQ is a redox-cycling compound. It accepts an electron from NADPH-cytochrome P-450 reductase in the ER of the hepatocytes and thereby becomes a free radical (259). The DQ radical recycles to the non-radical form by donating its unpaired electron to molecular oxygen (O_2), producing superoxide (260). ROS generally account for the DQ induced metabolic changes.

In the present study, ROS were found to affect the cholesterol biosynthesis at the transcriptional level as indicated by the increased mRNA levels of key cholesterol biosynthetic enzymes, including HMG CoA reductase and squalene epoxidase in mouse and HepG2 cells. In agreement with our results, Recuero et al., (2009) reported that ROS produced by xanthine/xanthine oxidase increased the mRNA levels of cholesterol biosynthetic genes in human neuronal cells (255). Moreover, ROS have been shown to regulate the enzymatic activity of HMG CoA reductase by certain

modifications (245, 246). Therefore, ROS might be involved in the regulation of the cholesterol biosynthesis on transcriptional and post-translational levels.

Further, at the first time, we report that ROS increased SREBP2 mRNA and nuclear protein levels in the livers of mice. There are three different SREBPs: SREBP-1a, -1c and -2. SREBP-1a and -1c are isoforms produced from a single gene by alternate splicing (69). SREBP 2 isoform preferentially regulates genes involved in cholesterol homeostasis including all the cholesterol biosynthetic enzymes while SREBP1c mainly controls the fatty acid synthesis (127). Under normal conditions, SREBPs are activated and translocated into nuclei after the processes of translocation and protease cleavage when cellular cholesterol is depleted, and suppressed by the replete cholesterol (77, 78). This is considered as a major regulatory mechanism of SREBPs while other regulations are also suggested, including phosphorylation and sumylation, which affected its activity and stability in nuclei (129, 228). In addition, the transcription of SREBP2 is under its own control. Therefore, the increased nuclear SREBP2 accounted for, at least partially, the increased mRNA of HMGCR and SQLE in the liver of mice treated with DQ.

Interestingly, DQ treatment increased SREBP2 but reduced SREBP1 in hepatic nuclei of mice. The balance between SREBP1 and SREBP2 are important in maintaining the normal lipids biosynthesis, as demonstrated by Shimano et al., (1997) (159, 226). The changes induced by DQ might represent the cellular priorities of metabolic needs in order to survive the unfavorable condition, and SREBP 1 and 2 serve as the switch to direct energy to the critical reactions. It also is proposed as a survival strategy for yeast that the activation of SREBP homologue in yeast, which induces the synthesis of sterol, under hypoxia is a necessary process for cells to survive through the adverse condition (75, 158).

In summary, our results demonstrated that DQ induced oxidative stress increased plasma cholesterol, and elevated HMG CoA and squalene epoxidase transcription in the liver of mice as well in HepG2 cells, which may be mediated, at least partially, by increasing nuclear SREBP2. These findings suggest that ROS play an importance role in regulation of cholesterol biosynthesis, and SREBP2 may mediate this response. This study makes ROS generators or scavengers potentially useful for clinical usage in order to interfere with problems related to cholesterol biosynthesis.

CHAPTER SEVEN

SUMMARY AND GENERAL DISCUSSION

Antioxidant enzymes play important roles in maintaining the cellular redox homeostasis and protecting cells from the damage caused by ROS. The deficiencies of antioxidant enzymes cause various health problems in animals due to the consequences of disrupted redox balance. ROS, which could be toxic or function as cellular signaling molecules, carry the primary interest in the exploration of antioxidant deficiency induced biological alterations. Several transcriptional factors, enzymes and small antioxidant molecules have been identified as ROS responsive agents that mediate the signal transduction of ROS although the exact regulatory mechanism remains largely unknown.

SOD1, mainly located in cytosol, has been appreciated for decades as an important antioxidant enzyme in the clearance of superoxide. Generally, superoxide is converted into hydrogen peroxide by superoxide dismutase and the latter is further converted to water by glutathione peroxide or catalase. Apparently SOD1 regulates the cellular level of superoxide and could influence the cellular redox balance. Numbers of studies show that the deficiency of SOD1 leads to abnormities of different tissues and organs in the genetic knockout models (2-9). The abnormal lipid deposition in liver and heart discovered in many studies indicates the potential role of SOD1 in lipid metabolism (9, 121). The association or indirect link between ROS and energy or lipid metabolism also suggested the possible regulatory role of SOD1 (192, 240-244). Obesity model caused by over expression of glutathione peroxidase 1, discovered in our lab, strongly supports the importance of redox balance in the regulation of energy and lipid homeostasis (131). The accidental observation of severe dyslipidemia in SOD1 mice further intrigued us to investigate the metabolic change, specifically lipid metabolism, caused by the knockout of SOD1 and the molecular mechanism behind this interesting

phenotype. This dissertation was aimed to demonstrate the indispensible role of SOD1 in maintaining the normal lipid metabolism.

To address the question of the regulatory role of SOD1 in lipid metabolism and explore possible strategies to counteract the abnormal changes induced by the knockout of SOD1, several hypotheses have been developed and examined by separate studies with different approaches. The activation of cholesterol biosynthetic pathway significantly attracted our attention because of the biological significance of cholesterol. It is known that both fatty acids and cholesterol are synthesized with difference pathways. However, both pathways begin with the same substrate, cellular acetyl CoA, which is the small unit of energy in cells. While cholesterol is well known as an essential structural component of cells and a precursor of important hormones, it is possible that it is also used as an energy carrier for storage or excretion, where cholesterol synthesis is activated under the positive energy balance as an alternative way to store or eliminate the excessive energy. It seemed to really happen in SOD-/- mice as stated in Chapter Three, which drove us to exam the cholesterol biosynthetic pathway closely in the following studies, where triglyceride was also included.

In Chapter Three, the lipid disorder was first characterized in both young and adult SOD1-/- mice followed by molecular measurements of related pathways. The knockout of SOD1 causes hypercholesterolemia and hypotriglyceridemia with irregular lipid accumulation in liver, heart, kidney, muscle and testis. In contrast to the suppressed accumulation of fatty acids/triglyceride, the cholesterol synthetic pathway was consistently activated in SOD1-/- mice as indicated by increased mRNA and protein levels of related genes at 3 wk and 9 wk of age. The significant increase of SREBP2 and decrease of SREBP1 in SOD1-/- mice suggested the switch-like function of these two proteins under unfavorable conditions. It was obvious that the knockout of SOD1 shifted the energy from fatty acid/triglyceride into cholesterol synthesis by

activation the classical biosynthetic pathway.

In Chapter Four, experiments were designed to test the hypothesis that the metabolic changes induced by the knockout of SOD1 depended on dietary energy, which could be reversed by high fat diet. However, high fat diet reduced body weight of SOD1-/- mice by 17% and (V)LDL triglyceride by 15%, although the plasma total cholesterol, total triglyceride and fecal cholesterol in SOD1-/- mice were not significantly affected. High fat diet significantly increased levels of nuclear SREBP1 and SREBP2 proteins in both genotypes while did not reverse the trend induced by SOD1-/- under normal feeding. These results indicate that the increased dietary energy did not reverse the metabolic changes and the activation of cholesterol biosynthesis might not be affected by high fat diet in SOD1-/- mice.

In Chapter Five, experiments were conducted to test the hypothesis that dietary Cu may counteract the metabolic changes induced by the knockout of SOD1 as SOD1 is the major Cu-containing protein. Interestingly, Cu deficiency did not affect the concentrations of blood lipids in SOD1-/- mice while high Cu was only found to reduce hepatic triglyceride with no effect on plasma cholesterol and triglyceride and hepatic cholesterol. An additional finding was that the expression of SOD1 protein was negatively related to dietary Cu level in WT mice, which was opposite to the changes of total enzyme activity. SREBPs proteins showed remarkable changes but only partially matched the predictions of the phenotype. Therefore, dietary supplementation of excess Cu was unable to reverse the consequence of SOD1 deficiency in mice.

In Chapter Six, experiments were conducted to test the hypothesis that ROS were the primary factors in regulation of cholesterol biosynthesis as observed in the SOD1-/- mice. Surprisingly, significant increases, of 23% and 29%, total plasma cholesterol were observed within two hours in mice injected with DQ at 10mg/kg BW and

30mg/kg BW, respectively; we also found that mRNA of HMG CoA reductase and squalene epoxidase were elevated by 18% and 13%, respectively, compared with control. HepG2 cells also showed a similar response to DQ treatment with increased HMGCR mRNA levels. These results suggest that ROS may play an important role in regulation of cholesterol biosynthesis which is possibly mediated by SREBP2.

The lipid disorder in SOD1-/- mice did not depend on age and diets. Oxidative stress induced by DQ showed positive effects on the transcription of cholesterol biosynthetic genes in mice and cells model as well as on the concentrations of plasma cholesterol in mice. Oxidative stress have been shown to increase with impaired SOD1 activity in animals on the Cu deficient diet, which also increased plasma cholesterol as a result of elevated biosynthesis. This may suggest that the loss of SOD1 activity is the primary factor of Cu deficiency-induced lipid disorder.

High fat diet has also been reported to increase oxidative stress in animals, while similar increase is observed in obese patients (164, 181-183, 213, 261-263). High fat diet may aggravate oxidative stress in SOD1-/- mice, which could explain the further loss of body weight and reduced plasma triglyceride. Therefore, extra caution should be taken in using high fat diet to improve body weight of patients whose antioxidant system is impaired.

This dissertation indicates a possible way to interfere with lipid metabolism by SOD1 or ROS generators, which could switch fatty acid synthesis to cholesterol synthesis and the latter could be degraded or excreted from bodies. This work provides promising tools for treating obesity. However, the detrimental effect of oxidative stress should also be considered.

In summary, the major findings of this dissertation include: 1) knockout of SOD1 caused dyslipidemia as well as abnormal cholesterol and triglyceride deposition among tissues and organs; 2) SOD1 deficiency activated cholesterol biosynthetic

pathway and was transcriptionally associated with increased SREBP2 protein; 3) knockout of SOD1 altered the ratio of SREBP1 and SREBP2 proteins as well as their target genes and plasma cholesterol and triglyceride; 4) high fat diet exacerbated the loss of body weight in SOD1-/- mice without benefits on the lipid disorder; 5) dietary excess Cu did not rescue the lipid disorder in SOD1-/- mice while the similarities of hypercholesterolemia caused by dietary Cu deficiency and by knockout of SOD1were observed; 6) the DQ-induced oxidative stress elevated the plasma cholesterol along with increased transcription of cholesterol synthetic genes *in vivo* and *in vitro*. It could be concluded that the impaired lipid metabolism in the SOD1-/- mice resulted from the loss of SOD1 function in scavenging superoxide anion.. However, further studies are needed to dissect the exact molecular mechanism of the regulatory role of SOD1 and its interaction with ROS in lipid metabolism.

REFERENCES

1. Semenza GL. Life with oxygen. Science. 2007 Oct 5;318:62-4.

2. Busuttil RA, Garcia AM, Cabrera C, Rodriguez A, Suh Y, Kim WH, Huang TT, Vijg J. Organ-specific increase in mutation accumulation and apoptosis rate in CuZn-superoxide dismutase-deficient mice. Cancer Res. 2005 Dec 15;65:11271-5.

3. Kessova IG, Cederbaum AI. Mitochondrial alterations in livers of Sod1-/- mice fed alcohol. Free Radic Biol Med. 2007 May 15;42:1470-80.

4. Elchuri S, Oberley TD, Qi W, Eisenstein RS, Jackson Roberts L, Van Remmen H, Epstein CJ, Huang TT. CuZnSOD deficiency leads to persistent and widespread oxidative damage and hepatocarcinogenesis later in life. Oncogene. 2005 Jan 13;24:367-80.

5. Imamura Y, Noda S, Hashizume K, Shinoda K, Yamaguchi M, Uchiyama S, Shimizu T, Mizushima Y, Shirasawa T, Tsubota K. Drusen, choroidal neovascularization, and retinal pigment epithelium dysfunction in SOD1-deficient mice: a model of age-related macular degeneration. Proc Natl Acad Sci U S A. 2006 Jul 25;103:11282-7.

6. Olofsson EM, Marklund SL, Karlsson K, Brannstrom T, Behndig A. In vitro glucose-induced cataract in copper-zinc superoxide dismutase null mice. Exp Eye Res. 2005 Dec;81:639-46.

7. Matzuk MM, Dionne L, Guo Q, Kumar TR, Lebovitz RM. Ovarian function in superoxide dismutase 1 and 2 knockout mice. Endocrinology. 1998 Sep;139:4008-11.

8. Reaume AG, Elliott JL, Hoffman EK, Kowall NW, Ferrante RJ, Siwek DF, Wilcox HM, Flood DG, Beal MF, et al. Motor neurons in Cu/Zn superoxide dismutase-deficient mice develop normally but exhibit enhanced cell death after axonal injury. Nat Genet. 1996 May;13:43-7.

9. Kostrominova TY, Pasyk KA, Van Remmen H, Richardson AG, Faulkner JA. Adaptive changes in structure of skeletal muscles from adult Sod1 homozygous knockout mice. Cell Tissue Res. 2007 Mar;327:595-605.

10. Halliwell B. Oxygen and nitrogen are pro-carcinogens. Damage to DNA by reactive oxygen, chlorine and nitrogen species: measurement, mechanism and the effects of nutrition. Mutat Res. 1999 Jul 15;443:37-52.

11. Frimer AA. Superoxide chemistry in non-aqueous media. Basic Life Sci. 1988;49:29-38.

12. Waghray M, Cui Z, Horowitz JC, Subramanian IM, Martinez FJ, Toews GB, Thannickal VJ. Hydrogen peroxide is a diffusible paracrine signal for the induction of epithelial cell death by activated myofibroblasts. FASEB J. 2005 May;19:854-6.

13. Gutteridge JM, Maidt L, Poyer L. Superoxide dismutase and Fenton chemistry. Reaction of ferric-EDTA complex and ferric-bipyridyl complex with hydrogen peroxide without the apparent formation of iron(II). Biochem J. 1990 Jul 1;269:169-74.

14. Buechter DD. Free radicals and oxygen toxicity. Pharm Res. 1988 May;5:253-60.

15. Sies H, Cadenas E. Oxidative stress: damage to intact cells and organs. Philos Trans R Soc Lond B Biol Sci. 1985 Dec 17;311:617-31.

16. Davies SM, Poljak A, Duncan MW, Smythe GA, Murphy MP. Measurements of protein carbonyls, ortho- and meta-tyrosine and oxidative phosphorylation complex activity in mitochondria from young and old rats. Free Radic Biol Med. 2001 Jul 15;31:181-90.

17. Fraga CG, Shigenaga MK, Park JW, Degan P, Ames BN. Oxidative damage to DNA during aging: 8-hydroxy-2'-deoxyguanosine in rat organ DNA and urine. Proc Natl Acad Sci U S A. 1990 Jun;87:4533-7.

18. Hwang ES, Kim GH. Biomarkers for oxidative stress status of DNA, lipids, and proteins in vitro and in vivo cancer research. Toxicology. 2007 Jan 5;229:1-10.

19. May JM, de Haen C. The insulin-like effect of hydrogen peroxide on pathways of lipid synthesis in rat adipocytes. J Biol Chem. 1979 Sep 25;254:9017-21.

20. Czech MP, Lawrence JC, Jr., Lynn WS. Activation of hexose transport by concanavalin A in isolated brown fat cells. Effects of cell surface modification with neuraminidase and trypsin on lectin and insulin action. J Biol Chem. 1974 Dec 10;249:7499-505.

21. McCubrey JA, Lahair MM, Franklin RA. Reactive oxygen species-induced activation of the MAP kinase signaling pathways. Antioxid Redox Signal. 2006 Sep-Oct;8:1775-89.

22. Singh I, Pahan K, Khan M, Singh AK. Cytokine-mediated induction of ceramide production is redox-sensitive. Implications to proinflammatory cytokine-mediated apoptosis in demyelinating diseases. J Biol Chem. 1998 Aug 7;273:20354-62.

23. Chandel NS, Maltepe E, Goldwasser E, Mathieu CE, Simon MC, Schumacker PT. Mitochondrial reactive oxygen species trigger hypoxia-induced transcription. Proc Natl Acad Sci U S A. 1998 Sep 29;95:11715-20.

24. Griendling KK, Ushio-Fukai M. Reactive oxygen species as mediators of angiotensin II signaling. Regul Pept. 2000 Jul 28;91:21-7.

25. Shetty V, Neubert TA. Characterization of Novel Oxidation Products of Cysteine in an Active Site Motif Peptide of PTP1B. J Am Soc Mass Spectrom. 2009 May 3.

26. Barrett WC, DeGnore JP, Keng YF, Zhang ZY, Yim MB, Chock PB. Roles of superoxide radical anion in signal transduction mediated by reversible regulation of protein-tyrosine phosphatase 1B. J Biol Chem. 1999 Dec 3;274:34543-6.

27. Nguyen T, Sherratt PJ, Pickett CB. Regulatory mechanisms controlling gene expression mediated by the antioxidant response element. Annu Rev Pharmacol Toxicol. 2003;43:233-60.

28. Nguyen T, Nioi P, Pickett CB. The Nrf2-antioxidant response element signaling pathway and its activation by oxidative stress. J Biol Chem. 2009 May 15;284:13291-5.

29. Schmidt KN, Amstad P, Cerutti P, Baeuerle PA. The roles of hydrogen peroxide and superoxide as messengers in the activation of transcription factor NF-kappa B. Chem Biol. 1995 Jan;2:13-22.

30. Ammendola R, Mesuraca M, Russo T, Cimino F. The DNA-binding efficiency of Sp1 is affected by redox changes. Eur J Biochem. 1994 Oct 1;225:483-9.

31. Seto E, Lewis B, Shenk T. Interaction between transcription factors Sp1 and YY1. Nature. 1993 Sep 30;365:462-4.

32. Fu Y, Cheng WH, Porres JM, Ross DA, Lei XG. Knockout of cellular glutathione peroxidase gene renders mice susceptible to diquat-induced oxidative stress. Free Radic Biol Med. 1999 Sep;27:605-11.

33. Yoshida T, Maulik N, Engelman RM, Ho YS, Das DK. Targeted disruption of the

mouse Sod I gene makes the hearts vulnerable to ischemic reperfusion injury. Circ Res. 2000 Feb 18;86:264-9.

34. Muller FL, Liu Y, Van Remmen H. Complex III releases superoxide to both sides of the inner mitochondrial membrane. J Biol Chem. 2004 Nov 19;279:49064-73.

35. Fridovich I. Superoxide dismutases: defence against endogenous superoxide radical. Ciba Found Symp. 1978 Jun 6-8:77-93.

36. Huie RE, Padmaja S. The reaction of no with superoxide. Free Radic Res Commun. 1993;18:195-9.

37. Hurst JK. Whence nitrotyrosine? J Clin Invest. 2002 May;109:1287-9.

38. Greenacre SA, Ischiropoulos H. Tyrosine nitration: localisation, quantification, consequences for protein function and signal transduction. Free Radic Res. 2001 Jun;34:541-81.

39. Drew B, Leeuwenburgh C. Aging and the role of reactive nitrogen species. Ann N Y Acad Sci. 2002 Apr;959:66-81.

40. Wiseman H, Halliwell B. Damage to DNA by reactive oxygen and nitrogen species: role in inflammatory disease and progression to cancer. Biochem J. 1996 Jan 1;313 (Pt 1):17-29.

41. Zelko IN, Mariani TJ, Folz RJ. Superoxide dismutase multigene family: a comparison of the CuZn-SOD (SOD1), Mn-SOD (SOD2), and EC-SOD (SOD3) gene structures, evolution, and expression. Free Radic Biol Med. 2002 Aug 1;33:337-49.

42. Crapo JD, Oury T, Rabouille C, Slot JW, Chang LY. Copper,zinc superoxide dismutase is primarily a cytosolic protein in human cells. Proc Natl Acad Sci U S A. 1992 Nov 1;89:10405-9.

43. Liochev SI, Fridovich I. Copper- and zinc-containing superoxide dismutase can act as a superoxide reductase and a superoxide oxidase. J Biol Chem. 2000 Dec 8;275:38482-5.

44. Rosen DR. Mutations in Cu/Zn superoxide dismutase gene are associated with familial amyotrophic lateral sclerosis. Nature. 1993 Jul 22;364:362.

45. Gurney ME, Pu H, Chiu AY, Dal Canto MC, Polchow CY, Alexander DD, Caliendo J, Hentati A, Kwon YW, et al. Motor neuron degeneration in mice that express a human Cu,Zn superoxide dismutase mutation. Science. 1994 Jun 17;264:1772-5.

46. Ripps ME, Huntley GW, Hof PR, Morrison JH, Gordon JW. Transgenic mice expressing an altered murine superoxide dismutase gene provide an animal model of amyotrophic lateral sclerosis. Proc Natl Acad Sci U S A. 1995 Jan 31;92:689-93.

47. Yamanobe T, Okada F, Iuchi Y, Onuma K, Tomita Y, Fujii J. Deterioration of ischemia/reperfusion-induced acute renal failure in SOD1-deficient mice. Free Radic Res. 2007 Feb;41:200-7.

48. Iuchi Y, Okada F, Onuma K, Onoda T, Asao H, Kobayashi M, Fujii J. Elevated oxidative stress in erythrocytes due to a SOD1 deficiency causes anaemia and triggers autoantibody production. Biochem J. 2007 Mar 1;402:219-27.

49. Dimayuga FO, Wang C, Clark JM, Dimayuga ER, Dimayuga VM, Bruce-Keller AJ. SOD1 overexpression alters ROS production and reduces neurotoxic inflammatory signaling in microglial cells. J Neuroimmunol. 2007 Jan;182:89-99.

50. Huang CY, Fujimura M, Noshita N, Chang YY, Chan PH. SOD1 down-regulates NF-kappaB and c-Myc expression in mice after transient focal cerebral ischemia. J Cereb Blood Flow Metab. 2001 Feb;21:163-73.

51. Rao AK, Ziegler YS, McLeod IX, Yates JR, Nardulli AM. Effects of Cu/Zn superoxide dismutase on estrogen responsiveness and oxidative stress in human breast cancer cells. Mol Endocrinol. 2008 May;22:1113-24.

52. Sentman ML, Granstrom M, Jakobson H, Reaume A, Basu S, Marklund SL. Phenotypes of mice lacking extracellular superoxide dismutase and copper- and zinc-containing superoxide dismutase. J Biol Chem. 2006 Mar 17;281:6904-9.

53. Dietschy JM, Turley SD. Control of cholesterol turnover in the mouse. J Biol Chem. 2002 Feb 8;277:3801-4.

54. Lange Y, Ye J, Rigney M, Steck TL. Regulation of endoplasmic reticulum cholesterol by plasma membrane cholesterol. J Lipid Res. 1999 Dec;40:2264-70.

55. Maxfield FR, Wustner D. Intracellular cholesterol transport. J Clin Invest. 2002 Oct;110:891-8.

56. Zannis VI, Koukos G, Drosatos K, Vezeridis A, Zanni EE, Kypreos KE, Chroni A. Discrete roles of apoA-I and apoE in the biogenesis of HDL species: lessons learned from gene transfer studies in different mouse models. Ann Med. 2008 Feb;40 Suppl 1:14-28.

57. Zannis VI, Chroni A, Krieger M. Role of apoA-I, ABCA1, LCAT, and SR-BI in the biogenesis of HDL. J Mol Med. 2006 Apr;84:276-94.

58. Shelness GS, Sellers JA. Very-low-density lipoprotein assembly and secretion. Curr Opin Lipidol. 2001 Apr;12:151-7.

59. Spady DK, Meddings JB, Dietschy JM. Kinetic constants for receptor-dependent and receptor-independent low density lipoprotein transport in the tissues of the rat and hamster. J Clin Invest. 1986 May;77:1474-81.

60. Durrington P. Dyslipidaemia. Lancet. 2003 Aug 30;362:717-31.

61. Brown MS, Goldstein JL. A receptor-mediated pathway for cholesterol homeostasis. Science. 1986 Apr 4;232:34-47.

62. Abifadel M, Varret M, Rabes JP, Allard D, Ouguerram K, Devillers M, Cruaud C, Benjannet S, Wickham L, et al. Mutations in PCSK9 cause autosomal dominant hypercholesterolemia. Nat Genet. 2003 Jun;34:154-6.

63. Young SG, Hubl ST, Chappell DA, Smith RS, Claiborne F, Snyder SM, Terdiman JF. Familial hypobetalipoproteinemia associated with a mutant species of apolipoprotein B (B-46). N Engl J Med. 1989 Jun 15;320:1604-10.

64. Garcia CK, Wilund K, Arca M, Zuliani G, Fellin R, Maioli M, Calandra S, Bertolini S, Cossu F, et al. Autosomal recessive hypercholesterolemia caused by mutations in a putative LDL receptor adaptor protein. Science. 2001 May 18;292:1394-8.

65. Soutar AK, Naoumova RP. Mechanisms of disease: genetic causes of familial hypercholesterolemia. Nat Clin Pract Cardiovasc Med. 2007 Apr;4:214-25.

66. Yokode M, Hammer RE, Ishibashi S, Brown MS, Goldstein JL. Diet-induced hypercholesterolemia in mice: prevention by overexpression of LDL receptors. Science. 1990 Nov 30;250:1273-5.

67. Polychronopoulos E, Panagiotakos DB, Polystipioti A. Diet, lifestyle factors and

hypercholesterolemia in elderly men and women from Cyprus. Lipids Health Dis. 2005;4:17.

68. Hua X, Yokoyama C, Wu J, Briggs MR, Brown MS, Goldstein JL, Wang X. SREBP-2, a second basic-helix-loop-helix-leucine zipper protein that stimulates transcription by binding to a sterol regulatory element. Proc Natl Acad Sci U S A. 1993 Dec 15;90:11603-7.

69. Shimomura I, Shimano H, Horton JD, Goldstein JL, Brown MS. Differential expression of exons 1a and 1c in mRNAs for sterol regulatory element binding protein-1 in human and mouse organs and cultured cells. J Clin Invest. 1997 Mar 1;99:838-45.

70. Hua X, Sakai J, Ho YK, Goldstein JL, Brown MS. Hairpin orientation of sterol regulatory element-binding protein-2 in cell membranes as determined by protease protection. J Biol Chem. 1995 Dec 8;270:29422-7.

71. Sun LP, Seemann J, Goldstein JL, Brown MS. Sterol-regulated transport of SREBPs from endoplasmic reticulum to Golgi: Insig renders sorting signal in Scap inaccessible to COPII proteins. Proc Natl Acad Sci U S A. 2007 Apr 17;104:6519-26.

72. Edwards PA, Tabor D, Kast HR, Venkateswaran A. Regulation of gene expression by SREBP and SCAP. Biochim Biophys Acta. 2000 Dec 15;1529:103-13.

73. Goldstein JL, DeBose-Boyd RA, Brown MS. Protein sensors for membrane sterols. Cell. 2006 Jan 13;124:35-46.

74. Radhakrishnan A, Ikeda Y, Kwon HJ, Brown MS, Goldstein JL. Sterol-regulated transport of SREBPs from endoplasmic reticulum to Golgi: oxysterols block transport by binding to Insig. Proc Natl Acad Sci U S A. 2007 Apr 17;104:6511-8.

75. Espenshade PJ, Hughes AL. Regulation of sterol synthesis in eukaryotes. Annu Rev Genet. 2007;41:401-27.

76. Radhakrishnan A, Sun LP, Kwon HJ, Brown MS, Goldstein JL. Direct binding of cholesterol to the purified membrane region of SCAP: mechanism for a sterol-sensing domain. Mol Cell. 2004 Jul 23;15:259-68.

77. Korn BS, Shimomura I, Bashmakov Y, Hammer RE, Horton JD, Goldstein JL, Brown MS. Blunted feedback suppression of SREBP processing by dietary cholesterol in transgenic mice expressing sterol-resistant SCAP(D443N). J Clin Invest. 1998 Dec 15;102:2050-60.

78. Sakai J, Rawson RB, Espenshade PJ, Cheng D, Seegmiller AC, Goldstein JL, Brown MS. Molecular identification of the sterol-regulated luminal protease that cleaves SREBPs and controls lipid composition of animal cells. Mol Cell. 1998 Oct;2:505-14.

79. Briggs MR, Yokoyama C, Wang X, Brown MS, Goldstein JL. Nuclear protein that binds sterol regulatory element of low density lipoprotein receptor promoter. I. Identification of the protein and delineation of its target nucleotide sequence. J Biol Chem. 1993 Jul 5;268:14490-6.

80. Wang X, Sato R, Brown MS, Hua X, Goldstein JL. SREBP-1, a membrane-bound transcription factor released by sterol-regulated proteolysis. Cell. 1994 Apr 8;77:53-62.

81. Shimano H, Horton JD, Hammer RE, Shimomura I, Brown MS, Goldstein JL. Overproduction of cholesterol and fatty acids causes massive liver enlargement in transgenic mice expressing truncated SREBP-1a. J Clin Invest. 1996 Oct 1;98:1575-84.

82. Ziouzenkova O, Perrey S, Asatryan L, Hwang J, MacNaul KL, Moller DE, Rader DJ, Sevanian A, Zechner R, et al. Lipolysis of triglyceride-rich lipoproteins generates PPAR ligands: evidence for an antiinflammatory role for lipoprotein lipase. Proc Natl Acad Sci U S A. 2003 Mar 4;100:2730-5.

83. Riserus U, Sprecher D, Johnson T, Olson E, Hirschberg S, Liu A, Fang Z, Hegde P, Richards D, et al. Activation of PPAR{delta} promotes reversal of multiple metabolic abnormalities, reduces oxidative stress and increases fatty acid oxidation in moderately obese men. Diabetes. 2007 Nov 16.

84. Dreyer C, Keller H, Mahfoudi A, Laudet V, Krey G, Wahli W. Positive regulation of the peroxisomal beta-oxidation pathway by fatty acids through activation of peroxisome proliferator-activated receptors (PPAR). Biol Cell. 1993;77:67-76.

85. Kalaany NY, Gauthier KC, Zavacki AM, Mammen PP, Kitazume T, Peterson JA, Horton JD, Garry DJ, Bianco AC, Mangelsdorf DJ. LXRs regulate the balance between fat storage and oxidation. Cell Metab. 2005 Apr;1:231-44.

86. DeBose-Boyd RA, Ou J, Goldstein JL, Brown MS. Expression of sterol regulatory element-binding protein 1c (SREBP-1c) mRNA in rat hepatoma cells requires endogenous LXR ligands. Proc Natl Acad Sci U S A. 2001 Feb 13;98:1477-82.

87. Schultz JR, Tu H, Luk A, Repa JJ, Medina JC, Li L, Schwendner S, Wang S,

Thoolen M, et al. Role of LXRs in control of lipogenesis. Genes Dev. 2000 Nov 15;14:2831-8.

88. Millatt LJ, Bocher V, Fruchart JC, Staels B. Liver X receptors and the control of cholesterol homeostasis: potential therapeutic targets for the treatment of atherosclerosis. Biochim Biophys Acta. 2003 Mar 17;1631:107-18.

89. Venkateswaran A, Laffitte BA, Joseph SB, Mak PA, Wilpitz DC, Edwards PA, Tontonoz P. Control of cellular cholesterol efflux by the nuclear oxysterol receptor LXR alpha. Proc Natl Acad Sci U S A. 2000 Oct 24;97:12097-102.

90. Janowski BA, Grogan MJ, Jones SA, Wisely GB, Kliewer SA, Corey EJ, Mangelsdorf DJ. Structural requirements of ligands for the oxysterol liver X receptors LXRalpha and LXRbeta. Proc Natl Acad Sci U S A. 1999 Jan 5;96:266-71.

91. Kliewer SA, Sundseth SS, Jones SA, Brown PJ, Wisely GB, Koble CS, Devchand P, Wahli W, Willson TM, et al. Fatty acids and eicosanoids regulate gene expression through direct interactions with peroxisome proliferator-activated receptors alpha and gamma. Proc Natl Acad Sci U S A. 1997 Apr 29;94:4318-23.

92. Caro JF, Amatruda JM. The regulation of lipid synthesis in freshly isolated and primary cultures of hepatocytes from fasted rats: the primary role of insulin. Metabolism. 1982 Jan;31:14-8.

93. Geelen MJ, Beynen AC, Christiansen RZ, Lepreau-Jose MJ, Gibson DM. Short-term effects of insulin and glucagon on lipid synthesis in isolated rat hepatocytes. Covariance of acetyl-CoA carboxylase activity and the rate of 3H2O incorporation into fatty acids. FEBS Lett. 1978 Nov 15;95:326-30.

94. Koning AJ, Roberts CJ, Wright RL. Different subcellular localization of Saccharomyces cerevisiae HMG-CoA reductase isozymes at elevated levels corresponds to distinct endoplasmic reticulum membrane proliferations. Mol Biol Cell. 1996 May;7:769-89.

95. Holdgate GA, Ward WH, McTaggart F. Molecular mechanism for inhibition of 3-hydroxy-3-methylglutaryl CoA (HMG-CoA) reductase by rosuvastatin. Biochem Soc Trans. 2003 Jun;31:528-31.

96. Istvan ES, Palnitkar M, Buchanan SK, Deisenhofer J. Crystal structure of the catalytic portion of human HMG-CoA reductase: insights into regulation of activity and catalysis. EMBO J. 2000 Mar 1;19:819-30.

97. Istvan ES, Deisenhofer J. The structure of the catalytic portion of human HMG-CoA reductase. Biochim Biophys Acta. 2000 Dec 15;1529:9-18.

98. Ravid T, Doolman R, Avner R, Harats D, Roitelman J. The ubiquitin-proteasome pathway mediates the regulated degradation of mammalian 3-hydroxy-3-methylglutaryl-coenzyme A reductase. J Biol Chem. 2000 Nov 17;275:35840-7.

99. Song BL, Javitt NB, DeBose-Boyd RA. Insig-mediated degradation of HMG CoA reductase stimulated by lanosterol, an intermediate in the synthesis of cholesterol. Cell Metab. 2005 Mar;1:179-89.

100. Burg JS, Powell DW, Chai R, Hughes AL, Link AJ, Espenshade PJ. Insig regulates HMG-CoA reductase by controlling enzyme phosphorylation in fission yeast. Cell Metab. 2008 Dec;8:522-31.

101. Marrero PF, Haro D, Hegardt FG. Phosphorylation of HMG-CoA reductase induced by mevalonate accelerates its rate of degradation in isolated rat hepatocytes. FEBS Lett. 1986 Mar 3;197:183-6.

102. Sato R, Goldstein JL, Brown MS. Replacement of serine-871 of hamster 3-hydroxy-3-methylglutaryl-CoA reductase prevents phosphorylation by AMP-activated kinase and blocks inhibition of sterol synthesis induced by ATP depletion. Proc Natl Acad Sci U S A. 1993 Oct 15;90:9261-5.

103. Lei KY. Dietary copper: cholesterol and lipoprotein metabolism. Annu Rev Nutr. 1991;11:265-83.

104. al-Othman AA, Rosenstein F, Lei KY. Copper deficiency alters plasma pool size, percent composition and concentration of lipoprotein components in rats. J Nutr. 1992 Jun;122:1199-204.

105. Bunce GE. Hypercholesterolemia of copper deficiency is linked to glutathione metabolism and regulation of hepatic HMG-CoA reductase. Nutr Rev. 1993 Oct;51:305-7.

106. Hamilton IM, Gilmore WS, Strain JJ. Marginal copper deficiency and atherosclerosis. Biol Trace Elem Res. 2000 Winter;78:179-89.

107. Kim S, Chao PY, Allen KG. Inhibition of elevated hepatic glutathione abolishes copper deficiency cholesterolemia. FASEB J. 1992 Apr;6:2467-71.

108. Carr TP, Lei KY. In vivo apoprotein catabolism of high density lipoproteins in copper-deficient, hypercholesterolemic rats. Proc Soc Exp Biol Med. 1989 Sep;191:370-6.

109. Lefevre M, Keen CL, Lonnerdal B, Hurley LS, Schneeman BO. Copper deficiency-induced hypercholesterolemia: effects on HDL subfractions and hepatic lipoprotein receptor activity in the rat. J Nutr. 1986 Sep;116:1735-46.

110. Young NL, Harvey PW, Elovson J. Radioimmunoassay of rat apolipoprotein B peptides in lipoproteins and tissues. Anal Biochem. 1987 May 1;162:311-8.

111. Yount NY, McNamara DJ, Al-Othman AA, Lei KY. The effect of copper deficiency on rat hepatic 3-hydroxy-3-methylglutaryl coenzyme A reductase activity. J Nutr Biochem. 1990 Jan;1:21-7.

112. Tang Z, Gasperkova D, Xu J, Baillie R, Lee JH, Clarke SD. Copper deficiency induces hepatic fatty acid synthase gene transcription in rats by increasing the nuclear content of mature sterol regulatory element binding protein 1. J Nutr. 2000 Dec;130:2915-21.

113. Lei KY. Oxidation, excretion, and tissue distribution of [26-14C] cholesterol in copper-deficient rats. J Nutr. 1978 Feb;108:232-7.

114. Loudianos G, Gitlin JD. Wilson's disease. Semin Liver Dis. 2000;20:353-64.

115. Huster D, Purnat TD, Burkhead JL, Ralle M, Fiehn O, Stuckert F, Olson NE, Teupser D, Lutsenko S. High copper selectively alters lipid metabolism and cell cycle machinery in the mouse model of Wilson disease. J Biol Chem. 2007 Mar 16;282:8343-55.

116. Ho YS, Gargano M, Cao J, Bronson RT, Heimler I, Hutz RJ. Reduced fertility in female mice lacking copper-zinc superoxide dismutase. J Biol Chem. 1998 Mar 27;273:7765-9.

117. Lowry OH, Rosebrough NJ, Farr AL, Randall RJ. Protein measurement with the Folin phenol reagent. J Biol Chem. 1951 Nov;193:265-75.

118. Folch J, Lees M, Sloane Stanley GH. A simple method for the isolation and purification of total lipides from animal tissues. J Biol Chem. 1957 May;226:497-509.

119. Xia XG, Zhou H, Samper E, Melov S, Xu Z. Pol II-expressed shRNA knocks

down Sod2 gene expression and causes phenotypes of the gene knockout in mice. PLoS Genet. 2006 Jan;2:e10.

120. Lebovitz RM, Zhang H, Vogel H, Cartwright J, Jr., Dionne L, Lu N, Huang S, Matzuk MM. Neurodegeneration, myocardial injury, and perinatal death in mitochondrial superoxide dismutase-deficient mice. Proc Natl Acad Sci U S A. 1996 Sep 3;93:9782-7.

121. Uchiyama S, Shimizu T, Shirasawa T. CuZn-SOD deficiency causes ApoB degradation and induces hepatic lipid accumulation by impaired lipoprotein secretion in mice. J Biol Chem. 2006 Oct 20;281:31713-9.

122. Brown MS, Goldstein JL. A proteolytic pathway that controls the cholesterol content of membranes, cells, and blood. Proc Natl Acad Sci U S A. 1999 Sep 28;96:11041-8.

123. Goldstein JL, Brown MS. Regulation of the mevalonate pathway. Nature. 1990 Feb 1;343:425-30.

124. Pallottini V, Montanari L, Cavallini G, Bergamini E, Gori Z, Trentalance A. Mechanisms underlying the impaired regulation of 3-hydroxy-3-methylglutaryl coenzyme A reductase in aged rat liver. Mech Ageing Dev. 2004 Sep;125:633-9.

125. Beg ZH, Stonik JA, Brewer HB, Jr. 3-Hydroxy-3-methylglutaryl coenzyme A reductase: regulation of enzymatic activity by phosphorylation and dephosphorylation. Proc Natl Acad Sci U S A. 1978 Aug;75:3678-82.

126. Cappel RE, Gilbert HF. Thiol/disulfide exchange between 3-hydroxy-3-methylglutaryl-CoA reductase and glutathione. A thermodynamically facile dithiol oxidation. J Biol Chem. 1988 Sep 5;263:12204-12.

127. Horton JD, Goldstein JL, Brown MS. SREBPs: activators of the complete program of cholesterol and fatty acid synthesis in the liver. J Clin Invest. 2002 May;109:1125-31.

128. Zeng L, Lu M, Mori K, Luo S, Lee AS, Zhu Y, Shyy JY. ATF6 modulates SREBP2-mediated lipogenesis. EMBO J. 2004 Feb 25;23:950-8.

129. Sundqvist A, Bengoechea-Alonso MT, Ye X, Lukiyanchuk V, Jin J, Harper JW, Ericsson J. Control of lipid metabolism by phosphorylation-dependent degradation of the SREBP family of transcription factors by SCF(Fbw7). Cell Metab. 2005 Jun;1:379-91.

130. Griffin MJ, Wong RH, Pandya N, Sul HS. Direct interaction between USF and SREBP-1c mediates synergistic activation of the fatty-acid synthase promoter. J Biol Chem. 2007 Feb 23;282:5453-67.

131. McClung JP, Roneker CA, Mu W, Lisk DJ, Langlais P, Liu F, Lei XG. Development of insulin resistance and obesity in mice overexpressing cellular glutathione peroxidase. Proc Natl Acad Sci U S A. 2004 Jun 15;101:8852-7.

132. Tirosh O, Pardo M, Schwartz B, Miskin R. Long-lived alphaMUPA transgenic mice show reduced SOD2 expression, enhanced apoptosis and reduced susceptibility to the carcinogen dimethylhydrazine. Mech Ageing Dev. 2005 Dec;126:1262-73.

133. Li Y, Huang TT, Carlson EJ, Melov S, Ursell PC, Olson JL, Noble LJ, Yoshimura MP, Berger C, et al. Dilated cardiomyopathy and neonatal lethality in mutant mice lacking manganese superoxide dismutase. Nat Genet. 1995 Dec;11:376-81.

134. Rivals I, Personnaz L, Taing L, Potier MC. Enrichment or depletion of a GO category within a class of genes: which test? Bioinformatics. 2007 Feb 15;23:401-7.

135. Bindea G, Mlecnik B, Hackl H, Charoentong P, Tosolini M, Kirilovsky A, Fridman WH, Pages F, Trajanoski Z, Galon J. ClueGO: a Cytoscape plug-in to decipher functionally grouped gene ontology and pathway annotation networks. Bioinformatics. 2009 Apr 15;25:1091-3.

136. Williams PT. Changes in body weight and waist circumference affect incident hypercholesterolemia during 7 years of follow-up. Obesity (Silver Spring). 2008 Sep;16:2163-8.

137. Magkos F, Tsekouras YE, Prentzas KI, Basioukas KN, Matsama SG, Yanni AE, Kavouras SA, Sidossis LS. Acute exercise-induced changes in basal VLDL-triglyceride kinetics leading to hypotriglyceridemia manifest more readily after resistance than endurance exercise. J Appl Physiol. 2008 Oct;105:1228-36.

138. Andreoli MF, Gonzalez MA, Martinelli MI, Mocchiutti NO, Bernal CA. Effects of dietary conjugated linoleic acid at high-fat levels on triacylglycerol regulation in mice. Nutrition. 2009 Apr;25:445-52.

139. Iannello S, Cavaleri A, Milazzo P, Cantarella S, Belfiore F. Low fasting serum triglyceride level as a precocious marker of autoimmune disorders. MedGenMed. 2003 Aug 7;5:20.

140. Stevens FJ, Argon Y. Protein folding in the ER. Semin Cell Dev Biol. 1999 Oct;10:443-54.

141. Appierto V, Tiberio P, Villani MG, Cavadini E, Formelli F. PLAB induction in fenretinide-induced apoptosis of ovarian cancer cells occurs via a ROS-dependent mechanism involving ER stress and JNK activation. Carcinogenesis. 2009 May;30:824-31.

142. Travers KJ, Patil CK, Wodicka L, Lockhart DJ, Weissman JS, Walter P. Functional and genomic analyses reveal an essential coordination between the unfolded protein response and ER-associated degradation. Cell. 2000 Apr 28;101:249-58.

143. Haynes CM, Titus EA, Cooper AA. Degradation of misfolded proteins prevents ER-derived oxidative stress and cell death. Mol Cell. 2004 Sep 10;15:767-76.

144. Tan SX, Teo M, Lam YT, Dawes IW, Perrone GG. Cu, Zn superoxide dismutase and NADP(H) homeostasis are required for tolerance of endoplasmic reticulum stress in Saccharomyces cerevisiae. Mol Biol Cell. 2009 Mar;20:1493-508.

145. Ye J, Rawson RB, Komuro R, Chen X, Dave UP, Prywes R, Brown MS, Goldstein JL. ER stress induces cleavage of membrane-bound ATF6 by the same proteases that process SREBPs. Mol Cell. 2000 Dec;6:1355-64.

146. Wakil SJ. Fatty acid synthase, a proficient multifunctional enzyme. Biochemistry. 1989 May 30;28:4523-30.

147. Camps L, Reina M, Llobera M, Bengtsson-Olivecrona G, Olivecrona T, Vilaro S. Lipoprotein lipase in lungs, spleen, and liver: synthesis and distribution. J Lipid Res. 1991 Dec;32:1877-88.

148. Merkel M, Weinstock PH, Chajek-Shaul T, Radner H, Yin B, Breslow JL, Goldberg IJ. Lipoprotein lipase expression exclusively in liver. A mouse model for metabolism in the neonatal period and during cachexia. J Clin Invest. 1998 Sep 1;102:893-901.

149. Tein I, De Vivo DC, Hale DE, Clarke JT, Zinman H, Laxer R, Shore A, DiMauro S. Short-chain L-3-hydroxyacyl-CoA dehydrogenase deficiency in muscle: a new cause for recurrent myoglobinuria and encephalopathy. Ann Neurol. 1991 Sep;30:415-9.

150. Robinson BH, Sherwood WG, Taylor J, Balfe JW, Mamer OA. Acetoacetyl

CoA thiolase deficiency: a cause of severe ketoacidosis in infancy simulating salicylism. J Pediatr. 1979 Aug;95:228-33.

151. Middleton B. The kinetic mechanism and properties of the cytoplasmic acetoacetyl-coenzyme A thiolase from rat liver. Biochem J. 1974 Apr;139:109-21.

152. Hartlage P, Eller G, Carter L, Roesel A, Hommes F. Mitochondrial acetoacetyl-CoA thiolase deficiency. Biochem Med Metab Biol. 1986 Oct;36:198-206.

153. Bennett MJ, Hosking GP, Smith MF, Gray RG, Middleton B. Biochemical investigations on a patient with a defect in cytosolic acetoacetyl-CoA thiolase, associated with mental retardation. J Inherit Metab Dis. 1984;7:125-8.

154. Mattiazzi M, D'Aurelio M, Gajewski CD, Martushova K, Kiaei M, Beal MF, Manfredi G. Mutated human SOD1 causes dysfunction of oxidative phosphorylation in mitochondria of transgenic mice. J Biol Chem. 2002 Aug 16;277:29626-33.

155. Muller FL, Song W, Jang YC, Liu Y, Sabia M, Richardson A, Van Remmen H. Denervation-induced skeletal muscle atrophy is associated with increased mitochondrial ROS production. Am J Physiol Regul Integr Comp Physiol. 2007 Sep;293:R1159-68.

156. Spiegelman BM. Transcriptional control of energy homeostasis through the PGC1 coactivators. Novartis Found Symp. 2007;286:3-6; discusssion -12, 162-3, 96-203.

157. Jahnke VE, Sabido O, Freyssenet D. Control of mitochondrial biogenesis, ROS level, and cytosolic Ca2+ concentration during the cell cycle and the onset of differentiation in L6E9 myoblasts. Am J Physiol Cell Physiol. 2009 May;296:C1185-94.

158. Hughes AL, Todd BL, Espenshade PJ. SREBP pathway responds to sterols and functions as an oxygen sensor in fission yeast. Cell. 2005 Mar 25;120:831-42.

159. Shimano H, Shimomura I, Hammer RE, Herz J, Goldstein JL, Brown MS, Horton JD. Elevated levels of SREBP-2 and cholesterol synthesis in livers of mice homozygous for a targeted disruption of the SREBP-1 gene. J Clin Invest. 1997 Oct 15;100:2115-24.

160. McPherson R, Gauthier A. Molecular regulation of SREBP function: the Insig-SCAP connection and isoform-specific modulation of lipid synthesis. Biochem Cell Biol. 2004 Feb;82:201-11.

161. De Felice B, Santillo M, Seru R, Damiano S, Matrone G, Wilson RR, Mondola P. Modulation of 3-hydroxy-3-methylglutaryl-CoA reductase gene expression by CuZn superoxide dismutase in human fibroblasts and HepG2 cells. Gene Expr. 2004;12:29-38.

162. Mondola P, Seru R, Santillo M, Damiano S, Bifulco M, Laezza C, Formisano P, Rotilio G, Ciriolo MR. Effect of Cu,Zn superoxide dismutase on cholesterol metabolism in human hepatocarcinoma (HepG2) cells. Biochem Biophys Res Commun. 2002 Jul 19;295:603-9.

163. Obesity: preventing and managing the global epidemic. Report of a WHO consultation. World Health Organ Tech Rep Ser. 2000;894:i-xii, 1-253.

164. Furukawa S, Fujita T, Shimabukuro M, Iwaki M, Yamada Y, Nakajima Y, Nakayama O, Makishima M, Matsuda M, Shimomura I. Increased oxidative stress in obesity and its impact on metabolic syndrome. J Clin Invest. 2004 Dec;114:1752-61.

165. Atabek ME, Vatansev H, Erkul I. Oxidative stress in childhood obesity. J Pediatr Endocrinol Metab. 2004 Aug;17:1063-8.

166. Ozata M, Mergen M, Oktenli C, Aydin A, Sanisoglu SY, Bolu E, Yilmaz MI, Sayal A, Isimer A, Ozdemir IC. Increased oxidative stress and hypozincemia in male obesity. Clin Biochem. 2002 Nov;35:627-31.

167. Vincent HK, Taylor AG. Biomarkers and potential mechanisms of obesity-induced oxidant stress in humans. Int J Obes (Lond). 2006 Mar;30:400-18.

168. Woods SC, Seeley RJ, Porte D, Jr., Schwartz MW. Signals that regulate food intake and energy homeostasis. Science. 1998 May 29;280:1378-83.

169. Vachharajani V, Granger DN. Adipose tissue: a motor for the inflammation associated with obesity. IUBMB Life. 2009 Apr;61:424-30.

170. Guerre-Millo M. Adipose tissue and adipokines: for better or worse. Diabetes Metab. 2004 Feb;30:13-9.

171. Bluher M. Adipose Tissue Dysfunction in Obesity. Exp Clin Endocrinol Diabetes. 2009 Apr 8.

172. Pearce J. Fatty acid synthesis in liver and adipose tissue. Proc Nutr Soc. 1983 Jun;42:263-71.

173. Lin J, Yang R, Tarr PT, Wu PH, Handschin C, Li S, Yang W, Pei L, Uldry M, et al. Hyperlipidemic effects of dietary saturated fats mediated through PGC-1beta coactivation of SREBP. Cell. 2005 Jan 28;120:261-73.

174. Yang F, Vought BW, Satterlee JS, Walker AK, Jim Sun ZY, Watts JL, DeBeaumont R, Saito RM, Hyberts SG, et al. An ARC/Mediator subunit required for SREBP control of cholesterol and lipid homeostasis. Nature. 2006 Aug 10;442:700-4.

175. Canto C, Gerhart-Hines Z, Feige JN, Lagouge M, Noriega L, Milne JC, Elliott PJ, Puigserver P, Auwerx J. AMPK regulates energy expenditure by modulating NAD+ metabolism and SIRT1 activity. Nature. 2009 Apr 23;458:1056-60.

176. Lee AH, Scapa EF, Cohen DE, Glimcher LH. Regulation of hepatic lipogenesis by the transcription factor XBP1. Science. 2008 Jun 13;320:1492-6.

177. Haslam DW, James WP. Obesity. Lancet. 2005 Oct 1;366:1197-209.

178. Aggoun Y. Obesity, metabolic syndrome, and cardiovascular disease. Pediatr Res. 2007 Jun;61:653-9.

179. Heptulla R, Smitten A, Teague B, Tamborlane WV, Ma YZ, Caprio S. Temporal patterns of circulating leptin levels in lean and obese adolescents: relationships to insulin, growth hormone, and free fatty acids rhythmicity. J Clin Endocrinol Metab. 2001 Jan;86:90-6.

180. Chen Q, Vazquez EJ, Moghaddas S, Hoppel CL, Lesnefsky EJ. Production of reactive oxygen species by mitochondria: central role of complex III. J Biol Chem. 2003 Sep 19;278:36027-31.

181. Busquets S, Almendro V, Barreiro E, Figueras M, Argiles JM, Lopez-Soriano FJ. Activation of UCPs gene expression in skeletal muscle can be independent on both circulating fatty acids and food intake. Involvement of ROS in a model of mouse cancer cachexia. FEBS Lett. 2005 Jan 31;579:717-22.

182. Cury-Boaventura MF, Curi R. Regulation of reactive oxygen species (ROS) production by C18 fatty acids in Jurkat and Raji cells. Clin Sci (Lond). 2005 Mar;108:245-53.

183. Yang S, Zhu H, Li Y, Lin H, Gabrielson K, Trush MA, Diehl AM. Mitochondrial adaptations to obesity-related oxidant stress. Arch Biochem Biophys. 2000 Jun 15;378:259-68.

184. Fujita T. Aldosterone in salt-sensitive hypertension and metabolic syndrome. J Mol Med. 2008 Jun;86:729-34.

185. D'Autreaux B, Toledano MB. ROS as signalling molecules: mechanisms that generate specificity in ROS homeostasis. Nat Rev Mol Cell Biol. 2007 Oct;8:813-24.

186. Maddux BA, See W, Lawrence JC, Jr., Goldfine AL, Goldfine ID, Evans JL. Protection against oxidative stress-induced insulin resistance in rat L6 muscle cells by mircomolar concentrations of alpha-lipoic acid. Diabetes. 2001 Feb;50:404-10.

187. Rudich A, Tirosh A, Potashnik R, Hemi R, Kanety H, Bashan N. Prolonged oxidative stress impairs insulin-induced GLUT4 translocation in 3T3-L1 adipocytes. Diabetes. 1998 Oct;47:1562-9.

188. Ali MH, Schlidt SA, Chandel NS, Hynes KL, Schumacker PT, Gewertz BL. Endothelial permeability and IL-6 production during hypoxia: role of ROS in signal transduction. Am J Physiol. 1999 Nov;277:L1057-65.

189. Muller FL, Song W, Liu Y, Chaudhuri A, Pieke-Dahl S, Strong R, Huang TT, Epstein CJ, Roberts LJ, 2nd, et al. Absence of CuZn superoxide dismutase leads to elevated oxidative stress and acceleration of age-dependent skeletal muscle atrophy. Free Radic Biol Med. 2006 Jun 1;40:1993-2004.

190. Miao L, Clair DK. Regulation of Superoxide Dismutase Genes: Implications in Diseases. Free Radic Biol Med. 2009 May 25.

191. Pfluger PT, Herranz D, Velasco-Miguel S, Serrano M, Tschop MH. Sirt1 protects against high-fat diet-induced metabolic damage. Proc Natl Acad Sci U S A. 2008 Jul 15;105:9793-8.

192. St-Pierre J, Drori S, Uldry M, Silvaggi JM, Rhee J, Jager S, Handschin C, Zheng K, Lin J, et al. Suppression of reactive oxygen species and neurodegeneration by the PGC-1 transcriptional coactivators. Cell. 2006 Oct 20;127:397-408.

193. Andersen G, Wegner L, Yanagisawa K, Rose CS, Lin J, Glumer C, Drivsholm T, Borch-Johnsen K, Jorgensen T, et al. Evidence of an association between genetic variation of the coactivator PGC-1beta and obesity. J Med Genet. 2005 May;42:402-7.

194. Ropelle ER, Pauli JR, Cintra DE, Frederico MJ, de Pinho RA, Velloso LA, De Souza CT. Acute exercise modulates the Foxo1/PGC-1alpha pathway in the liver of diet-induced obesity rats. J Physiol. 2009 May 1;587:2069-76.

195. de Haan JB, Witting PK, Stefanovic N, Pete J, Daskalakis M, Kola I, Stocker R, Smolich JJ. Lack of the antioxidant glutathione peroxidase-1 does not increase atherosclerosis in C57BL/J6 mice fed a high-fat diet. J Lipid Res. 2006 Jun;47:1157-67.

196. Mickelsen O, Takahashi S, Craig C. Experimental obesity. I. Production of obesity in rats by feeding high-fat diets. J Nutr. 1955 Dec 10;57:541-54.

197. Prentice AM, Sonko BJ, Murgatroyd PR, Goldberg GR. Obesity as an adaptation to a high-fat diet. Am J Clin Nutr. 1994 Oct;60:640-2.

198. Fearnside JF, Dumas ME, Rothwell AR, Wilder SP, Cloarec O, Toye A, Blancher C, Holmes E, Tatoud R, et al. Phylometabonomic patterns of adaptation to high fat diet feeding in inbred mice. PLoS ONE. 2008;3:e1668.

199. Peters JC. Dietary fat and body weight control. Lipids. 2003 Feb;38:123-7.

200. Lissner L, Levitsky DA, Strupp BJ, Kalkwarf HJ, Roe DA. Dietary fat and the regulation of energy intake in human subjects. Am J Clin Nutr. 1987 Dec;46:886-92.

201. Stubbs RJ, Harbron CG, Murgatroyd PR, Prentice AM. Covert manipulation of dietary fat and energy density: effect on substrate flux and food intake in men eating ad libitum. Am J Clin Nutr. 1995 Aug;62:316-29.

202. Schutz Y, Flatt JP, Jequier E. Failure of dietary fat intake to promote fat oxidation: a factor favoring the development of obesity. Am J Clin Nutr. 1989 Aug;50:307-14.

203. Wang XD, Vatamaniuk MZ, Wang SK, Roneker CA, Simmons RA, Lei XG. Molecular mechanisms for hyperinsulinaemia induced by overproduction of selenium-dependent glutathione peroxidase-1 in mice. Diabetologia. 2008 Aug;51:1515-24.

204. Jaillard T, Roger M, Galinier A, Guillou P, Benani A, Leloup C, Casteilla L, Penicaud L, Lorsignol A. Hypothalamic reactive oxygen species are required for insulin-induced food intake inhibition. A NADPH oxidase-dependent mechanism. Diabetes. 2009 Apr 23.

205. Perez-de-Arce K, Foncea R, Leighton F. Reactive oxygen species mediates homocysteine-induced mitochondrial biogenesis in human endothelial cells: modulation by antioxidants. Biochem Biophys Res Commun. 2005 Dec

16;338:1103-9.

206. Espenshade PJ. SREBPs: sterol-regulated transcription factors. J Cell Sci. 2006 Mar 15;119:973-6.

207. van der Velde AE, Vrins CL, van den Oever K, Kunne C, Oude Elferink RP, Kuipers F, Groen AK. Direct intestinal cholesterol secretion contributes significantly to total fecal neutral sterol excretion in mice. Gastroenterology. 2007 Sep;133:967-75.

208. Sterzing PR, McGilliard AD, Allen RS. Fine structural localization of cholesterol during fat absorption by bovine intestinal mucosa. J Dairy Sci. 1971 Oct;54:1449-56.

209. de Vogel-van den Bosch HM, de Wit NJ, Hooiveld GJ, Vermeulen H, van der Veen JN, Houten SM, Kuipers F, Muller M, van der Meer R. A cholesterol-free, high-fat diet suppresses gene expression of cholesterol transporters in murine small intestine. Am J Physiol Gastrointest Liver Physiol. 2008 May;294:G1171-80.

210. Satchithanandam S, Reicks M, Calvert RJ, Cassidy MM, Kritchevsky D. Coconut oil and sesame oil affect lymphatic absorption of cholesterol and fatty acids in rats. J Nutr. 1993 Nov;123:1852-8.

211.Brussaard JH, Katan MB, Hautvast JG. Faecal excretion of bile acids and neutral steroids on diets differing in type and amount of dietary fat in young healthy persons. Eur J Clin Invest. 1983 Apr;13:115-22.

212. Lin CC, Yin MC. Effects of cysteine-containing compounds on biosynthesis of triacylglycerol and cholesterol and anti-oxidative protection in liver from mice consuming a high-fat diet. Br J Nutr. 2008 Jan;99:37-43.

213. Matsuzawa-Nagata N, Takamura T, Ando H, Nakamura S, Kurita S, Misu H, Ota T, Yokoyama M, Honda M, et al. Increased oxidative stress precedes the onset of high-fat diet-induced insulin resistance and obesity. Metabolism. 2008 Aug;57:1071-7.

214. Sekiya M, Hiraishi A, Touyama M, Sakamoto K. Oxidative stress induced lipid accumulation via SREBP1c activation in HepG2 cells. Biochem Biophys Res Commun. 2008 Oct 31;375:602-7.

215. Waris G, Felmlee DJ, Negro F, Siddiqui A. Hepatitis C virus induces proteolytic cleavage of sterol regulatory element binding proteins and stimulates their phosphorylation via oxidative stress. J Virol. 2007 Aug;81:8122-30.

216. Bizeau ME, MacLean PS, Johnson GC, Wei Y. Skeletal muscle sterol regulatory element binding protein-1c decreases with food deprivation and increases with feeding in rats. J Nutr. 2003 Jun;133:1787-92.

217. Commerford SR, Peng L, Dube JJ, O'Doherty RM. In vivo regulation of SREBP-1c in skeletal muscle: effects of nutritional status, glucose, insulin, and leptin. Am J Physiol Regul Integr Comp Physiol. 2004 Jul;287:R218-27.

218. McCord JM, Fridovich I. Superoxide dismutase. An enzymic function for erythrocuprein (hemocuprein). J Biol Chem. 1969 Nov 25;244:6049-55.

219. Inarrea P, Moini H, Han D, Rettori D, Aguilo I, Alava MA, Iturralde M, Cadenas E. Mitochondrial respiratory chain and thioredoxin reductase regulate intermembrane Cu,Zn-superoxide dismutase activity: implications for mitochondrial energy metabolism and apoptosis. Biochem J. 2007 Jul 1;405:173-9.

220. Tainer JA, Getzoff ED, Richardson JS, Richardson DC. Structure and mechanism of copper, zinc superoxide dismutase. Nature. 1983 Nov 17-23;306:284-7.

221. Bertinato J, Iskandar M, L'Abbe MR. Copper deficiency induces the upregulation of the copper chaperone for Cu/Zn superoxide dismutase in weanling male rats. J Nutr. 2003 Jan;133:28-31.

222. Lawrence CB, Davies NT, Mills CF, Nicol F. Studies on the effects of copper deficiency on rat liver mitochondria. I. Changes in mitochondrial composition. Biochim Biophys Acta. 1985 Oct 9;809:351-61.

223. Chen H, Huang G, Su T, Gao H, Attieh ZK, McKie AT, Anderson GJ, Vulpe CD. Decreased hephaestin activity in the intestine of copper-deficient mice causes systemic iron deficiency. J Nutr. 2006 May;136:1236-41.

224. Zhu JH, Zhang X, McClung JP, Lei XG. Impact of Cu, Zn-superoxide dismutase and Se-dependent glutathione peroxidase-1 knockouts on acetaminophen-induced cell death and related signaling in murine liver. Exp Biol Med (Maywood). 2006 Dec;231:1726-32.

225. Lei XG, Zhu JH, McClung JP, Aregullin M, Roneker CA. Mice deficient in Cu,Zn-superoxide dismutase are resistant to acetaminophen toxicity. Biochem J. 2006 Nov 1;399:455-61.

226. Shimano H, Horton JD, Shimomura I, Hammer RE, Brown MS, Goldstein JL. Isoform 1c of sterol regulatory element binding protein is less active than isoform 1a

in livers of transgenic mice and in cultured cells. J Clin Invest. 1997 Mar 1;99:846-54.

227. Wilson J, Kim S, Allen KG, Baillie R, Clarke SD. Hepatic fatty acid synthase gene transcription is induced by a dietary copper deficiency. Am J Physiol. 1997 Jun;272:E1124-9.

228. Hirano Y, Murata S, Tanaka K, Shimizu M, Sato R. Sterol regulatory element-binding proteins are negatively regulated through SUMO-1 modification independent of the ubiquitin/26 S proteasome pathway. J Biol Chem. 2003 May 9;278:16809-19.

229. Bengoechea-Alonso MT, Punga T, Ericsson J. Hyperphosphorylation regulates the activity of SREBP1 during mitosis. Proc Natl Acad Sci U S A. 2005 Aug 16;102:11681-6.

230. Bureau I, Gueux E, Mazur A, Rock E, Roussel AM, Rayssiguier Y. Female rats are protected against oxidative stress during copper deficiency. J Am Coll Nutr. 2003 Jun;22:239-46.

231. Sukalski KA, LaBerge TP, Johnson WT. In vivo oxidative modification of erythrocyte membrane proteins in copper deficiency. Free Radic Biol Med. 1997;22:835-42.

232. Carroll MC, Outten CE, Proescher JB, Rosenfeld L, Watson WH, Whitson LJ, Hart PJ, Jensen LT, Cizewski Culotta V. The effects of glutaredoxin and copper activation pathways on the disulfide and stability of Cu,Zn superoxide dismutase. J Biol Chem. 2006 Sep 29;281:28648-56.

233. Freeman BA, Crapo JD. Biology of disease: free radicals and tissue injury. Lab Invest. 1982 Nov;47:412-26.

234. Wissing D, Mouritzen H, Jaattela M. TNF-induced mitochondrial changes and activation of apoptotic proteases are inhibited by A20. Free Radic Biol Med. 1998 Jul 1;25:57-65.

235. Thannickal VJ, Fanburg BL. Reactive oxygen species in cell signaling. Am J Physiol Lung Cell Mol Physiol. 2000 Dec;279:L1005-28.

236. Zangar RC, Davydov DR, Verma S. Mechanisms that regulate production of reactive oxygen species by cytochrome P450. Toxicol Appl Pharmacol. 2004 Sep 15;199:316-31.

237. Schrader M, Fahimi HD. The peroxisome: still a mysterious organelle. Histochem Cell Biol. 2008 Apr;129:421-40.

238. Ushio-Fukai M. Localizing NADPH oxidase-derived ROS. Sci STKE. 2006 Aug 22;2006:re8.

239. Szasz T, Thompson JM, Watts SW. A comparison of reactive oxygen species metabolism in the rat aorta and vena cava: focus on xanthine oxidase. Am J Physiol Heart Circ Physiol. 2008 Sep;295:H1341-H50.

240. Nakamura T, Sakamoto K. Forkhead transcription factor FOXO subfamily is essential for reactive oxygen species-induced apoptosis. Mol Cell Endocrinol. 2008 Jan 16;281:47-55.

241. Gross DN, Wan M, Birnbaum MJ. The role of FOXO in the regulation of metabolism. Curr Diab Rep. 2009 Jun;9:208-14.

242. Fredriksson K. FOXO, the spindle in the net for wasting diseases? J Physiol. 2008 Nov 15;586:5285.

243. Lage R, Dieguez C, Vidal-Puig A, Lopez M. AMPK: a metabolic gauge regulating whole-body energy homeostasis. Trends Mol Med. 2008 Dec;14:539-49.

244. Emerling BM, Weinberg F, Snyder C, Burgess Z, Mutlu GM, Viollet B, Budinger GR, Chandel NS. Hypoxic activation of AMPK is dependent on mitochondrial ROS but independent of an increase in AMP/ATP ratio. Free Radic Biol Med. 2009 May 15;46:1386-91.

245. Pallottini V, Martini C, Cavallini G, Bergamini E, Mustard KJ, Hardie DG, Trentalance A. Age-related HMG-CoA reductase deregulation depends on ROS-induced p38 activation. Mech Ageing Dev. 2007 Nov-Dec;128:688-95.

246. Pallottini V, Martini C, Pascolini A, Cavallini G, Gori Z, Bergamini E, Incerpi S, Trentalance A. 3-Hydroxy-3-methylglutaryl coenzyme A reductase deregulation and age-related hypercholesterolemia: a new role for ROS. Mech Ageing Dev. 2005 Aug;126:845-51.

247. Mason RP, Walter MF, Jacob RF. Effects of HMG-CoA reductase inhibitors on endothelial function: role of microdomains and oxidative stress. Circulation. 2004 Jun 1;109:II34-41.

248. Vecchione C, Brandes RP. Withdrawal of 3-hydroxy-3-methylglutaryl coenzyme A reductase inhibitors elicits oxidative stress and induces endothelial dysfunction in mice. Circ Res. 2002 Jul 26;91:173-9.

249. Satoh T, Hidaka Y, Kamei T. Regulation of squalene epoxidase activity in rat liver. J Lipid Res. 1990 Nov;31:2095-101.

250. Hidaka Y, Satoh T, Kamei T. Regulation of squalene epoxidase in HepG2 cells. J Lipid Res. 1990 Nov;31:2087-94.

251. Chugh A, Ray A, Gupta JB. Squalene epoxidase as hypocholesterolemic drug target revisited. Prog Lipid Res. 2003 Jan;42:37-50.

252. Nagai M, Sakakibara J, Nakamura Y, Gejyo F, Ono T. SREBP-2 and NF-Y are involved in the transcriptional regulation of squalene epoxidase. Biochem Biophys Res Commun. 2002 Jul 5;295:74-80.

253. Martin FM, Bydlon G, Friedman JS. SOD2-deficiency sideroblastic anemia and red blood cell oxidative stress. Antioxid Redox Signal. 2006 Jul-Aug;8:1217-25.

254. Friedman JS, Lopez MF, Fleming MD, Rivera A, Martin FM, Welsh ML, Boyd A, Doctrow SR, Burakoff SJ. SOD2-deficiency anemia: protein oxidation and altered protein expression reveal targets of damage, stress response, and antioxidant responsiveness. Blood. 2004 Oct 15;104:2565-73.

255. Recuero M, Vicente MC, Martinez-Garcia A, Ramos MC, Carmona-Saez P, Sastre I, Aldudo J, Vilella E, Frank A, et al. A free radical-generating system induces the cholesterol biosynthesis pathway: a role in Alzheimer's disease. Aging Cell. 2009 Apr;8:128-39.

256. Haudek VJ, Gundacker NC, Slany A, Wimmer H, Bayer E, Pable K, Gerner C. Consequences of Acute and Chronic Oxidative Stress upon the Expression Pattern of Proteins in Peripheral Blood Mononuclear Cells. J Proteome Res. 2008 Nov 4.

257. Brown MS, Goldstein JL. The SREBP pathway: regulation of cholesterol metabolism by proteolysis of a membrane-bound transcription factor. Cell. 1997 May 2;89:331-40.

258. Fu Y, Sies H, Lei XG. Opposite roles of selenium-dependent glutathione peroxidase-1 in superoxide generator diquat- and peroxynitrite-induced apoptosis and signaling. J Biol Chem. 2001 Nov 16;276:43004-9.

259. Farrington JA, Ebert M, Land EJ, Fletcher K. Bipyridylium quaternary salts and related compounds. V. Pulse radiolysis studies of the reaction of paraquat radical with oxygen. Implications for the mode of action of bipyridyl herbicides. Biochim Biophys Acta. 1973 Sep 26;314:372-81.

260. Atkinson JB, Hill KE, Burk RF. Centrilobular endothelial cell injury by diquat in the selenium-deficient rat liver. Lab Invest. 2001 Feb;81:193-200.

261. Morris EM, Whaley-Connell AT, Thyfault JP, Britton SL, Koch LG, Wei Y, Ibdah JA, Sowers JR. Low Aerobic Capacity and High-Fat Diet Contribute to Oxidative Stress and IRS-1 Degradation in the Kidney. Am J Nephrol. 2009 Feb 20;30:112-9.

262. Dong F, Li Q, Sreejayan N, Nunn JM, Ren J. Metallothionein prevents high-fat diet induced cardiac contractile dysfunction: role of peroxisome proliferator activated receptor gamma coactivator 1alpha and mitochondrial biogenesis. Diabetes. 2007 Sep;56:2201-12.

263. Zhang X, Dong F, Ren J, Driscoll MJ, Culver B. High dietary fat induces NADPH oxidase-associated oxidative stress and inflammation in rat cerebral cortex. Exp Neurol. 2005 Feb;191:318-25.